UNIVERSITY OF PALERMO

PhD Research Course in Biomedicine and Neuroscience, curriculum in Experimental Oncobiology,
Department of Experimental Biomedicine and Clinical Neurosciences

SSD BIO/10

STUDY ON P53 GAIN OF FUNCTION

IN 3AB-OS CANCER STEM CELLS

THE DOCTOR

Michela Marcatti

THE COORDINATOR

Prof. Renza Vento

THE TUTOR

Prof. Renza Vento

THE CO-TUTOR

Doct. Martin Jansson

XXV CYCLE

ACHIEVEMENT YEAR TITLE 2015

I dedicate this thesis to

my dad and my husband,

the two men of my life

INDEX

INTRODUCTION

OSTEOSARCOMA

Osteosarcoma (OS) is a highly malignant mesenchymal tumor of bone in which the malignant cells produce osteoid (1). It is one of the most common primary, non-hematologic bone malignancies in children that occurs most frequently in patients between the ages of 10 and 25 years (2). Before the advent of multi-agent chemotherapy, amputation provided a long-term survival rate of about 20%. The use of multi-agent chemotherapy combined with aggressive surgery has improved the long-term survival in these patients to approximately 60% (3).Interestingly, survival of patients treated with chemotherapy alone is only 20%, suggesting that populations of tumor cells in a large percentage of osteosarcomas are highly resistant to chemotherapy. Despite intensive efforts in both surgical and medical management, the survival rate has not improved over the last 30 years and fully 40% of osteosarcoma patients die of their disease. Osteosarcoma can arise in any bone, but occurs primarily in the juxta-epiphyseal regions of rapidly growing long bones (Fig.1).

Fig.1. Radiographic appearance of osteosarcoma of the knee. (http://www.mypacs.net)

Osteosarcoma often begins as a process destructive of medullary bone that progresses to destroy cortical bone, usually with an associated soft-tissue component. The histopathologic appearance of high-grade intramedullary osteosarcoma is one of malignant spindle cells producing osteoid and immature bone. Cytogenetic evaluation has revealed numerous complex chromosomal abnormalities that change both within and between individual tumors in osteosarcoma (4). Molecular analyses have revealed a variety of genetic alterations in osteosarcoma, including inactivation of p53 and retinoblastoma tumor suppressor genes, downreguation of INK4α and overexpression of oncogenes such as MDM2 (5). For example, alterations of the retinoblastoma gene (RB1) have been shown in up to 70% of reported cases, and loss of heterozygosity for RB1 has been shown to be a marker of poor prognosis (6). Moreover, the gene INK4α, that encodes for negative regulators of cell cycle p16 and p14, is deleted in 10% of OS (7) and their protein products are considered biomarker of survival in patients with osteosarcoma (8). Major signaling pathway alterations also have been implicated, such as the pathway of Wnt, that has been associated with metastasis and poor prognosis (9). Abnormal expression of growth factors, such as TGF-b3, also has been associated with poor outcome. The use of novel effective therapeutic approaches and treatment strategies in patients who are resistant to current therapy could provide an improvement in outcome in patients. Improvements in outcome in paediatric OS have been achieved without the addition of novel agents, but rather through optimization of the dose, combination, schedule, and duration of treatment using standard systemic chemotherapy. Over the last decade, technological advances in research and medicine have provided detailed descriptions of factors that contribute to the malignant phenotype of this disease with the hope of finding new therapeutic treatments and strategies (10). Most of the phase III of clinical trials are combination treatments of conventional chemotherapy agents (11). OS overexpress several receptor tyrosine kinases (RTKs) including ErbB2, IGF-1R, PDGFR, VEGFR, and

activate the downstream signal-transduction pathways. Using of multi-RTKs in OS may be a powerful tool for the outcome of these tumors (12). Many tyrosine kinase inhibitors have been preclinically and clinically evaluated for OS desease, such as Imatinib and Dasatinib. Ongoing trials include the phase I/II study of dasatinib in combination with ifosfamide, carboplatin, and etoposide in young patients with metastatic or recurrent malignant solid tumors, including OS (10). The vascular endothelial growth factor (VEGF) pathway is involved in angiogenesis and is crucial for tumor growth and progression. It presents three isofroms, (VEGFR-1, -2, and -3) of which OS cell lines express the isoform VEGFR-3, that has been associated with poor survival (13). Cediranib (AZD 2171), sorafenib, and sunitinib. Combination of cediranib with the EGFR inhibitor gefitinib were tested in a phase I trial in patients with advanced solid tumors and demonstrated positive response in one OS patient (14). The insulin-like growth factor-1 receptor (IGF-1R) 1R has been implicated in the development of sarcomas and inhibition of its function has been demonstrated to reduce growth in OS (15). More than 25 antibodies and small molecules that specifically inhibit IGF-1R have undergone preclinical and clinical testing in both adults and children alone (16,17). However, despite clear evidence of clinical benefits in some pediatric patients, several drug companies have curtailed or eliminated anti-IGF-1R programs because the observed clinical benefits of targeting this pathway in single and multi-agent strategies did not met the primary endpoints in many adult trials. The current development of anti-IGF-1R therapy is being reviewed.

Activation of the mTOR pathway is implicated in the development and progression of OS (18) which makes mTOR an appealing target for therapeutic intervention. Rapamycin (sirolimus) and rapalogs (everolimus, temsirolimus, and ridaforolimus) are immunosuppressive macrocyclic lactone antibiotics that inhibit the kinase activity of mTORC1 while mTORC2 is generally rapamycin- insensitive (19). The response to these

compounds alone or in combination with other has been tested in preclinical and clinical trials (20, 21, 22, 23**,** 24) without a really good results. Novel small-molecule inhibitors that are mTOR-selective or dual mTOR/PI3K inhibitors have entered clinical trials. A key focus in the development of these drugs will be to establish the effectiveness of combination strategies with other targeted therapies and standard cytotoxic agents. IGF-1R signals through Akt and is suggested to be involved in resistance to mTOR inhibitors. Combined inhibition of IGF-1R and mTOR has been evaluated. Antibodies targeting IGF-1R (R1507, figitumumab, cixutumumab) in combination with rapamycin and rapalogs showed enhanced activity compared to the single agents (25, 26, 27). Further use of mTOR inhibitors in the treatment of OS patients is under investigation as single-dose therapy and multi-agent therapy in order to determine effective dosing schedules and additive combinations. PI3K and Akt activation may drive tumorigenesis in OS by regulating effectors that are different from mTORC1. Inhibition of Akt signaling reduces tumor survival and enhance the effectiveness of cytotoxic chemotherapy by increasing apoptosis (28, 29). The development of specific inhibitors of PI3K/Akt pathway is under investigation. Many growth factor receptors associated with the biology of OS (IGF-1R, EGFR,VEGFR, and PDGFR) activate the MAPK/ERK pathway to make it a powerful target for therapeutic intervention. AZD6244 is a potent and specific inhibitor for MEK 1/2 and demonstrated effective tumor growth inhibition of OS (30)**.** Cyclin-dependent kinases regulate orderly progression through the cell cycle. The use of inhibitors of cdks activity, such as seliciclib, alvocidib and dinaciclib induces cell cycle arrest and apoptosis of several OS cell lines (31) **.** Mutations in p53 (32) and amplification of MDM2 have been reported in OS (33). Antagonist of MDM2 and inhibitor of MDM2/p53 axis are under investigation (34, 35). Histone deacetylases (HDACs) regulate acetylation of histone lysine residues which triggers transcriptional activity promoting cell transformation and proliferation. Deregulation of histone acetylation is associated with disease pathogenesis

by promoting alterations in chromatin structure and gene transcription. HDAC inhibitors induce growth arrest and cell death by epigenetic changes in many preclinical and clinical cancer models (10). During programmed cell death, Smac, an endogenous pro-apoptotic protein of the mitochondria is released and promotes apoptosis via inhibition or proteasomal degradation of the inhibitor of apoptosis (IAP) family of proteins. Overexpression of Smac has been shown to sensitize OS cells *in vitro* to chemotherapeutic drug-induced apoptosis (36)**.** Thus, the use of small-molecule drugs that act as Smac mimetics in OS cells that overexpress IAP might be a potent strategy to elicit a pro-apoptotic anti-cancer response (37)**.** LCL161 demonstrated tumor growth delay in five of six OS xenografts and intermediate activity in one xenograft in the PPTP (37). The future application of small-molecule Smac mimetics as a treatment for OS warrants further investigation in multi-agent therapies with chemotherapy or other targeted therapies inclusive of agents that target apoptosis. The identification of new therapeutic drugs using strategies which target cell proliferation (multi-tyrosine kinase receptor inhibitors), angiogenesis (VEGF inhibitors), apoptosis, and DNA cytotoxicity in combination with standard chemotherapy has demonstrated promise in preclinical and early-phase clinical trials for OS (10). The emergence of numerous anti-cancer agents and the small number of OS patients eligible for early-phase clinical trials present another challenge in the clinical testing of novel compounds. The systematic preclinical evaluation of new agents in paediatric cancer has received huge support by the efforts of the Pediatric Pharmacoepidemiology Training Program (PPTP) supported by National Cancer Institute (NCI) (38). Since 2007, this program has facilitated the comprehensive analysis of more than 50 novel and standard agents in *in vitro* and *in vivo* panels of childhood cancers. The PPTP has demonstrated that OS xenografts provide a rapid and efficient platform to test new therapies for anti-tumor effects, offering a link between preclinical and clinical testing

with the potential of benefits to paediatric patients (10). In figure 2 the most important targets and therapies above discussed are shown.

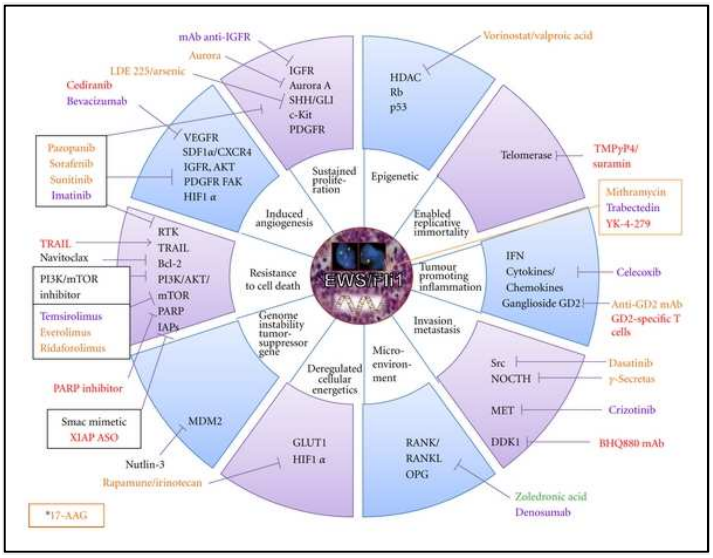

Fig.2. Targets and therapies in preclinical and clinical development in children and adolescent bone sarcomas. The different colours described the current clinical development of the drugs. (Red) Preclinical; (Orange) Phase I; (Blue) Phase II; (Green) Phase III(all in pediatric studies); (Black) Phase I or II in adults: all solid tumours (http://www.hindawi.com/journals/sarcoma/2012/301975).

CANCER STEM CELLS (CSCs)

Tumor microenvironment plays an important role in cell behavior and tumorigenesis. This network consists of different cell populations with normal and tumor cells in contact to each other. Within a tumor, only a minor subset of tumor cells are able to proliferate and divide unlimitedly to generate the tumor mass. This sub-population is defined as cancer stem cells (CSCs) (39). The name "CSCs" refer to the fact that they share many properties with normal stem cells (SCs), including activation of main cell signalling pathways such as Wnt, Notch, Hedgehog and others. Deregulation of some of these important signalling pathways in CSCs is involved in tumorigenesis (40, 41). CSCs behave like normal stem cells in many other aspects such as multipotency, membrane transport, DNA repair and the ability to regulate self-renewal, differentiate in response to oncogenic mutations and external stimulations, drug resistance (Fig.3).

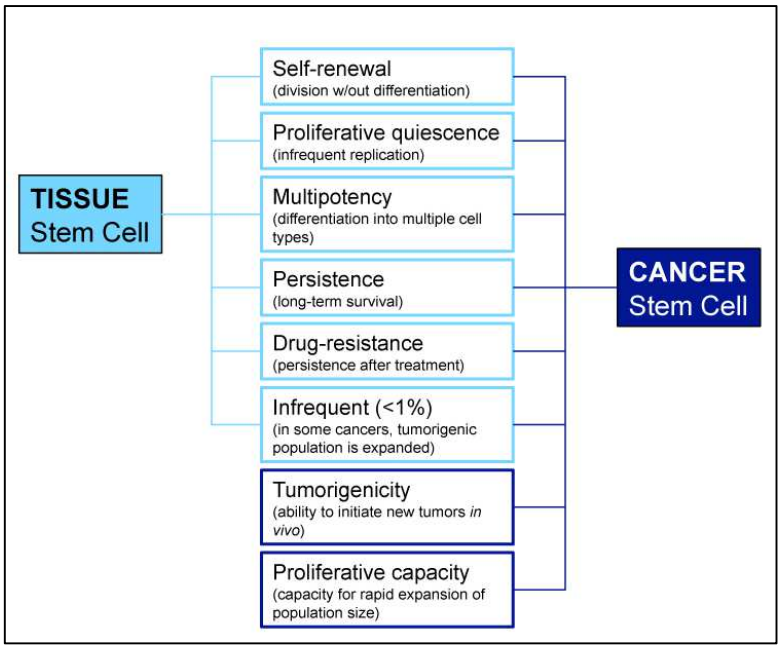

Fig.3. Features of cancer stem cells (CSCs) and tissue stem cells (SC) (Cancer Stem Cells lab-http://kirshner.bio.purdue.edu/

In cell culture, animal models and cancer patients it has been observed that these cells are responsible for cancer therapy failure using several molecular mechanisms, including

apoptosis resistance, drug-efflux pumps, enhanced DNA repair efficiency, detoxification enzyme expression and quiescence (42) For instance, in breast and AML (acute myeloid leukemia) CSCs, BCL2 and BCLXL are highly expressed (43, 44). Similarly, in primary GBM (glioblastoma) cultures CD133+ CSCs have elevated expression of BCL2 and BCLXL compared to their more differentiated CD133-progeny (45). Besides an elevated apoptotic threshold, CSCs display high expression of drug efflux pumps, like ATP-binding cassette (ABC) transporter family proteins (42), important for efflux of chemotherapy across the plasma membrane. Various ABC transporter proteins are highly expressed in hematopoietic stem cells (HSC) and in AML CSCs (CD34+/CD38-) compared to the non-stem (CD34+/CD38+) cells (46). Also in GBM and melanoma high expression of drug efflux pumps in CSCs are reported (47)**.** A recent observation is that CSCs may display quiescent properties to escape the selectivity of classical chemotherapy for cancer cells that are highly proliferative (42). Quiescent cells not only affects chemotherapy sensitivity, but also have a high DNA repair activity through an increased expression of DNA repair genes, such as ATM, ATR and Wee1 (42). Many chemotherapeutic agents and radiotherapy work by inducing DNA damage and cells that effectively repair DNA damage, such as CSCs, can potentially survive to therapeutic treatment. Various reports have shown that CSCs, such as GBM and breast CSCs, present high DNA repair activity, which makes them resistant to radiation and chemotherapy (48). In conclusion, there are many ways for CSCs to resist tumor therapy. Figure 2 illustrates the reasons for therapy resistance in CSCs (Fig.4).

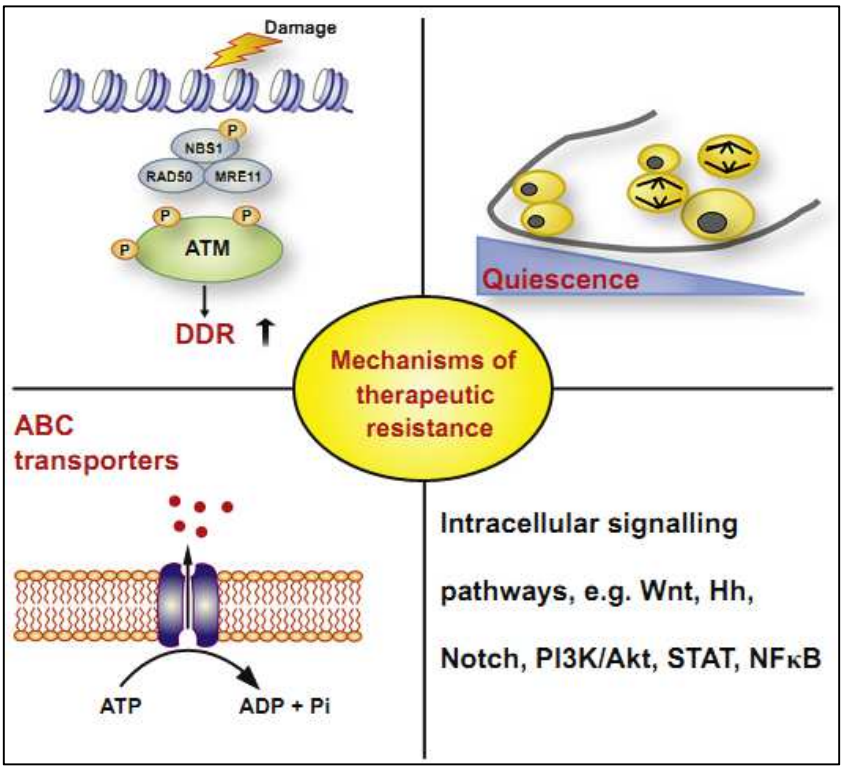

Fig.4. Main mechanisms of CSCs theraphy resistance. (Medicine-Oncology, book edited by Juan Manuel Mejia- Arangure, ISBN 978-953-51-0990-7, Published: April 17, 2013 under CC BY 3.0 license; Dong W, Zhu H et al; DOI: 105.5772/55075)

CSCs are characterized by the presence of several cell surface markers, such as CD133, CD44, CD13, CXCR1, Lgr5 and others. Identification of CSC markers and their roles in molecular mechanisms of tumorigenesis is critical to understanding tumor cell behavior in the tumor microenvironment and the development of new therapeutic modalities. Specific cell surface markers can help to identify, isolate and characterize both normal and cancer stem cells (39). Various groups and companies developed immunotoxins that directly target CSC markers. For instance, they produced antibodies against the stem cell marker CD133 conjugated to paclitaxel or cytolethal distending toxin (Cdt) target cells expressing CD133 and show *in vitro* and *in vivo* elimination of tumors (49, 50). However, CD133 expression is also expressed in normal stem cells surface, which should be protected from such therapies at all times. To minimize toxicity and deliver drug to cancer selectivity, photochemical internalization (PCI) has been developed. With this technique is possible to release drug in the tumor area specifically (51). Antibodies without toxins targeting other cell surface molecules

are shown to be efficient in killing CSCs as well. For example, antibodies against CD47 gave promising effects in various cancers. CD47 is a receptor that is involved in inhibition of phagocytosis signals and is highly expressed on CSCs compared to more differentiated cells. The block of this CD47 receptor affects phagocytosis of AML CSCs and thereby blocks tumor growth. In addition, it has been showed that CD47 inhibition blocks tumor growth in solid cancers like breast cancer, CRC, ovarian cancer and GBM (52, 53). Moreover, several antibodies have shown to delete essential signals from CSCs. For instance, direct targeting of breast CSCs can be achieved by using an antibody against CXCR1. The IL8 receptor CXCR1 is expressed almost exclusively on CSCs and Repertaxin, an inhibitor of CXCR1/2, or anti-CXCR1 treatment induces cell death in CXCR1+ breast CSCs, which appears to be mediated by AKT signaling inhibition (42). As described, CSCs require signaling pathways for their maintenance, suggesting that these may be attractive targets for therapy. For this reason, several compounds have been synthesized, such as Salinomycin, CUR199691 and DLL4, that inhibit Wint, Hedgeog and Notch pathways respectively (54, 55, 56). Antibodies can also target the CSC niche. For example, it has been observed that the use of Bevacizumab, an antibody against VEGF, induce GBM CSCs differentiation (57). In 2006 Jin et al. showed that using an antibody against CD44 decreased homing of AML cells and thereby promoting the AML CSCs to differentiate cancer cell progeny. This antibody also inhibited AML growth in mice (58). Another mechanism to target CSCs is to induce their differentiation by using specific protein, such as BMP4 (bone morphogenic protein 4) that induces GMB CSCs differentiation and inhibits their tumorigenicity (59). Altogether, direct CSCs targeting or CSCs differentiation induction are promising in the development of new tumor therapies, even if studies are needed to investigate the best combination treatments that does not give severe toxicities. Figure 5 describes the different effects between classical cancer therapies and CSCs specific therapies.

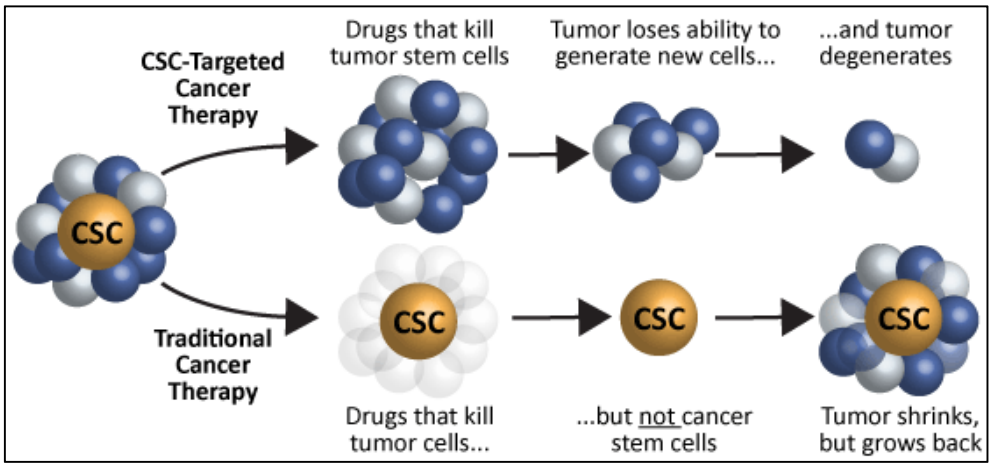

Fig.5. Traditional cancer therapies and CSCs specific therapies effects. (www.magrogenics.com/platform-cancer_stem_cells_csc.html)

P53

P53 is a tetrameric transcription factor consisting of three structural and functional domains: the amino-terminal transcriptional activation domain (TAD, residues 1–42); the DNA binding domain (DBD, aminoacidic residues 101–306); the carboxyl-terminal oligomerization domain (OD, residues 307–355) (Fig.6).

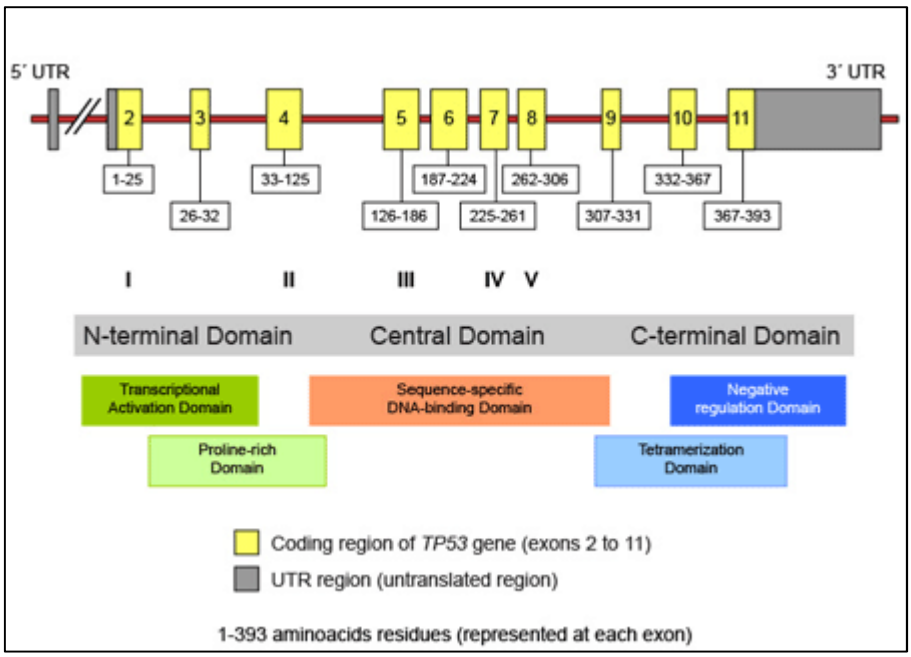

Fig.6. Structural organization of TP53 gene and p53 protein. (St. Jude Children's Research Hospital-website)

The protein p53 is normally kept at low expression levels through ubiquitylation and proteasomal degradation, mediated by several E3 ubiquitin ligase and MDM2 and MDM4 (60)**.** P53 turnover is controlled by the association of MDM2, MDM4, HAUSP (herpesvirus-associated ubiquitin-specific protease) and the adaptor protein DAXX (61, 62, 63, 64, 65) (Fig.7). HAUSP can deubiquitylate both MDM2 and p53. Under normal condition DAXX guides it towards MDM2 and MDM4. This minimize MDM2 auto-ubiquitylation and promotes p53 ubiquitylation and turnover.

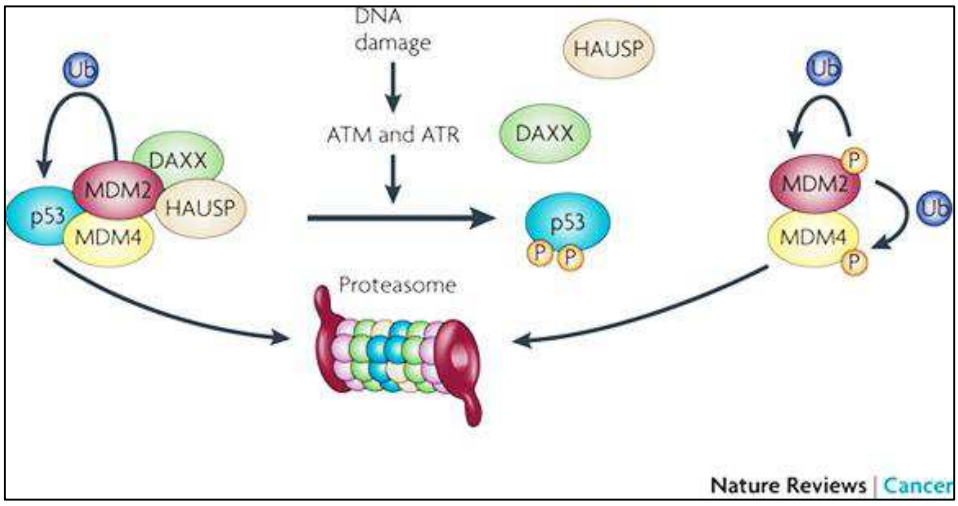

Fig.7. Mechanism of p53 turnover

P53 is activated in response of cellular stresses, including DNA damage and hyperproliferation (66)**.** Once induced, p53 regulates the expression of a wide range of genes, leading to the biological outcomes of repair, growth arrest, senescence or apoptosis (67) (Fig.8).

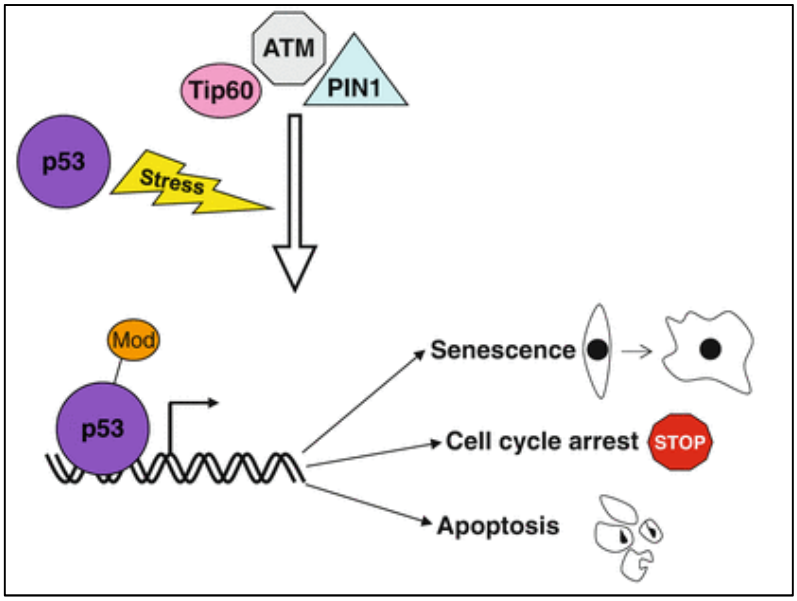

Fig.8. Activation of transcription by p53 wild type. Stress signals, such as DNA damage and activation of oncogenes, cause post-translational modifications of p53, mediated by interaction with stress-sensing molecules like Tip60, ATM and PIN1. Once activated, p53 can induce cell cycle arrest, senescence and apoptosis through transcriptional regulation of its target genes.

Upon these stress signals, p53 leads post-translational modifications such as phosphorylation, acetylation, sumoylation, ubiquitination (68) through the interaction with stress-sensing

molecules like TAT Interacting Protein 60 (Tip60) (69), Ataxia Telangiectasia Mutant (ATM), Rad-3 related protein kinase (ATR) and Peptidyl-prolyl cis-trans isomerase NIMA-interacting 1 (PIN1) (70, 71). These interaction determine the destruction of MDM2-DAXX-HAUSP complex and the rapid destruction of MDM2 and MDM4 with a consequent accumulation of stable p53 (72) (Fig.7).

More than half of all human cancers carry p53 gene mutations that can be divided empirically into three functionally non-exclusive categories: Loss of function, gain of function (GOF) mutations and dominant negative mutations (73).The first one are responsible for the loss of the tumor suppressor function of p53 and usually they are defective in sequence-specific transactivation of genes containing wild type (WT) p53 consensus binding sites. Most of these p53 mutations are missense mutations, mainly located within the DNA binding domain, that generate stable p53 proteins unable to bind canonical p53 consensus sequences (74). There are two classes of mutant p53. Class I mutants (e.g. mutants at codons 248 or 273) are characterized by an alteration in the residues which determine a sequence-specific binding to the DNA. Class II mutants (e.g. mutants at codon 175) show changes of p53 folding, abolishing completely the binding to the DNA and changing the capability to interact with other proteins (75). The mechanisms at the root of p53 GOF phenotype have not been fully elucidated. Mutant p53 may drive GOF phenotypes by acquiring new functions that result in uncontrolled proliferation, survival and motility (73). It has been showed that p53 mutants use several way in order to regulate the transcription of their targets by which can exert GOF function (Fig.9).

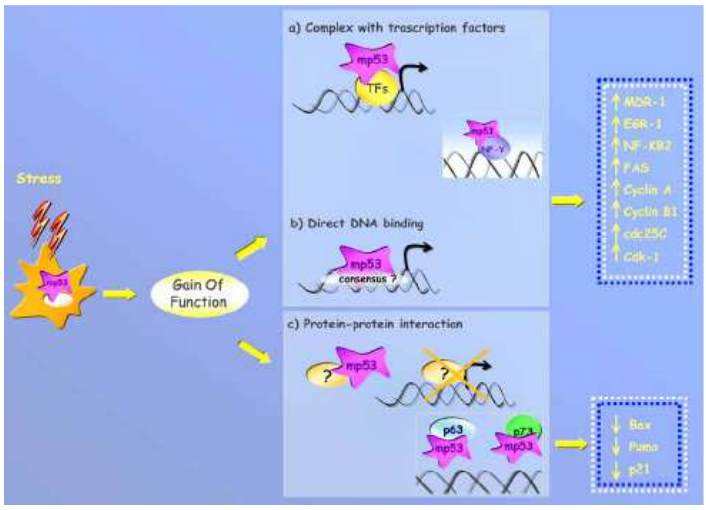

Fig.9: Mechanism of action of Mutant p53. Mutant p53 can be recruited on the promoter region of its gene targets by: a) interaction with other transcription factors; b) direct biding to DNA; c) interaction protein-protein (Donzelli S, Biagioni F et al; Curr Genomics,2008 May; 9 (3):200-7).

Although they cannot bind canonical p53 consensus elements by direct binding, they can be recruited to regulative elements on the chromatin through interaction with other protens and transcription factors, such as NF-Y(76), ETS1(77), ETS2 (78), p73 and p63 (79, 80)**,** Mre11, PLK2 and contribute to the regulation of their target genes (Fig.9). Moreover, it has been shown that mutant p53 can be recruited onto a subset of p63-responsive elements in the moters of genes upregulated and downregulated by p63 (81).

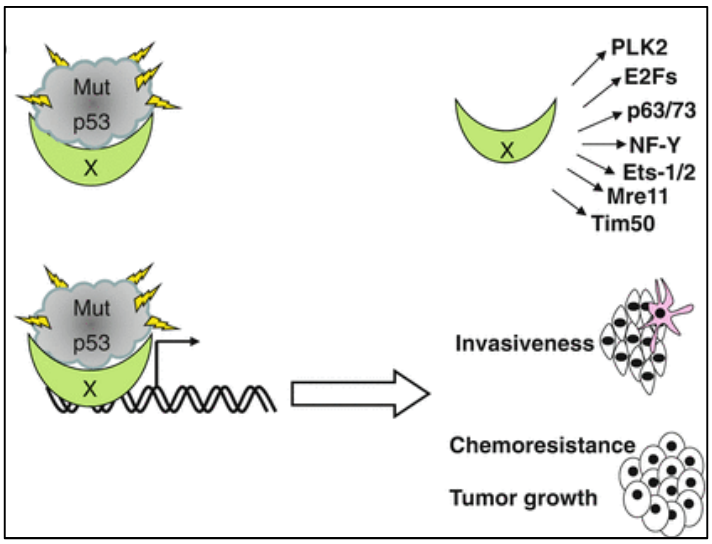

Fig.9. Activation of transcription by mutant p53. Mutant p53 acquires transcriptional activities by interacting with transcription factors such as NF-Y, Ets-1/2, p63/p73, E2Fs, PLK2, Mre11 and Tim50, which induce the recruitment of mutant p53 to regulatory regions on the chromatin.

It has been described that the transcription factor NF-Y binds to the CCAAT consensus motif present in the promoters of several cell cycle regulating genes, such as E2Fs and cyclines, and contributes to the modulation of their expression, through selective recruitment of acetylases and/or deacetylases (76). Upon DNA damage, the complex mutant p53/NF-Y drives the transcription of the cell cycle progressing genes cyclin A, B1 and B2, cdk1 and cdc25C, resulting in an increased DNA replication which constitutes an important aspect of mutant p53 GOF activities (76). Both WT p53 and mutant p53 are able to physically interact with the Polo-Like Kinase 2 (PLK2) protein, that plays a critical role in the arrest of cell in response to DNA damage (75). Another interactor of mutant p53 is Mre11. This protein forms with Rad50 and NBS1 a complex (MRN) involved in sensing DNA damage and recruiting the ATM kinase to the sites of DNA damage. When mutant p53 binds to Mre11 prevents the recruitment of the MRN complex to the sites of DNA double strand brakes (DSBs) leading to an impaired ATM response, that generate higher genetic instability (82). Since the interaction with novel partners confers mutant p53 new functions, many efforts are being made to identify additional interaction partners for mutant p53, especially in different contexts and in response to different stimuli (83). Moreover, mutant p53 can exerts its GOF function through the direct binding to the DNA. There is some evidence to show that mutant p53 binds to DNA on the chromosome, particularly in G/C rich areas around transcription start sites of some genes that are characterized by active chromatin marks (84). Furthermore, mutant p53 interact in a stereo-specific way with non-B DNA structures (85, 86). It has been shown that mutant p53 not only loses its suppressor functions but also can gain new oncogenic function contributing to the arising and maintenance of cancer (87). These mutants belong to the second category named gain of function (GOF) mutations. In dominant negative mutations, mutant p53 can form hetero-oligomers with wild type (WT) p53 abrogating WT p53 tumor suppressor functions. Usually, one allele of the p53 gene is mutated (point mutated),

generating a dominant negative mutant protein that may inactivate the co-expressed WT p53 resulting in weaker tumor suppression (p53:its mutations and their impact on transcription). This could be at the root of the increased cancer susceptibility of patients with Li-Fraumeni syndrome (88). Also GOF mutant p53 perform a dominant oncogenic role but it does not depend on complex formation with WT p53. Several laboratories have performed chromatin immunoprecipitation (ChIP) experiments to identify specific mutant p53 consensus sequences but, so far, no one has been identified (89). An important approach to detect the specific set of gene targets for each mutant p53 is the use of "ChIP-on-chip" and Chip-seq analyses and it could contribute to the identification of transcriptional activity of p53 mutants (90, 91, 92). In addition, a series of microarray analyses performed in different cell lines have shown that mutant p53 can modulate the expression of several genes (93). However, the scenario appears very complex because of the great heterogeneity of p53 mutations. In particular, each mutant of p53 can regulate the expression of a pattern of genes only partially overlapping with the ones of other p53 mutants. In fact, different mutations in p53 cause interaction with different sets of partners (75). The most known gain of function activity of mutant p53 is the induction of cell proliferation. Several studies have been conducted and the genes c-fos, c-myc, PCNA, cyclin A, B1, B2, cdk1 and cdc25c have been identified as specific targets of mutant p53, which can promote cell proliferation (75). Mutant p53 can exert its pro-invasive and pro-angiogenic activities mainly through the activation of its target genes ID4 and the chemokines CXCL1, CXCL5, CXCL8 and CXCL12 as well as MMP-13 and EGFR (75). Recently, p53 mutants have been involved in microRNA regulation. *Donzelli et al*. have shown that mutant p53R175H can induce the expression of miR-128-2 inducing chemoresistance in many cancers (94). It has been described that p53 mutants R175H, R273H and C135Y can downregulate the expression of miR-130b, which leads to upregulation of the transcriptional repressor ZEB1. This activates the ZEB1 signaling pathway which induces Epithelial-

Mesenchymal-Transition (EMT) (95). miR-155, which is upregulated in breast cancers, is activated by mutant p53 and promotes EMT through inhibition of genes such as ZNF652 (75). Moreover, mutant p53, recruited by ZEB1, binds the promoter region of miR-223, leading to mutant p53-mediated chemoresistance (96). The biological response to GOF p53 mutants was observed first in mouse tumor systems in which expression of a mutant p53 protein resulted in tumor formation (73). Using cell and animal model systems, expression of mutant p53 has been shown to result in oncogenic and proliferative processes (97) (increased tumorigenicity; increased growth in soft agar; decreased sensitivity to chemotherapeutic; increased resistance to γ-irradiation; accelerated chemical carcinogenesis; increased homologous recombination induced by ionizing radiation; destruction of the spindle check point activated topoisomerase I activity; increased DNA synthesis and increased growth rate; induction of gene amplification; cooperation with the TGF-β pathway; induction of cellular motility; invasive capability and metastasis; somatic cell reprogramming; increased tumor angiogenesis; promotion of chronic inflammation and associated cancer (75)**.** Several mouse models have been generated to test if the expression of p53 mutants in mice will induce GOF activity. For example, *Liu et al*. using a knock-in mouse line, demonstrated an increased metastatic potential in mice inheriting p53-R172H (homologous to human p53-R175H) (98, 99). Moreover, *Wang et al.* (100) showed some evidence of gain of function associated with genomic instability using a murine p53-R172H mutant transgenic model system. *Murphy et al.* (101) used the same mutant in a mammary epithelial murine cell model and find similar results. However, the most unequivocal demonstration of gain of function activity in mouse systems was shown when mutant p53 was stabilized by knockout of MDM2 or p16 (102). Being p53 mutated in more than 50 % of human cancers, restoration of p53 WT functions in cancers bearing mutant p53 represents a strategy for cancer therapy. In the era of translational cancer research, when the aim is to design specific therapy for each patient, the establishment of the characteristic

expression of gene such as p53 mutants is becoming of main importance. For this reason, many efforts have been made to establish differential signatures between normal and cancerous tissues and among the patients, in relation to various parameters altered in cancer, among which p53 (75)**.**

Human osteosarcoma cancer stem cells 3AB-OS

It is well known that solid tumors are organized hierarchically and that a distinct subpopulation of cells, named cancer stem cells (CSCs), is at the root of their growth and chemoresistance (103). It has been also demonstrated that CSCs are in the majority of tumors and in OS they seem to contribute to the initiation and development of the cancer (104). According to this, the research aimed at identifying the CSCs within the cancer cell population in order to identify specific therapies for tumor eradication. Recently, a human OS CSC line (3AB-OS) has been produced and isolated, for the first time, from the human osteosarcoma MG63 cell line by chemical treatment (105). In this regard, it has been shown that treating for a short time (24-72 h) MG63 cells with 3-aminobenzamide (3AB), a competitive inhibitor of poly (ADP-ribose) polymerase, their growth rate resulted markedly reduced and cells showed morphological features of osteocyte differentiation (106). Osteocyte differentiation was accompanied by a reprogramming of gene expression, with down-regulation of genes required for proliferation and up-regulation of those involved in osteoblastic differentiation. Studying the effects of the 3AB treatment for longer times (about 100 days) it was observed an increasing number of dead cells with a simultaneous and progressive enrichment of a new cell population, named 3AB-OS (107; Fig.10).

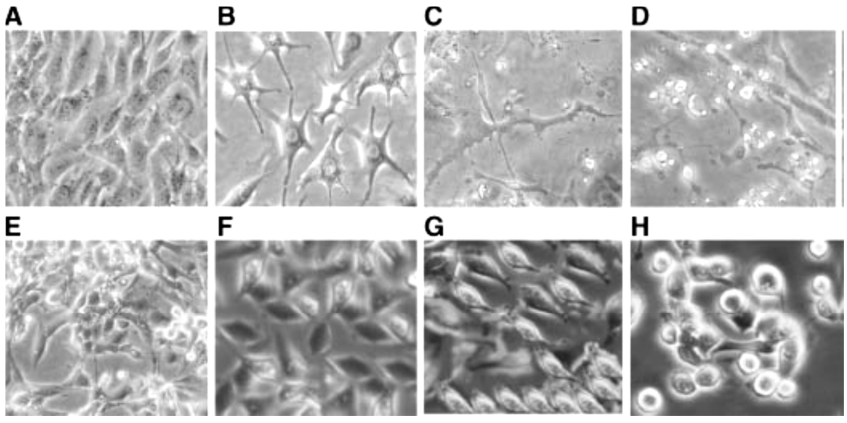

Fig.10. Production of 3AB-OS cells from human osteosarcoma MG-63 cells by prolonged 3AB treatment. The figure describes the morphology of MG-63 cells treated either with vehicle (control, A) or with 5mM3AB (B–H) analyzed by contrast phase microscopy as described in Materials and Methods and in Results Sections. Original magnification 200X.

The characterization of 3AB-OS cell population demonstrated that it is heterogeneous and stable. Moreover, after serial passages (currently, more than 200) in the absence of 3AB treatment this cells maintained their morphological and antigenic features. 3AB-OS cells showed the most important features of CSCs such as unlimited proliferative potential, ABCG2-dependent phenotype with high drug efflux capacity, strong expression of stemness and anti-apoptotic genes (105). Furthermore, they showed multi-lineage differentiation ability, favouring the mesenchymal lineage, with activation of myoblast differentiation and the appearance of muscle fibers in the tumor mass (108). Moreover, AB-OS CSCs showed a really good ability to growth in ultra-low attachment forming sarcospheres and they were be able to penetrate Matrigel with an invasion ability higher than MG63 parental cell of 2.6 fold genes (105). 3AB-OS cells showed a really high aggressive potential and when they were xenografted in athymic mice, in the presence of matrigel, they induced the formation of a great number of blood vessels (109). Overall, for the first time this provided a mouse model which recapitulate *in vivo* the key aspects of human osteosarcoma CSCs. During the multistep development of human tumors, the cells acquire a number of biological abilities such as unlimited proliferative signalling, evasion of growth suppressors, cell death resistance, replicative immortality, angiogenesis induction, invasion and metastasis activation. All these features are recognized as cancer hallmarks (110). The acquisition of these hallmarks results from genomic instability from which derives the genetic diversity that accelerates their acquisition. Recently, several studies suggested that tumor bioenergetics and CSCs might be related to each other (111, 112, 113, 114, 115). To characterize the energetic properties of 3AB-OS CSCs, their bioenergetics features were analyzed comparing them with the parental MG63 OS cells. Through these analyses it has been demonstrated that 3AB-OS cells depend on glycolytic metabolism more strongly than MG63 cells. Moreover, 3AB-OS cells show lower levels of mitochondrial respiration, are more sensitivity to glucose depletion or

glycolytic inhibitors and show a reduced sensitivity to inhibitors of oxidative phosphorylation. Furthermore, 3AB-OS have more fragmented mitochondria, respect to MG63 cells, which rapidly networked in the presence of glucose-rich medium. When they growth in low glucose conditions they completely lose these structures. Overall, the above findings suggested that the energy metabolism of 3AB-OS CSC strongly resemble that of normal stem cells and cancer cells, which are characterized by a glycolytic anaerobic metabolism (116). Cancer cells are characterized by multiple genetic/epigenetic changes that are responsible for chromosomal instability and tumor progression (117). Most of these changes consist in aberrations with loss or gain of gene function of many tumor suppressors. 3AB-OS cells have a large chromosomal complexity and molecular abnormalities characteristic of the most aggressive human cancers. Indeed, they have a hyper triploid karyotype and chromosome number ranging from 71 to 82, whereas MG63 cells have a hypotriploid karyotype and chromosome number ranging from 61 to 66. Moreover, 3AB-OS cells show monosomies, trisomies and nullisomies; they have 32 unidentifiable marker chromosomes and, compared with MG63, they have 49 copy number variations (gains/losses) affecting almost all the chromosomes (118). Intriguingly, the abnormalities evidenced in 3AB-OS cells are very similar to those described in a large number of pediatric and adult osteosarcomas, where karyotypes ranging from haploid to near hexaploid have been shown (119, 120, 121). Moreover, 3AB-OS cells showed losses/gains in agreement with those seen in osteosarcoma patients (119, 120, 121). By microarray analysis, where 3AB-OS cells have been compared with MG63 cells, the gene expression profile of 3AB-OS cells was studied. Employing KEGG and BioCarta analysis, 196 genes which resulted up-/down-regulated and which appeared to be involved in regulatory pathways of tumorigenesis and stemness (ECM-receptor interaction and cell communication; cell adhesion molecules; ABC transporters in general; Notch and Hedgehog signalling; MAPK signalling; cell cycle regulators; apoptosis) have been selected. Most of these genes have been reported in

osteosarcoma patients (122). Moreover, by human MicroRNA array analysis it was possible to identify 189 differentially expressed miRNAs and the analysis of mRNA/miRNA expression profiles appeared to be very similar to those reported in human OS patients (123, 124). Furthermore, to define a surface protein signature specific for 3AB-OS CSCs and MG63 cells, a cytometric analysis has been performed using an antibody-array consist in 245 membrane proteins. It has been also selected MAPK/ERK1/2 as a potential protein kinase-pathway correlated with pathways that characterize tumorigenesis and stemness of 3AB-OS cells (125) More than half of all cancers exhibit mutation at p53 locus on the short arm of chromosome I7 at I7p13 (126). Wild-type human p53 transcriptionally targets a large number of genes which mediates cell cycle arrest, DNA repair, senescence, apoptosis, and various metabolic processes. The loss of p53 function has been usually associated with an impairment of these functions (127). TP53 missense mutations represent the majority of cancer-associated mutations which lead to the expression of a full-length altered p53 protein which, in contrast to wild-type p53, has a prolonged half-life. These missense mutations even determine oncogenic or gain-of-function activity (128, 129). Recently (130), TP53 gene status/role in 3AB-OS CSC line has been studied and it has been shown that it is involved in promoting proliferation, invasiveness, resistance to apoptosis and stemness. In particular, it has been shown that, in comparison with parental MG63 cells (where TP53 gene is hyper methylated, rearranged and in single copy), 3AB-OS cells have TP53 gene unmethylated, rearranged and in multiple copies. Moreover, mutp53 (p53-R248W/P72R) is post-translationally stabilized and with nuclear localization. Interestingly, p53-R248W/P72R-knockdown by short-interfering RNA, reduced the growth and replication rate of 3AB-OS cells, markedly increasing cell cycle inhibitor levels and sensitizing 3AB-OS cells to TRAIL-induced apoptosis. Furthermore, the knockdown strongly decreased the levels of stemness and invasiveness genes. Recently, in 3AB-OS CSCs it has been described a predictive network for

let-7/98 and miR-29a, b, c, (two deeply down regulated miRNA family) and MSTN, CCND2, Lin28B, MEST, HMGA2, GHR (their anti-correlated and highly up regulated mRNAs). These miRNAs/mRNAs may represent new biomarkers for OS and could permit the identification of new potential therapeutic targets (118). These miRNAs will be overexpressed in 3AB-OS cells in order to study their effects on 3AB-OS stemness and behaviour. Moreover, it has been hypothesized that p53 mutation could be the “driver mutation” at the root of the dedifferentiation of MG63 cells into 3AB-OS CSCs (130). This PhD research project has been developed in order to demonstrated this hypothesis.

PROJECT AIM

During the last ten years the existence of cancer stem cells has been discussed. Numerous studies suggest that these cells have an important role in the development and maintenance of the tumor (42) The actual theory suggests that tumors consist of subsets of cells with functional heterogeneity among which there is a subset of cells with stem features (131) Therefore, the tumor can be imagined as a real organ where the various cells have very specific tasks and roles in the organization of the life of the tumor. The existence of cancer stem cells has been well supported by numerous studies and has been shown that they are resistant to cancer therapies causing the tumor recurrence (132).The understanding of the mechanisms at the roots of the growth, survival and expansion of cancer stem cells is crucial to detect specific treatments for tumor eradication. This PhD project has been developed at the University of Palermo, in the laboratories of the Section of Biochemistry, Polyclinic, of the DPT STEBICEF, coordinated by Prof. Renza Vento and in part in the laboratories of the Biothec Research and Innovation Centre (BRIC) at the University of Copenhagen directed by Professor Anders Lund. Professor Vento's research groups has produced a great number of paper on the study of the activation of apoptosis pathways after the treatments with several drugs in order to find specific targets for anti-tumor therapies. During the last years one of the lines of research developed in these laboratories concerned the study of the molecular mechanisms that might be at the origin of the cancer stem cell. Professor Lund's group has a great expertise in biomolecular biological studies focused on the analyses of genetic and epigenetic mechanisms in both tumor and normal cells line. My PhD research project is part of a more complex project on the 3AB-OS cancer stem cell line, coordinated by Professor Vento. Her research group, employing the osteosarcoma MG63 cells, has produced by chemical treatment a novel cell line which has been termed "3AB-OS" and which has been

patented (F12008A000238, Florence, 11/12/2008, Renza Vento, Riccardo Di Fiore). 3AB-OS cells show various features of cancer stem cells, including unlimited proliferative potential and expression of genes required for maintaining stem cell state (CD133, Oct3/4, hTERT, nucleostemin, Nanog) and for inhibiting apoptosis (HIF-1alpha, FLIP-L, Bcl-2, XIAP, IAPs and survivin). Moreover, 3AB-OS cells efficiently transdifferentiate, in vitro, into cells of all three primary germ layers (ectoderm, endoderm and mesoderm) and when injected into athimic mice, they recapitulate *in vivo* various features of human osteosarcoma. Thus, 3AB-OS cells can represent a useful model system to test *in vivo* novel antitumor approaches against human osteosarcoma. The research group has even genetically e molecularly characterized 3AB-OS cells. Overall, it has been suggested that 3AB-OS cells should represent an invaluable tool for studying the molecular mechanisms underlying osteosarcoma origin and stemness. Moreover, it has been shown that the energy metabolism of 3AB-OS CSCs strongly resemble that of normal stem cells and cancer cells, which are characterized by a glycolytic anaerobic metabolism (116). 3AB-OS cells have a large chromosomal complexity and molecular abnormalities characteristic of the most aggressive human cancers (118).

My participation in the research on 3AB-OS CSCs started when it has been showed that these cells contain a mutant p53 protein which could be responsible for their stemness properties. In particular, it has been shown that, compared with parental MG63 cells, where TP53 is not expressed and in single copy, 3AB-OS cells strongly express a mutp53 protein whose TP53 gene is rearranged and in multiple copies characterized by P72R polymorphism and hot spot mutation R248W. In addition, mp53 is stabilized by post-translational modifications (phosphorylation at Ser15 and acetylation at Lys 320, Lys 373-382). Depletion of mp53 by small-interfering-RNA induced a decrease in cell proliferation and migration accompanied by apoptosis resistance and by the coherent expression of genes controlling cell cycle, apoptosis and invasiveness. Moreover, mp53 knockdown affected the expression of

pluripotent markers as Oct3/4, Nanog, Sox2 and Nucleostemin, suggesting that it might affect pluripotency potential of 3AB-OS cells. Overall, the results suggested an oncogenic role of mp53 and its contribution to stemness and chemoresistance characteristics of 3AB-OS. The hypothesis was that p53-R248W/P72R could be at the root of the dedifferentiation of MG63 into 3AB-OS CSCs (130).

My PhD research project aimed to elucidate the molecular mechanisms underlying gain of function of this mutant p53 and to evaluate its potential contribution in maintenance of stemness properties of 3AB-OS cells.

RESULTS

Study of gain of function of p53-R248W/P72R in 3AB-OS cells

In order to evaluate whether, in 3AB-OS cells, p53-R248W/P72R has acquired GOF activities such as enhanced cell proliferation, invasiveness and resistance to apoptosis, we have determined the knockdown of the protein by small interfering RNA (siRNA) , transfecting 3AB-OS cells with either a p53-siRNA and a scramble siRNA (Scr-siRNA). First, we checked the efficiency of p53 silencing effects evaluating the changes on endogenous p53 levels. At 24–72 h after transfection, the content of the protein was assessed by western blot (Fig. 1A) and immunofluorescence (Fig. 1B) analyses. Both the analyses showed that p53-R248W/P72R levels potently lowered by p53-siRNA transfection. The lowering was already well evident at 24h after transfection where more than 35% decrease was observed. Then, it was maximal at 48h when more than 70% decrease in the level of the protein was evidenced. Thereafter, p53-R248W/P72R levels markedly went up, so that at 72 h after transfection, only a 22% decrease was observed. This suggested that, at that time, the transient silencing was in rapid recovery. Overall, the results suggested that the optimal silencing efficiency was reached at 48h after transfection. The knockdown of the protein was specific as no protein decrease was observed in cells transfected with Scr-siRNA.

A B

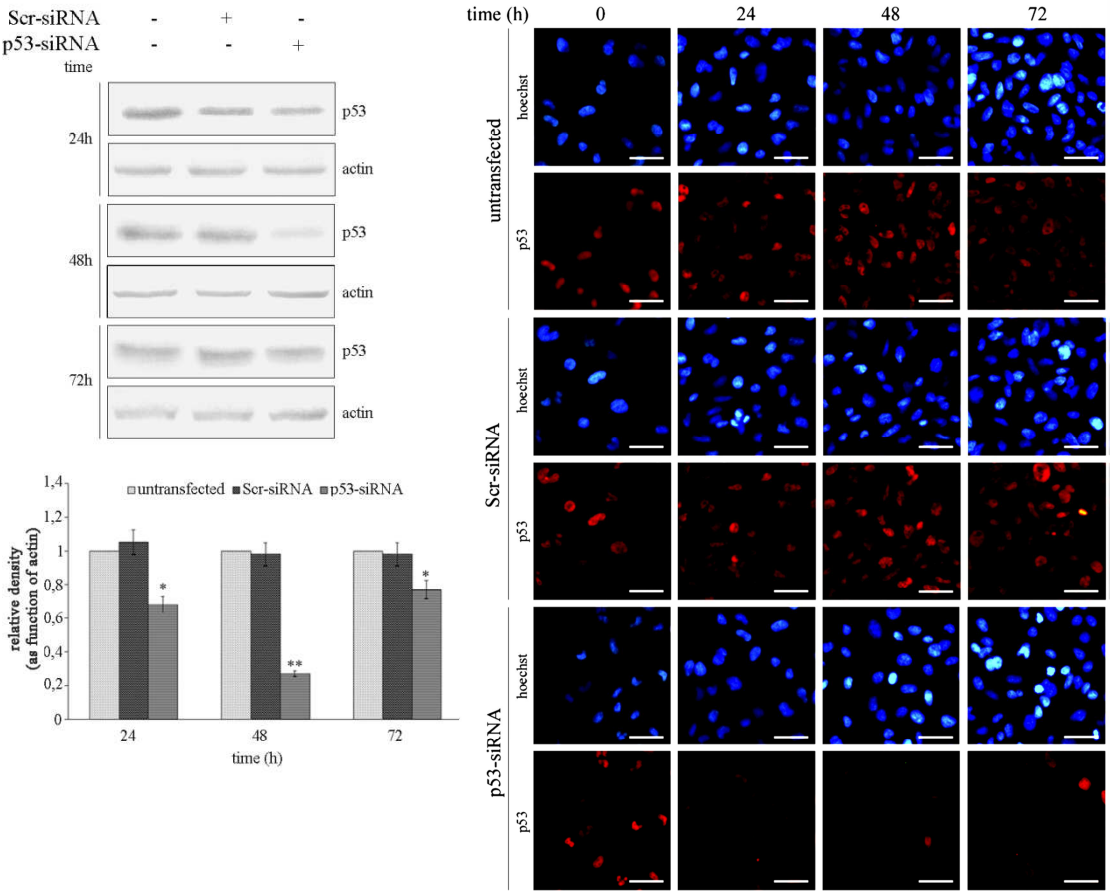

Fig. 1. Evaluation of knockdown efficiency of p53-R248W/P72R. 3AB-OS cells were transfected with scrambled siRNA (Scr-siRNA) or p53-siRNA and analyzed at 24–72 h after transfection. (A) Western blot analysis of p53-R248W/P72R and densitometric analysis of protein bands. Data (relative density normalized to actin) represent the mean with standard deviation (n = 4); *P b 0.05 and **P b 0.01 as compared to Scr-siRNA-transfected cells. (B) Immunofluorescence analysis by double staining cells with both Hoechst33342 dye (blue), to localize the nuclei, and anti-p53 antibody and Cy3-conjugated secondary antibody (red), to localize p53. The scale bar represents 25 μm. Images are representative of four independent experiments

p53-R248W/P72R-knockdown affects 3AB-OS cell proliferation rate

To evaluate whether p53-R248W/P72R-knockdown modified the growth of 3AB-OS cells, untransfected cells and cells transfected with Scr-siRNA or with p53-siRNA were microscopically observed and analysed (0–72 h) for cell number, percentage of cells in the S-phase of cell cycle (EdU incorporation) and percentage of viability. As Fig. 2A shows, in 3AB-OS silenced for p53-R248W/P72R, in comparison to untransfected or Scr-siRNA-transfected cells, cell number lowered. Fig. 2B also shows that p53-R248W/P72R silencing reduced the growth rate and the replication rate of 3ABOS cells, whereas the cell viability had

not been affected. The speed of cell growth and replication reflected the trend of p53-R248W/P72Rknockdown.

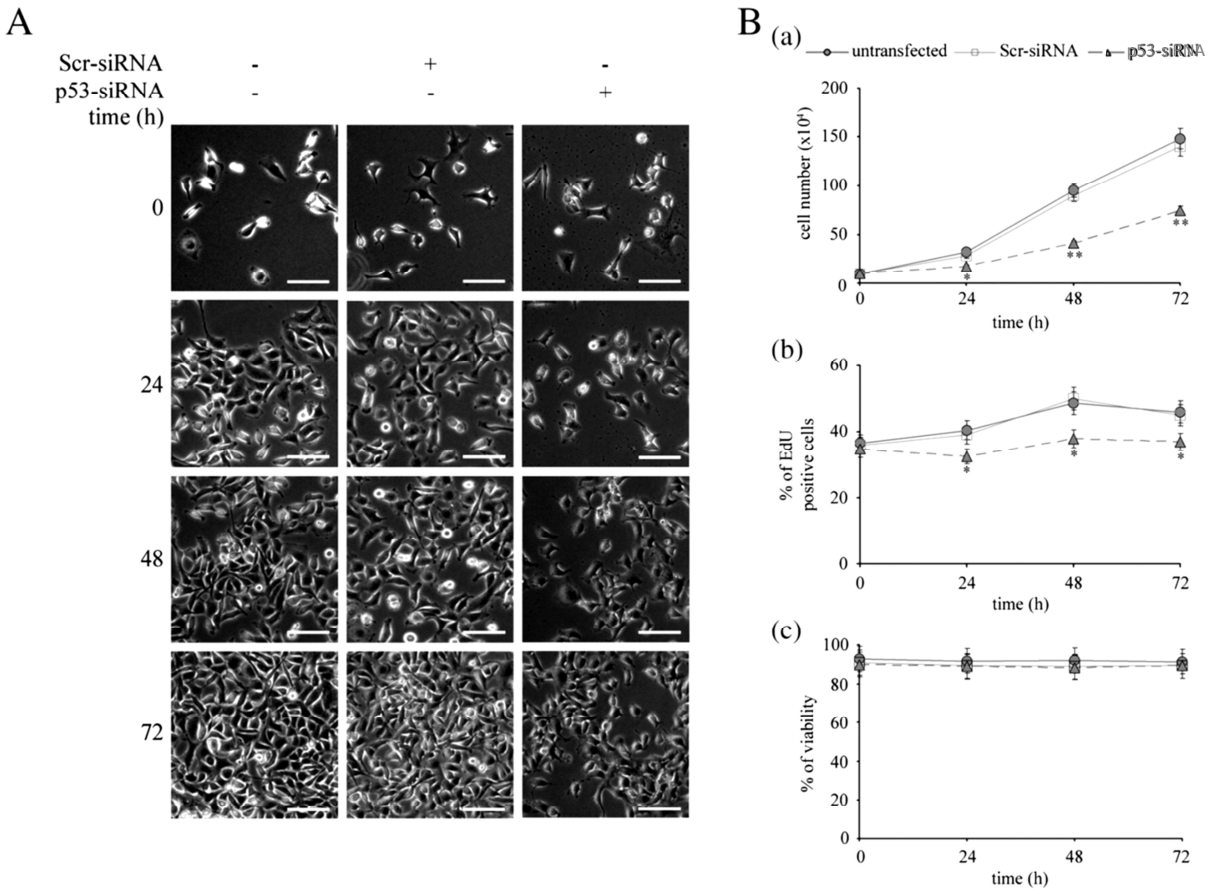

Fig.2. Effect of p53-R248W/P72R-knockdown on growth advantage of 3AB-OS cells. (A) Inverted phase contrast microscopy at 0–72 h after transfection. The scale bar represents 100 μm.Images are representative of four independent experiments. (B) Analysis of total cell number (a), percentage of cells in the S-phase of cell cycle (b) by EdU incorporation and percentage of cell viability (c). The data represent the mean with standard deviation (n = 4); *P < 0.05 and **P < 0.01 as compared to Scr-siRNA-transfected cells

Next, we examined the expression of several cell cycle-related proteins and genes at 48 h post transfection. In Fig. 3, western blot and real-time PCR analyses showed that the p53-R248W/P72R-knockdown markedly increased the levels of pRb, p130, p107, E2F1, E2F4, GADD45, p21 and p27,whereas it potently decreased CDK4 levels. No alteration in the expression of cyclins and other CDKs was observed.

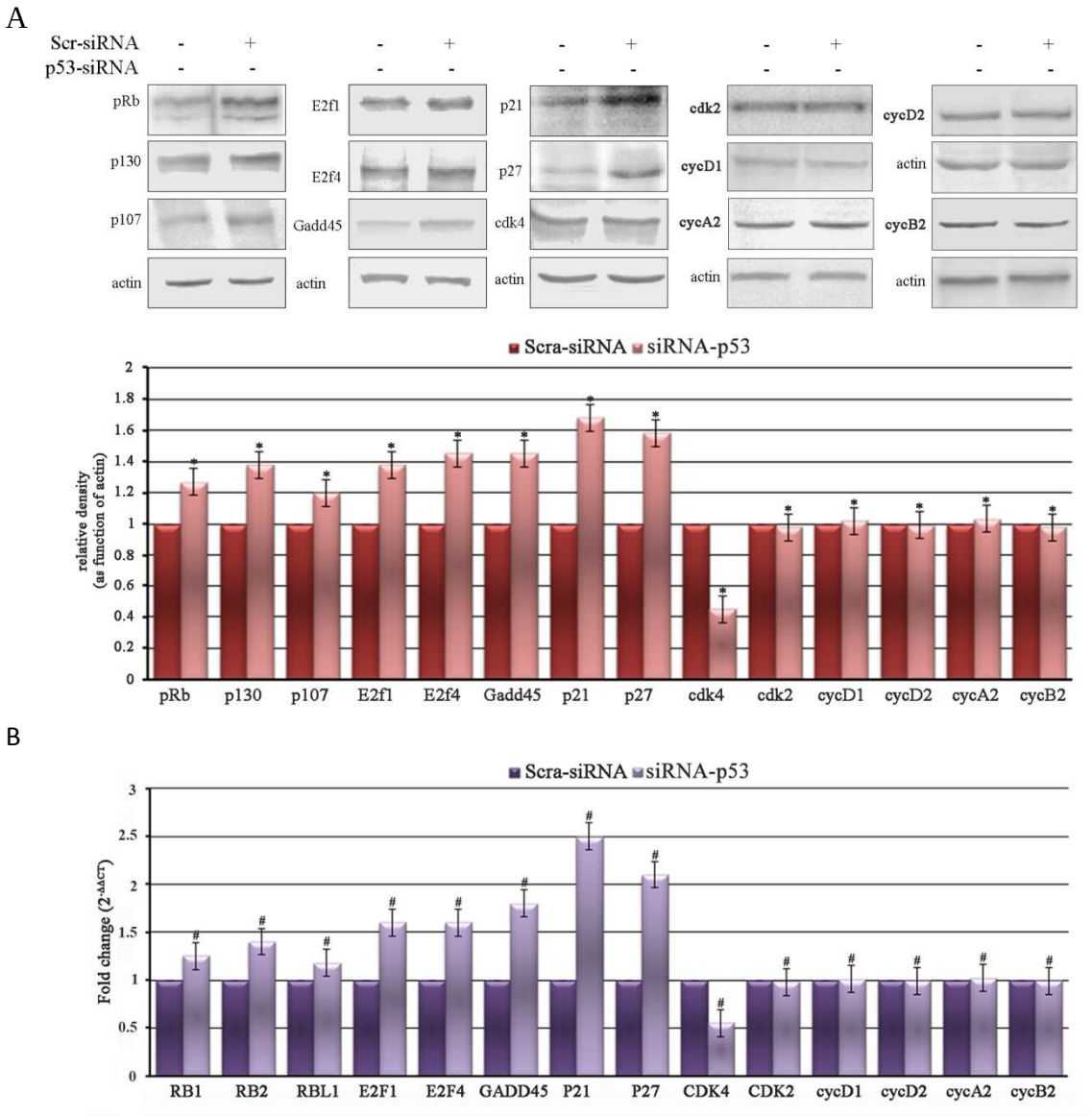

Fig.3. Analyses of cell-cycle regulators at 48 h after silencing. (A) Western blot analysis and quantification of protein bands by densitometric analysis; data (relative density normalized to actin) represent the mean with standard deviation (n = 4); *P < 0.05 as compared to Scr-siRNA-transfected cells. (B). Real-time PCR. Data (fold change) represent the mean with standard deviation (n = 4); #P < 0.005 as compared to Scr-siRNA-transfected cells.

p53-R248W/P72R-knockdown increases 3AB-OS sensitivity to apoptotic events.

Previous analyses demonstrated that 3AB-OS cells express low levels of the death receptors FAS and DR4 (118) and show strong resistance to TRAIL (TNF-related apoptosis inducing ligand). Here, we evaluated whether the p53-R248W/P72R-knockdown modifies the expression levels of DR4 (TRAIL-R1), KILLER/DR5 (TRAIL-R2) and FAS/CD95. In Fig. 4, western blot analyses show that at 48 h post-transfection p53-R248W/P72R knockdown

increased protein expression levels of DR4 and DR5, whereas no significant changes in FAS levels were observed. In order to evaluate TRAIL sensitivity, untransfected cells and cells transfected for 24h with Scr-siRNA or p53-siRNA were treated with TRAIL (40 ng/ml) for 36h.

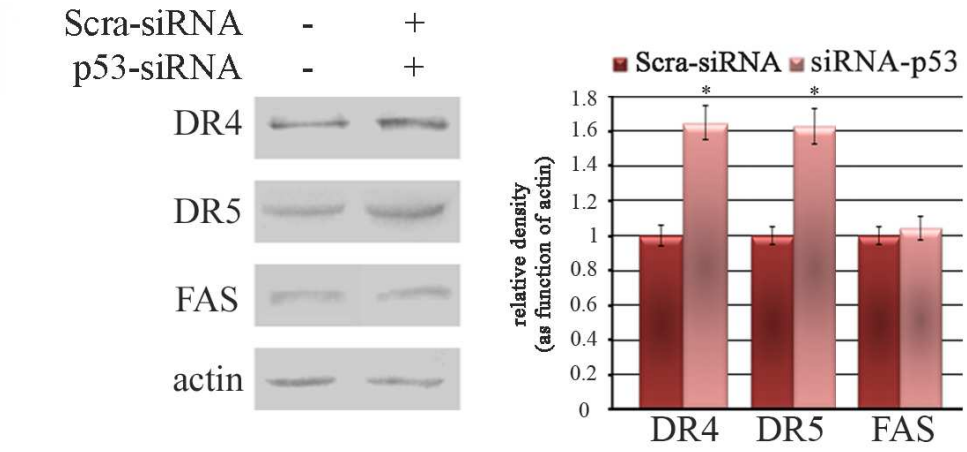

Fig. 4. Effect of p53-R248W/P72R-knockdown on DR4, DR5 and FAS receptors. Western blot analysis of DR4, DR5 and FAS receptors at 48 h after transfection and quantification of protein bands by densitometric analysis. Data (relative density normalized to actin) represent the mean with standard deviation (n = 4); *P < 0.005 as compared to ScrsiRNA-transfected cells.

In Fig. 5A, phase contrast microscopy shows that TRAIL markedly reduced cell number also inducing apoptosis in p53-silenced cells, as suggested by the presence of round-shaped cells floating in the medium, membrane blebbing and apoptotic body formation. Apoptosis was analyzed by staining nucleic acid with Hoechst 33342 to check chromatin condensation and nuclear fragmentation. As shown Fig. 5A, in p53-siRNA transfected cells, TRAIL induced typical apoptotic nuclei, exhibiting highly fluorescent condensed and fragmented chromatin. Apoptosis was also studied by flow cytometry of either DNA content (5B) or annexin V labelling (5C). The treatment with TRAIL resulted in 29% of cells accumulated in sub-G0–G1 phase with a 20% of early apoptotic cells (annexin V+/PI−) in p53-siRNA-transfected cells. The effects of TRAIL in both untransfected and Scr-siRNA transfected cells were much less conspicuous than in p53-siRNA-transfected cells. Collectively, these results demonstrate that p53-R248W/P72R knockdown sensitizes 3AB-OS cells to TRAIL induced apoptosis.

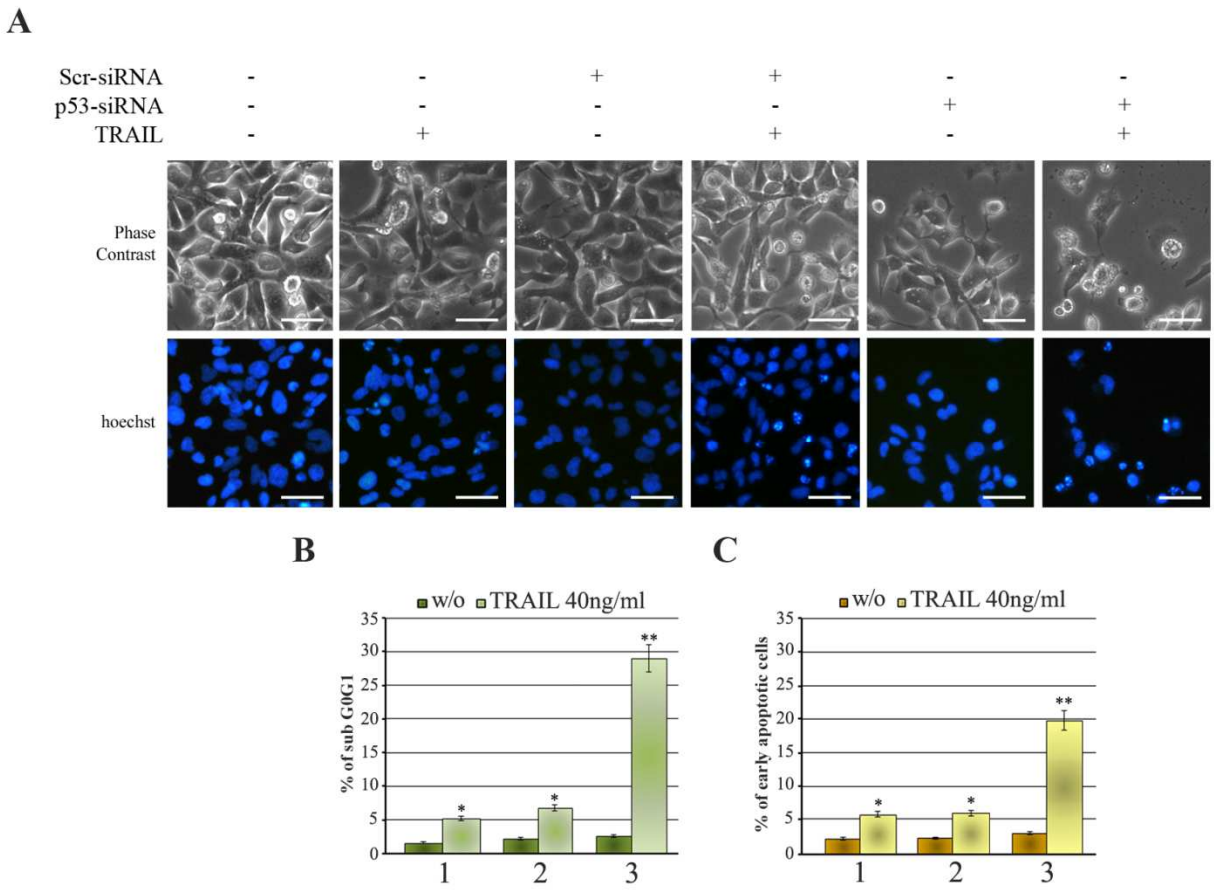

Fig.5. Effect of p53-R248W/P72R-knockdown on TRAIL-induced apoptosis. (A) Analysis of TRAIL-induced apoptosis by inverted phase contrast microscopy (upper panels) and fluorescence microscopy (Hoechst 33342 staining, bottom panels). The scale bar represents 25 μm. Images are representative of four independent experiments. (B) Percentages of cells in sub-G0–G1 phase evaluated by flow cytometric analysis of propidium iodide DNA staining, and percentages of early apoptotic cells (C) measured by flow cytometric analysis of annexin V labelling after TRAIL treatment (1, untransfected cells; 2, cells transfected with Scr-siRNA; 3, cells transfected with p53-siRNA). The data represent the mean with standard deviation (n = 4). *P < 0.05 and **P < 0.01 as compared to untreated cells.

It was also investigated, by cytofluorimetric analysis, if p53-R248W/P72R can attenuate mitochondrial apoptosis signalling pathways. DiOC6 staining revealed that the p53-R248W/P72R knockdown induced a significant decrease in fluorochrome uptake, indicating a loss of mitochondrial membrane potential $\Delta\psi m$ (Fig. 6A). To evaluate the mechanism involved, the expression levels of both anti-apoptotic (Bcl-2 and Bcl-XL) and pro-apoptotic (Bax and Puma) factors in p53-siRNA-transfected and Scr-siRNA transfected 3AB-OS cells were also investigated. In Figs. 6B and 6C, real-time PCR and western blot analyses showed that the p53-R248W/P72R knockdown significantly decreased Bcl-2 and Bcl-XL levels while

it increased Bax and Puma levels. These results well agreed with those obtained by cytofluorimetric analysis.

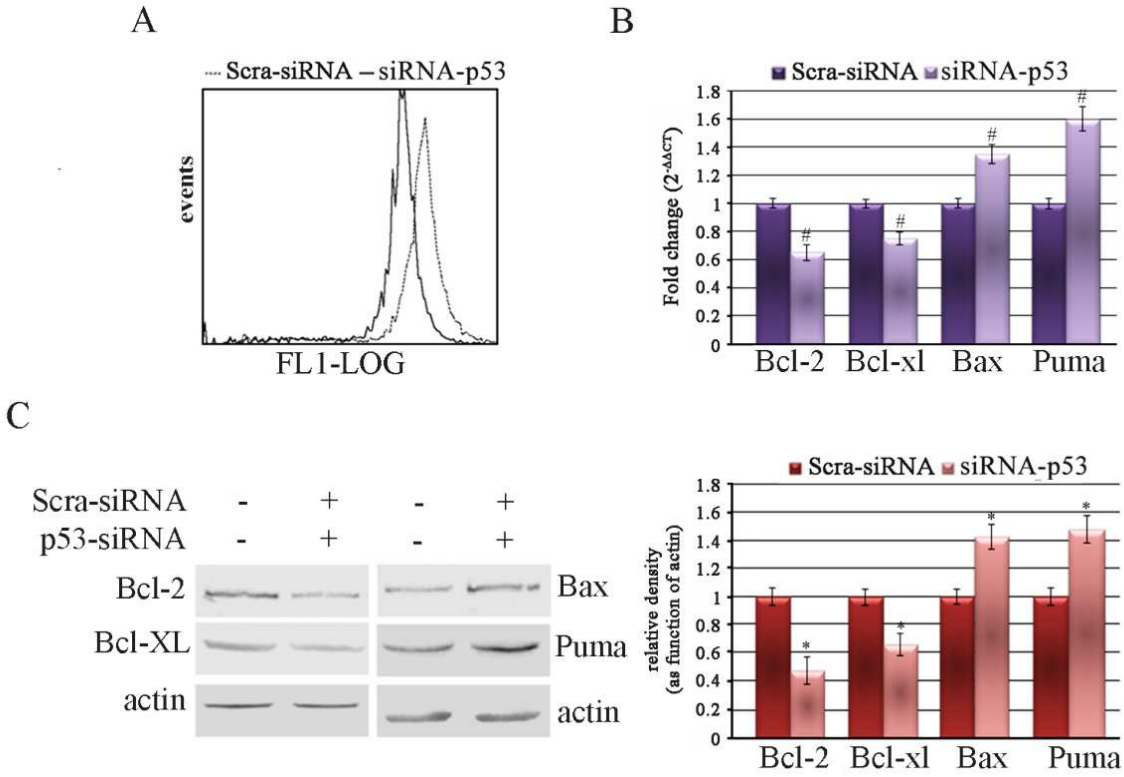

Fig.6. Effect of p53-R248W/P72R-knockdown on mitochondrial membrane potential and Bcl-2 familymembers (A) Citofluorimetric analysis by DiOC6 staining of mitochondrial membrane potential (Δψm). The decrease of fluorescence intensity indicates loss of Δψm. (B) Real-time PCR analysis of Bcl-2 family mRNAs at 48 h after transfection. Data represent the mean with standard deviation (n = 4); #P b 0.005 as compared to Scr-siRNA-transfected cells. (C) Western blot analysis of Bcl-2 family proteins at 48 h after transfection and quantification of protein bands by densitometric analysis. Data (relative density normalized to actin) represent the mean with standard deviation (n = 4); *P b 0.05 as compared to Scr-siRNA-transfected cells.

p53-R248W/P72R promotes cell invasiveness

To evaluate whether p53-R248W/P72R-knockdown influences 3ABOS cells invasiveness, Matrigel invasion trans-well assays were performed. As shown in figure 8, p53-siRNA transfection determined a potent decrease (−80%) of the invasive ability of 3AB-OS cells, whereas no statistically significant difference was observed in untransfected and Scr-siRNA transfected cells.

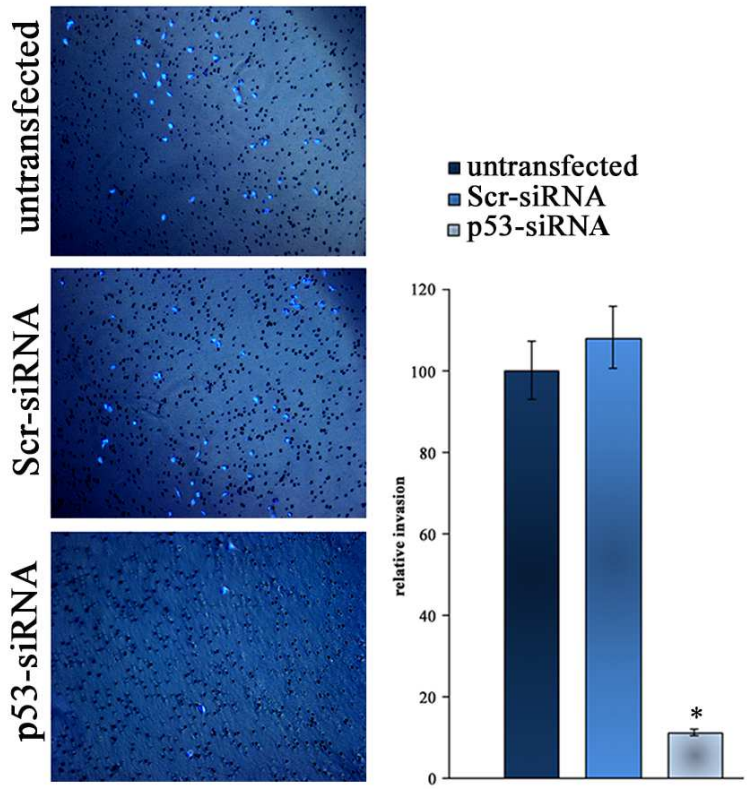

Fig.8. Effect of p53-R248W/P72R-knockdown on invasive properties of 3AB-OS cells. In vitro invasive capacity of untransfected cells and cells transfected with Scr-siRNA or p53-siRNA through the Matrigel-transwell membranes after 48 h of incubation. Fluorescence microscope imagines (left panel); data graphed (right panel) with the mean of the relative invasion ability of cells, normalized respect to the untransfected cells (standard deviation n = 4; *P < 0.05).

It was also examined the expression of a number of invasiveness related genes and proteins at 48 h post-transfection. In Figs. 9A and 9B, real-time PCR and western blot analyses showed that after the knockdown of p53-R248W/P72R the levels of matrix metalloproteinases 2 and 9 (MMP2 and MMP9), integrin alfa5 (ITGα5) and integrin alfaV (ITGαV) decreased, while the levels of the cell adhesion protein E-Cadherin increased. No alterations in the expression of proteins involved in mesenchymal phenotype (N-cadherin, β-catenin and vimentin) were observed.

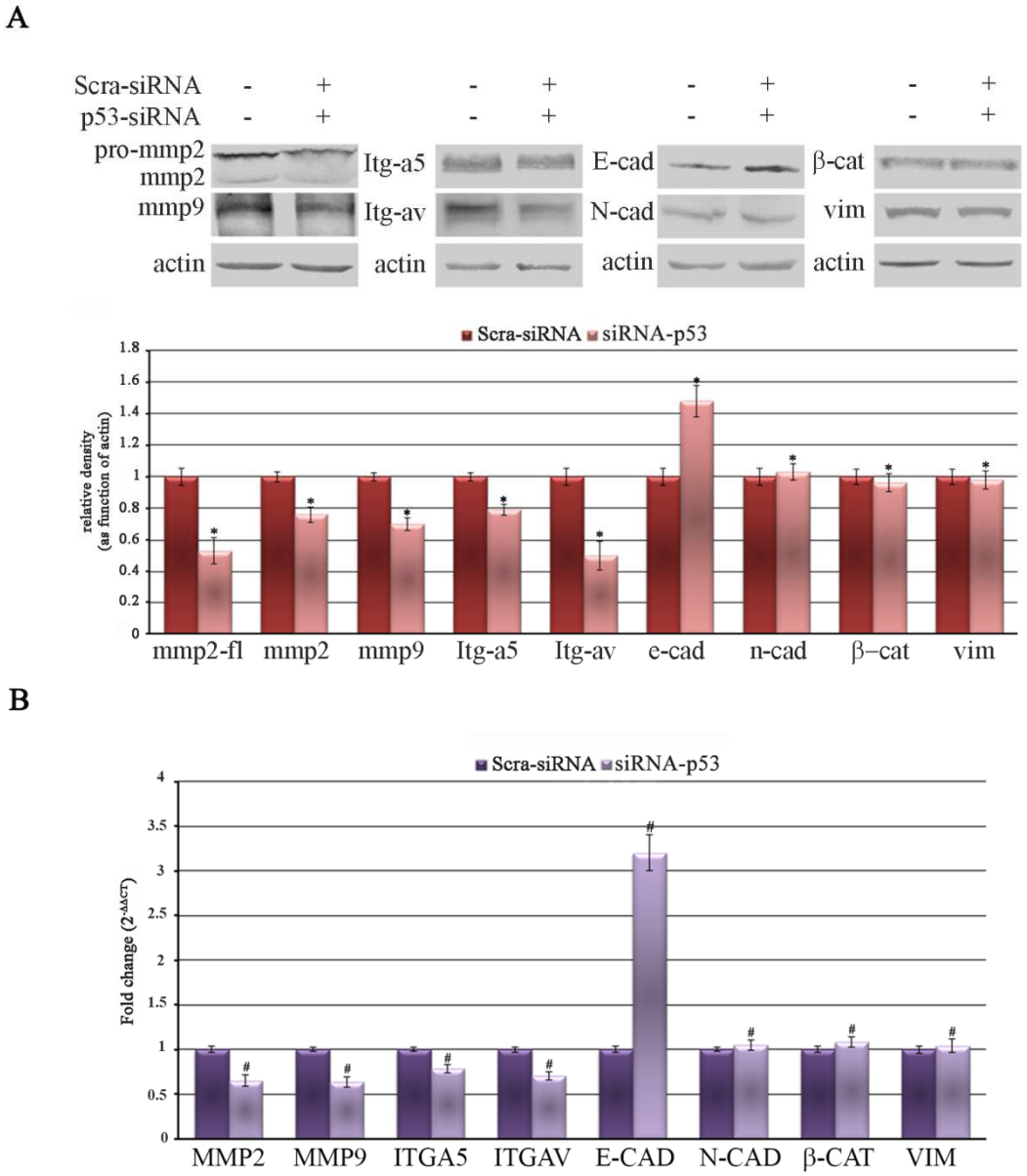

Fig.9. Effect of p53-R248W/P72R-knockdown on invasive properties of 3AB-OS cells. (A) Western blot analysis of both cell invasion and epithelial-mesenchymal-transition-related proteins at 48 h after transfection; quantification of protein bands by densitometric analysis. Data (relative density normalized to actin) represent the mean with standard deviation (n = 4); *P b 0.05 as compared to Scr-siRNA-transfected cells. (B) Real-time PCR analysis of both cell invasion and epithelial-mesenchymal-transition-related genes at 48 h after transfection. Data are the mean with standard deviation (n = 4); #P b 0.005 as compared to Scr-siRNA-transfected cells.

p53-R248W/P72R-knockdown affects the expression of stem-cell markers

Previously, it has been shown that 3AB-OS cells express a large number of genes required for maintaining stemness (105) and that they morphologically and functionally transdifferentiate in vitro into cells of all three primary germ layers (ectoderm, endoderm and mesoderm) (108).

Moreover, stemness markers were profoundly downregulated in differentiated cells. Here, fig.10 shows that undifferentiated 3AB-OS cells strongly expressed p53-R248W/P72R while it profoundly lowered in derived cell lineages.

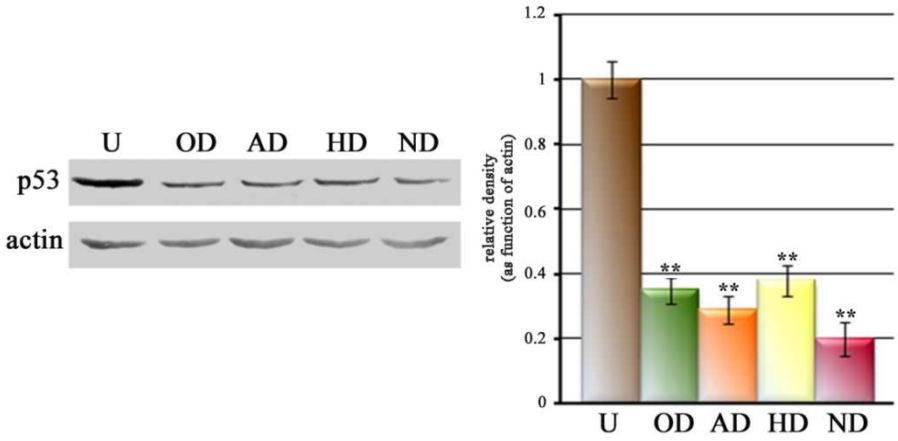

Fig. 10. Effect of p53-R248W/P72R-knockdown on various stem-cell markers in 3AB-OS cells. Western blot analysis of p53-R248W/P72R in undifferentiated (U) and differentiated 3AB-OS cells and quantification of protein bands by densitometric analysis. Data (relative density normalized to actin) represent the mean with standard deviation (n = 4);**P b 0.01 as compared to undifferentiated cells. Abbreviations: OD, osteogenic differentiation; AD, adipogenic differentiation; HD, hepatogenic differentiation; ND, neurogenic differentiation.

It was also investigated whether the knockdown of p53-R248W/P72R affected the expression of the most important stemness markers, such as Oct3/4, Nanog, Sox2, nucleostemin (ns) and CD133 that exhibited very high levels in untransfected 3ABOS cells. In Figs. 11A and 11B, western blot and real-time PCR analyses showed that in p53-R248W/P72R knockdown cells the levels of all the analyzed pluripotency markers potently decreased.

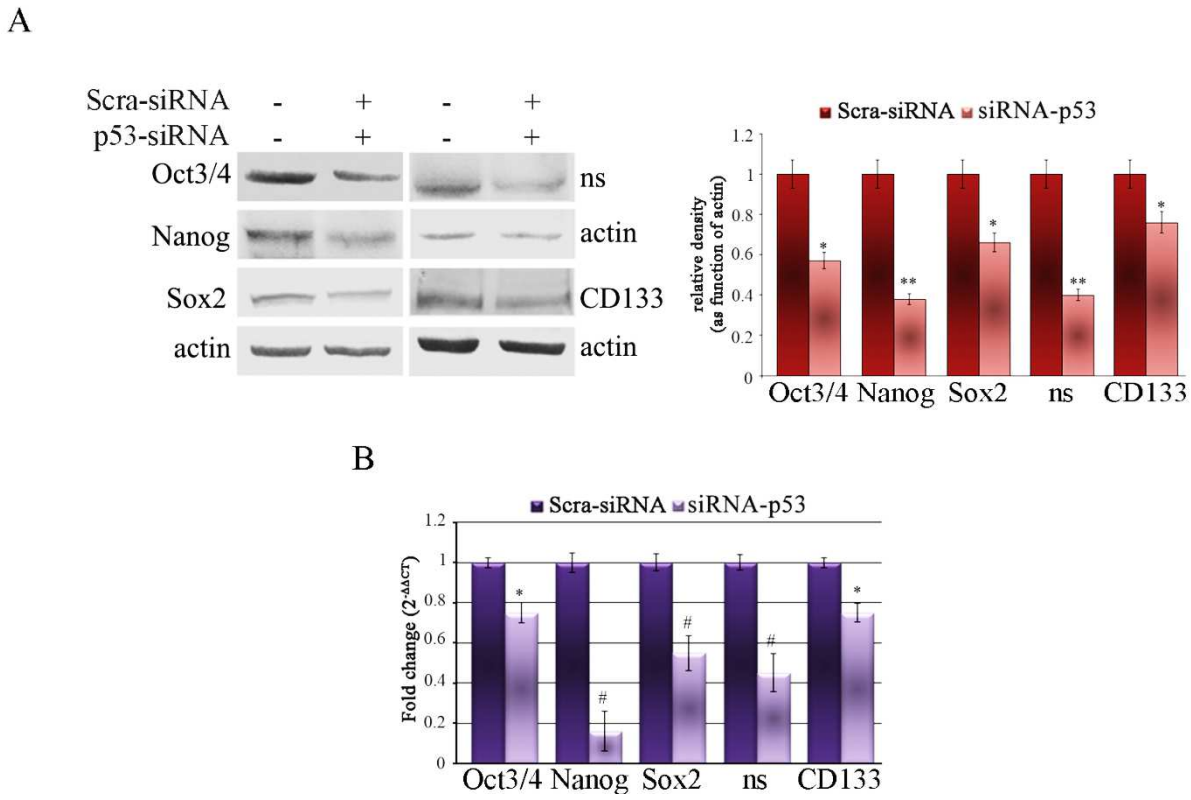

Fig. 11. Effect of p53-R248W/P72R-knockdown on various stem-cell markers in 3AB-OS cells. (A) Western blot analysis of stemness proteins at 48 h after transfection and quantification of protein bands by densitometric analysis. The data (relative density normalized to actin) represent the mean with standard deviation (n = 4);*P < 0.05 and **P < 0.01 as compared to Scr-siRNA-transfected cells. (B) Real-time PCR analysis of stemness genes at 48 h after transfection. Data represent the mean with standard deviation (n = 4); *P < 0.05 and $^{\#}$P < 0.005 as compared to Scr-siRNA-transfected cells.

Transient ectopic expression of p53-R248W/P72R in osteosarcoma MG63 cells.

The above-described findings suggested that the GOF property of p53-R248W/P72R could be at the root of 3AB-OS stemness. To evaluate this hypothesis, the effects of transient ectopic expression of P53-R248W/P72R were analyzed. MG63 cells were transfected with a pcDNA3.1 empty vector VECTOR) and with a pcDNA3.1 vector containing p53-R248W/P72R (R248W/P72R). First, it was evaluated p53-R248W/P72R protein expression and localization in both cellular lines by western blot, flowcytometry and immunofluorescence analyses (130). Figure. 12A shows that, as expected, p53 protein was not detectable in vector cells, while it was expressed in R248W/P72R cells. This was confirmed by a strong positivity for p53 (>75%) in R248W/P72R cells analyzed by cytometry (Fig.

12B). Moreover, p53 protein in R248W/P72R cells has a nuclear localization (Fig. 12C) like in 3AB-OS cells.

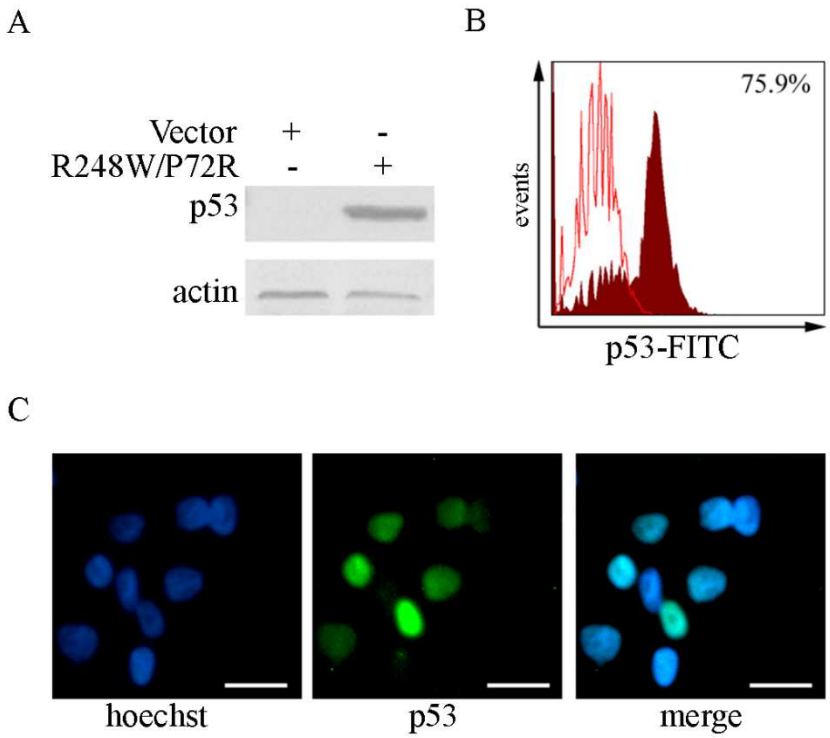

Fig.12. Transient ectopic expression of p53-R248W/P72R in osteosarcomaMG63 cells. (A) Western blot analysis of p53 in MG63 cells transfected with either pcDNA3.1-p53-R248W/P72R (R248W/P72R) or empty pcDNA3.1 vector (VECTOR). The images are representative of four independent experiments. (B) Cytometric analysis for p53 in R248W/P72R cells. The open histogram indicates isotype control, filled histogram, indicates the expression of p53. The images are representative of four independent experiments. (C) Immunofluorescence analysis of p53 in R248W/P72R cells, by double staining cells with both Hoechst 33342 dye (blue, left panel) to localize the nucleus and anti-p53 antibody and Cy2-conjugated secondary antibody (green, middle panel) to localize p53. In the right panel the merge of the two dyes is shown. The scale bar represents 25 μm. Images are representative of four independent experiments.

Thereafter, it was evaluated whether p53-R248W/P72R expression in MG63 cells promoted cancer stem-like features, as high proliferation rate, spheres formation, clonogenic growth, high migration and invasive ability. First, I compared R248W/P72R and VECTOR cells growth. As shown in Fig. 13A, R248W/P72R cells possess a higher proliferative output then VECTOR cells, exhibiting a doubling time of approximately 25 h, whereas vector cells show a doubling time of 33 h. This result was confirmed by cell cycle analyses performed by

cytometry and showing that R248W/P72R cells were confined mostly in the S-G2\M phase, while VECTOR cells were predominantly in G0\G1 (Fig. 13B).

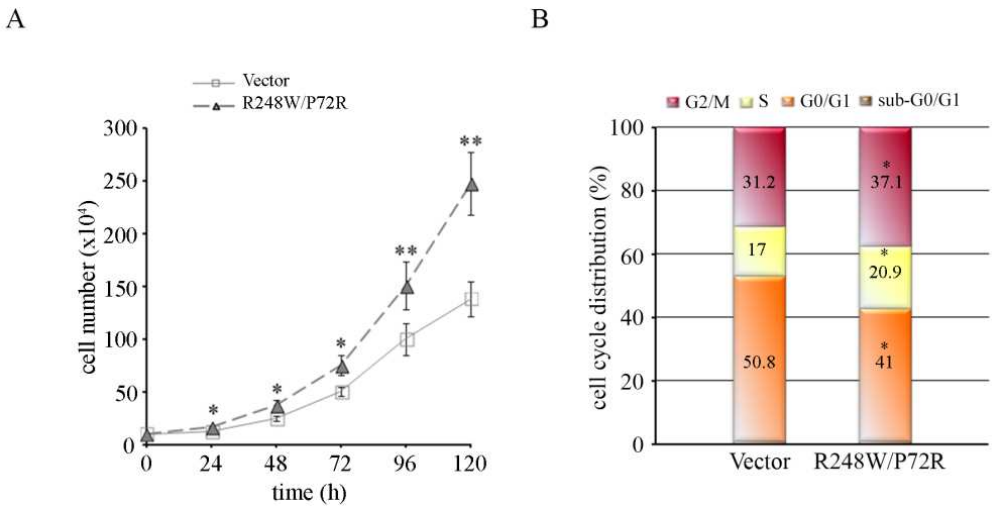

Fig.13. Transient ectopic expression of p53-R248W/P72R in osteosarcomaMG63 cells and its effect on cell proliferation. (A) Growth curves of VECTOR and R248W/P72R cells. The data represent the mean with standard deviation (n = 4); *P < 0.05 and **P < 0.01 as compared to vector cells. (B) Cell cycle distributions in VECTOR and R248W/P72R cells determined using flow cytometry. Results are indicated as relative percentage of total cell cycle (*P < 0.05, as compared to VECTOR cells).

It has been reported that cancer stem-like cells are able to form spheroid-like bodies under serum-free medium with bFGF and EGF (132) For this reason, sarcosphere forming ability of R248W/P72R cells compared to VECTOR cells was tested. Fig. 14 (A and B) shows that both vector and R248W/P72R cells were able to form sarcospheres. In particular, 5 days post seeding, vector cells formed sarcospheres with a mean diameter of 60.2 ± 5.7 μm and a frequency of approximately 1/54 (9.3 ± 1.5 spheres/500 cells), while R248W/P72R cells formed larger sarcospheres (mean diameter of 68.7 ± 7.6 μm) with a frequency of approximately 1/42 (12 ± 2.0 spheres/500 cells). After 10 days, R248W/P72R sarcospheres increased in size and number, showing a mean diameter of 110 ± 23 μm with 576 cells/sphere. Even VECTOR sarcospheres increased in size and number but less respect to the R248W/P72R sarcospheres (mean diameter of 74.9 ± 18.2 μm, containing about 214 cells/sphere). Thereafter, secondary and tertiary sarcosphere-forming ability was analyzed and

it was observed that (Fig. 14C) they maintained the same trend of the primary spheres. These data demonstrated that R248W/P72R cells acquired a higher in vitro self-renewing potential.

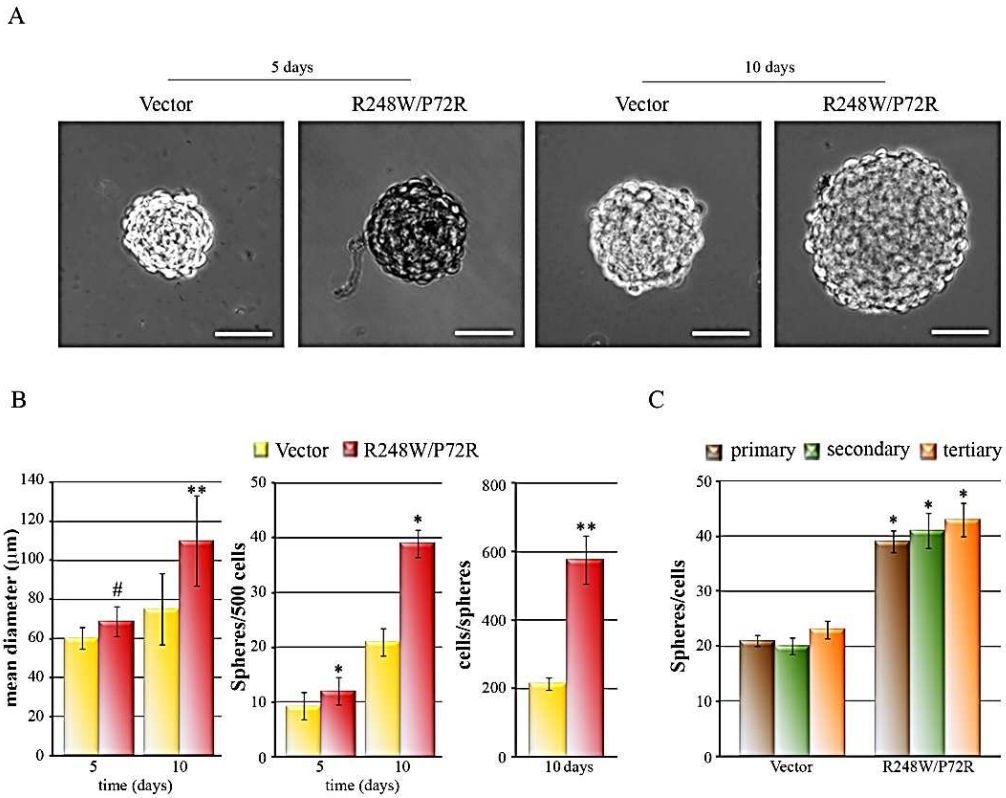

Fig.14.Transient ectopic expression of p53-R248W/P72R in osteosarcomaMG63 cells and its effect on sarcosphere-forming ability. (A) Phase contrast images of primary sarcospheres formed from VECTOR and R248W/P72R cells after 5 and 10 days post seeding. The scale bar represents 50 µm. Graphs summarizing size and number of sarcospheres from 500 cells (days 5 and 10) and number of cells/sphere on day 10. (B) Graph summarizing numbers of primary, secondary (generated from dissociated primary spheres) and tertiary (generated from dissociated secondary spheres) sarcospheres on day 10 from 500 cells. The data represent the mean with standard deviation (n = 4); *P < 0.05, **P < 0.01 and $^{\#}$P < 0.005 as compared to VECTOR cells.

As colony-forming ability is correlated with cell self-renewal (133), this ability was evaluated in MG63 cells after transient ectopic expression of the mutant p53 protein. As shown in Fig. 15 (A and B), R248W/P72R cells formed more and larger colonies than VECTOR cells.

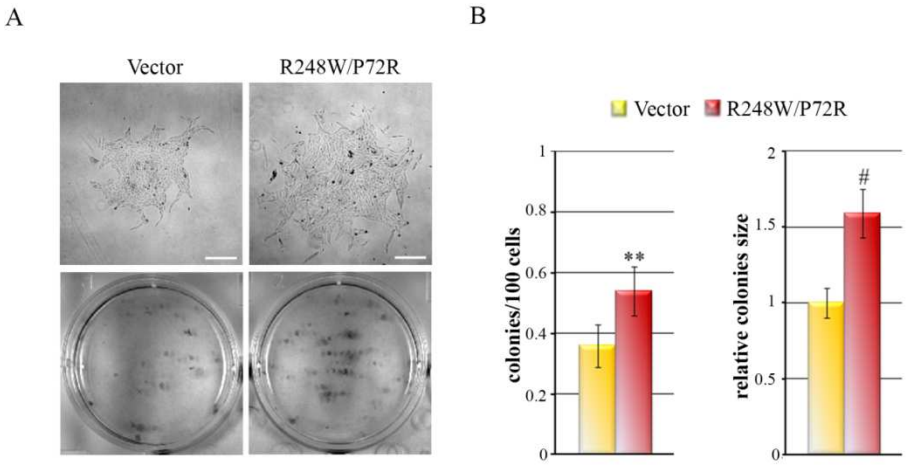

Fig.15. Transient ectopic expression of p53-R248W/P72R in osteosarcomaMG63 cells and its effect on colony-forming ability. Clonogenic growth of VECTOR and R248W/P72R cells after 10 days post seeding. A)Phase contrast images (top left panel; the scale bar represents 200 μm) and a picture (bottom left panel) of 6-well plate after staining with methylene blue are shown. B) Graphs summarizing plate efficiency (colonies/100 cells). The data represent the mean with standard deviation (n = 4); **P < 0.01 and $^{\#}$P < 0.005 as compared to VECTOR cells.

The motility and invasivity of the cells by wound healing and matrigel transwell invasion assays, respectively, were also evaluated. Compared with VECTOR cells, R248W/P72R cells showed higher migratory (Figs. 16A and B) and invasive (Figs. 17A and B) activities. These data suggested that p53-R248W/P72R expression can significantly promote the migratory and invasive function of MG63 cells.

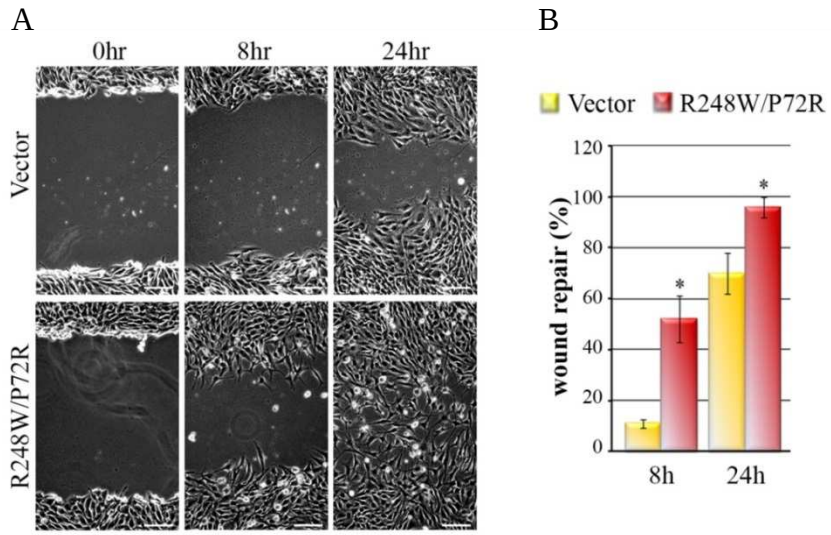

Fig.16. Effects of transient ectopic expression of p53-R248W/P72R on cell migration in MG63 cells. (A) Representative images from the scratch wound healing assay in MG63 cells transfected with either pcDNA3.1-p53-R248W/P72R (R248W/P72R) or empty pcDNA3.1 vector (Vector). Cells were scratched and wound margins were evaluated 0, 8 and 24 h later. The scale bar represents 100 μm. (B) Quantification of the scratch wound-healing assay is graphed. The data represent the mean with standard deviation (n = 4); *P < 0.05 as compared to VECTOR cells

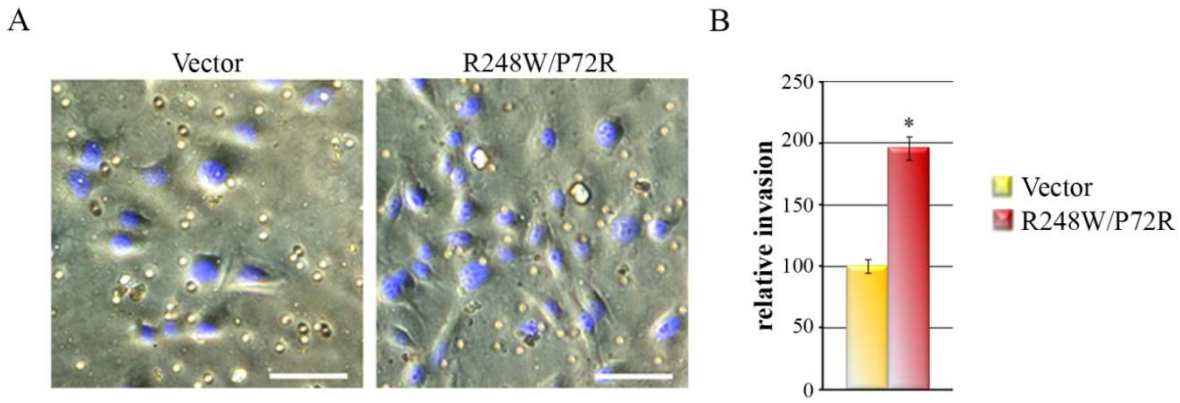

Fig.17. Effects of transient ectopic expression of p53-R248W/P72R on cell invasion in MG63 cells. (A) Representative images from the trans-well invasion assays in VECTOR and R248W/P72R cells. After 48 h of incubation, cells migrated to the underside of the insert were stained with Hoechst 33342. The scale bar represents 50 μm. (B) Graph of the relative invasion; the data represent the mean with standard deviation (n = 4; *P < 0.05).

In order to determine whether R248W/P72R cells could express the main cancer stem cell markers, the expression profile of two representative stem cell surface markers of OS, CD133 and ABCG2 was analyzed by flow cytometry (105) Fig. 18A shows a very low cell surface expression of CD133 and ABCG2 in both VECTOR cells (0.7% and 1.5%, respectively) and R248W/P72R cells (0.9% and 4.3%, respectively) and a high intracellular positivity (Fig. 18B), in both cellular conditions (24.5% of CD133 and 88.3% of ABCG2 in R248W/P72R cells; 8.3% of CD133 and 63.1% of ABCG2 in VECTOR cells). These results were confirmed by western blot analyses where the up-regulation (1,38 fold for CD133 and 1,25 fold for ABCG2) in R248W/P72R cells compared to VECTOR cells (Fig. 18B) was observed. Furthermore, the expression levels of the proteins that are involved in the regulation and maintenance of the stem cell phenotype, such as Nanog, OCT3/4, nucleostemin (NS) and Sox2 were analyzed. Western blot analyses (Fig. 18C) showed that these markers were significantly higher in R248W/P72R cells, with an increase of 1.56-fold, 1.22-fold and 1.37-fold for Nanog, OCT3/4 and ns, respectively (Fig. 18D). Significant changes in Sox2 levels were not observed. The above data demonstrated that the transient ectopic expression of mutant protein p53-R248W/P72R in MG63 cells, promotes cancer stem-like features.

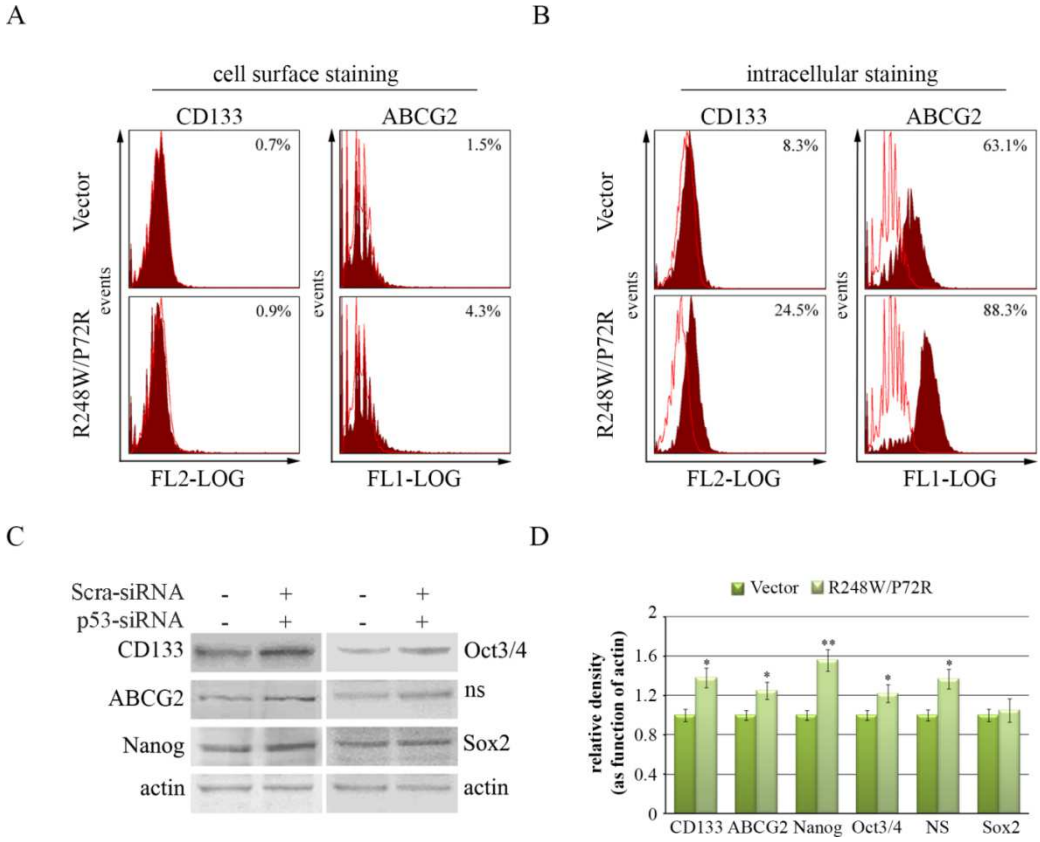

Fig.18. Effects of transient ectopic expression of p53-R248W/P72R on stemness markers expression inMG63 cells. (A) Cytometric analyses showing cell surface expression of CD133 (left panels) and ABCG2 (right panels) in VECTOR and R248W/P72R cells. The open histograms indicate isotype control; filled histograms indicate the expression of CD133 and ABCG2. (B) Cytometric analyses showing intracellular expression of CD133 (left panels) and ABCG2 (right panels) in VECTOR and R248W/P72R cells. The open histograms indicate isotype control; filled histograms indicate the expression of CD133 and ABCG2. (C and D) Western blot analysis of stemness proteins and relative densitometric analysis. The data (relative density normalized to actin) represent the mean with standard deviation (n = 4); *P < 0.05 and **P < 0.01 as compared to vector cells.

p53-R248W/P72R stable knockdown reduces cancer stem-like properties in human cancer stem cells 3AB-OS.

In order to confirm that p53-R248W/P72R is involved with the maintenance of 3AB-OS stemness the mutant p53 was silenced using stable RNAi system. Five days post selection the efficiency of silencing was evaluated by western blotting analysis, qPCR and immunoflurescence, comparing three cellular conditions: 3AB-OS, sh-scramble 3AB-OS (Scramble) and sh-p53 3AB-OS (sh-p53). As figure 19 (A, B and C) shows, the efficiency was more than 90%.

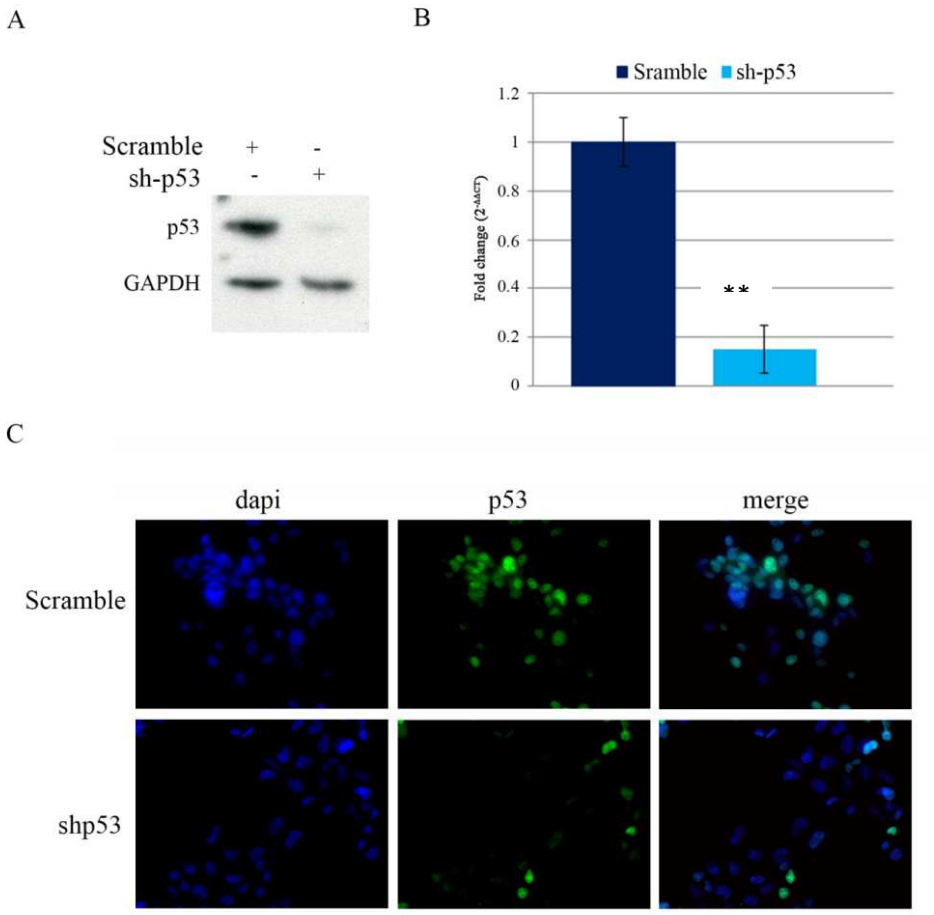

Fig. 19. Evaluation of stable knockdown efficiency of p53-R248W/P72R. 3AB-OS cells were transfected with scrambled shRNA (Scramble) or p53 shRNA (shp53) and analyzed at 5 days after infection. (A) Western blot analysis of p53-R248W/P72R. (B) Real time PCR analysis of p53-R248W/P72R 5 days post infection. Data represent the mean with standard deviation (n = 4); **P < 0.01 as compared to Scramble cells. (C) Immunofluorescence analysis by double staining cells with DAPI (blue), to localize the nuclei, and anti-p53 antibody and Alexa-fluo secondary antibody (green), to localize p53. Images are representative of four independent experiments

The cell line selected after p53-knockdown showed different aspects respect to the parental 3AB-OS and Scramble cells. Indeed, as shown in figure 20, the cells appeared bigger and polygonal and similar to each other respect to the control conditions. Moreover, there was a higher percentage of multinucleated giants cells respect to the Scramble and not silenced cells.

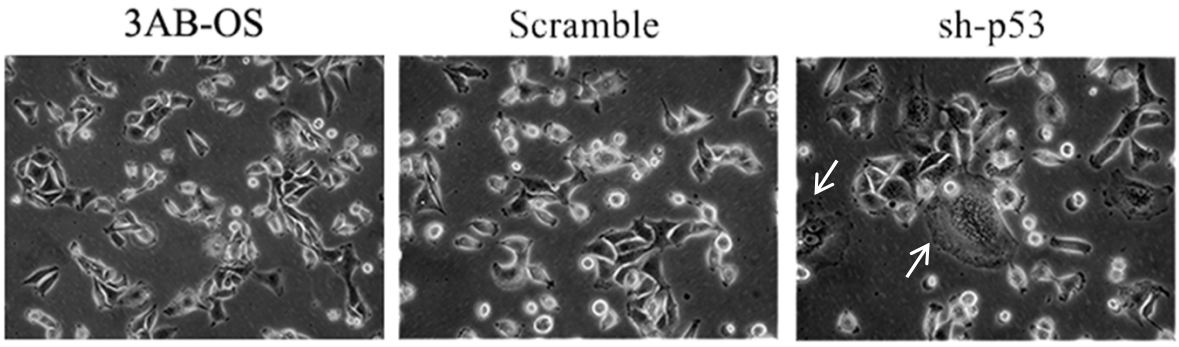

Fig.20. Morphologic analysis of stable p53-R248W/P72R knockdown cells. Inverted phase contrast microscopy after cells selection. The image shows 3AB-OS cells (left), Scramble (middle) and sh-p53 (right). The arrows evidenced the multinucleated giants cells.

Then, we evaluated whether p53-R248W/P72R stable knockdown affected 3AB-OS cancer stem-like features, such as proliferation rate, spheres and colonies formation, migration and expression levels of main stemness makers. First, we evaluated cell growth in sh-p53 cells compared with Scramble cells. MTS assay (fig.21A) showed in sh-p53 cells a decrease of cell proliferation confirmed by a decrease of S and G2/M cell cycle phases, accompanied by an increase in G1 cell cycle phase cell cycle (fig.21B) and a smaller percentage of EdU incorporation (fig.21C). As shown in figure 21D, p53R248W/P72R stable knockdown determined the decrease in expression levels of CycB1, CycD1, CDK6 that are important positive cell cycle regulators and the increase in p21 and p27, that represent negative regulators of cell cycle. These data were confirmed by real time PCR analyses (fig.21E) by which it has been observed a decrease in the expression levels of cycD1, cycD2, cycE1, cycE2 and an increase of CDKN2C, the inhibitor of CDK4. These results showed that after p53-R248W/P72R knockdown reduce the speed of the proliferation rate of 3AB-OS cells.

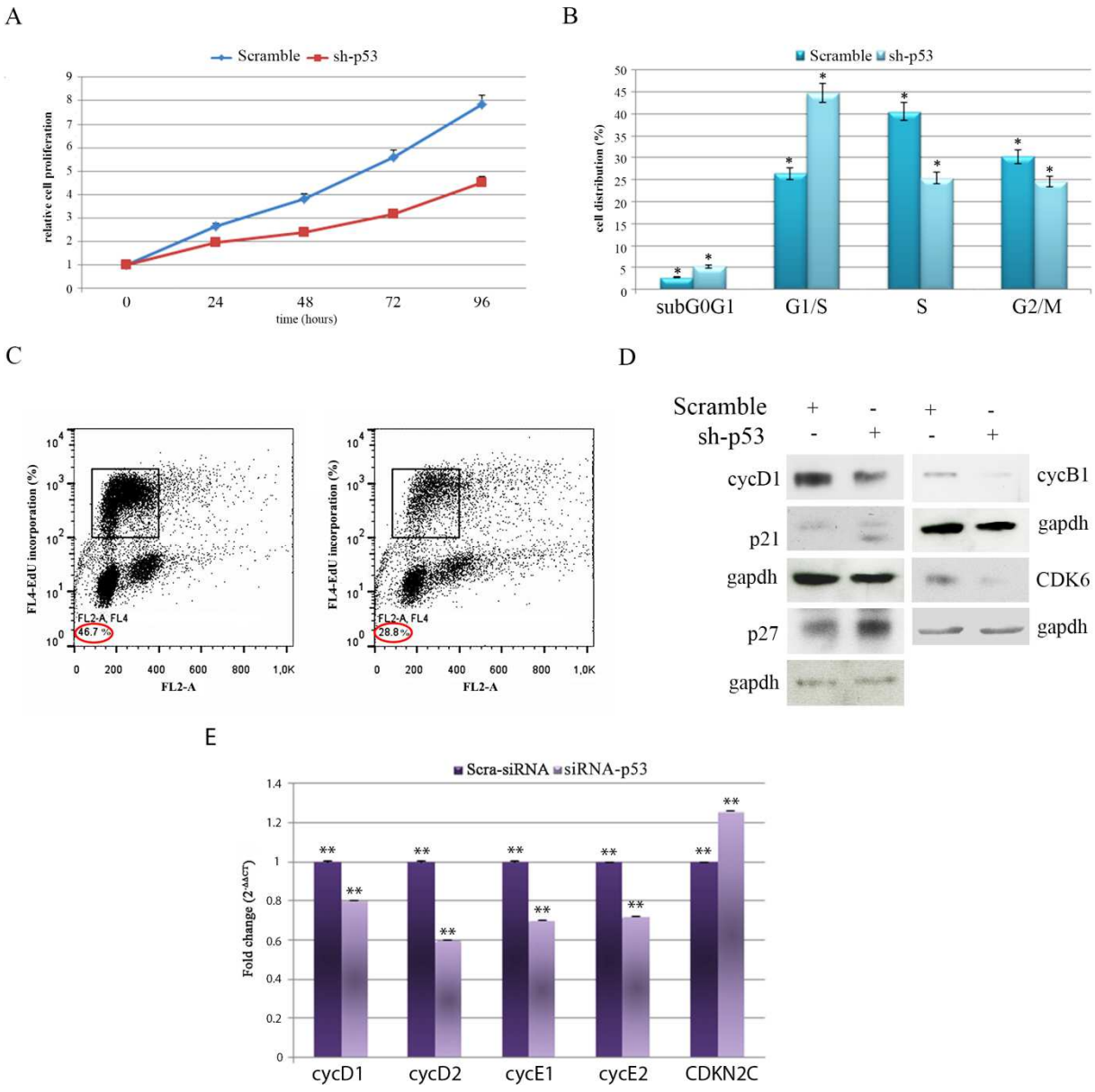

Fig.21. Effects of p53R248W/P72R: Proliferation rate. A) MTS assay performed among 0 and 96 hours after seeding; B) cell cycle distribution determined by flow cytometry. The data are indicated as relative percentage of total cell cycle (*P < 0.05 compared to the Scramble cells); C) Edu-incorporation assay performed by flow cytometry. D) western blotting analysis of important cell cycle regulators; E) Real-time PCR analysis of cell cycle regulators. Data represent the mean with standard deviation (n = 4); **P < 0.005 as compared to the Scramble cells.

These proliferation data, together with the increase in multinucleated giant cells, suggested that p53R248W/P72R stable knockdown could lead the cells to the acquisition of a senescent phenotype. In order to verify this hypothesis we performed β–galactosidase and Senescence Associated Heterochormatin Foci (SAHF) assays. There are many evidences that show high β-galactosidase levels in senescence cells (134). As figure 22A evidences there were more

blue cells in sh-p53 cells then in Scramble condition. These results suggest that silencing the mutant-p53 promotes the senescent state in 3AB-OS cells.

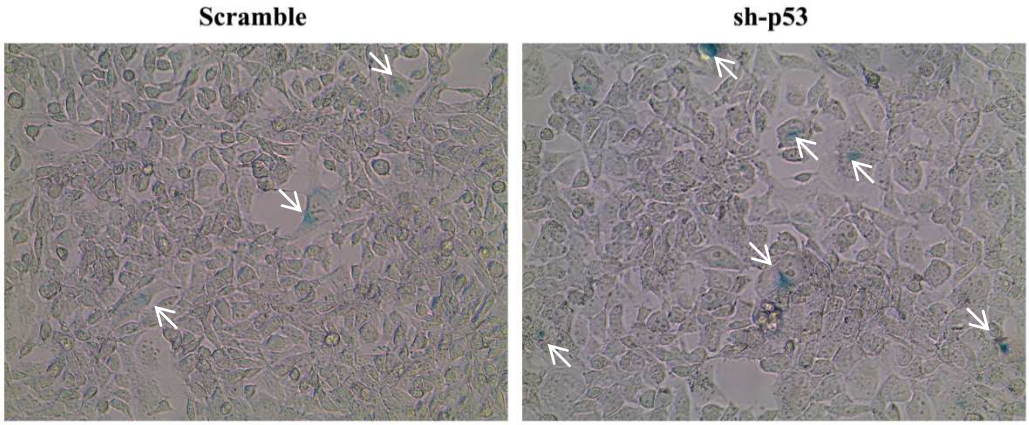

Fig. 22. Study of senescence state after p53-R248W/P72R stable knockdown. Contrast phase images of Scramble (left image) and sh-p53 (right image) after β-galactosidase assay; the blue cells senescent are evidenced by the arrows.

Thereafter, experiments were performed to understand if mutant p53 stable knockdown affected apoptosis. Western blotting analysis (Fig. 23A) showed that stable p53-R248W/P72R knockdown induced an increase in the levels of Bax and Bad, pro-apoptotic Bcl-2 family members, and a decrease in the levels of Bcl-2 the anti-apoptotic factors of the same family. The study of Lamin B shows in sh-p53 cells a decrease in its levels, while caspase-3 and PARP evidenced no significant differences in protein levels between Scramble and sh-p53 cells. Cell cycle analysis (fig.23B) shows a small increase in the subG0G1 phase in 3AB-OS-shp53 compared to the Scramble cells. Overall, these findings suggested that 3AB-OS cells with p53R248W/P72R knockdown are prone to the apoptotic event.

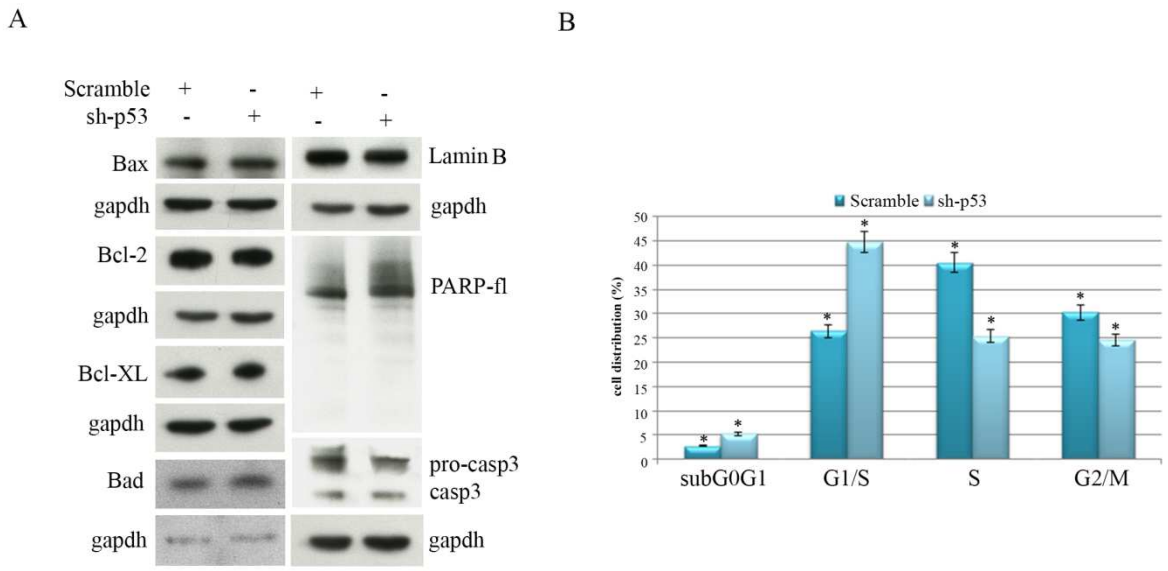

Fig.23. Effect of p53-R248W/P72R-knockdown on apoptosis. A) western blotting analisys of Bcl-2 family member and caspase-3 pathway; B)) cell cycle distribution determined by flow cytometry. The data are indicated as relative percentage of total cell cycle (*P<0.05 compared to the scramble cells).

Moreover, after p53 knockdown the cells showed a lower migratory ability and invasiveness then 3AB-OS and Scramble cells as shown by the data from wound healing, western blotting and qPCR analyses. Indeed, wound healing assay (Fig.24 A and B), performed by Incucyte System, showed that 3AB-OS and Scramble cells after the wound insult migrated faster than sh-p53 cells and after 16 hours only in 3AB-OS and Scramble cells the total repair of the scratch was observed.

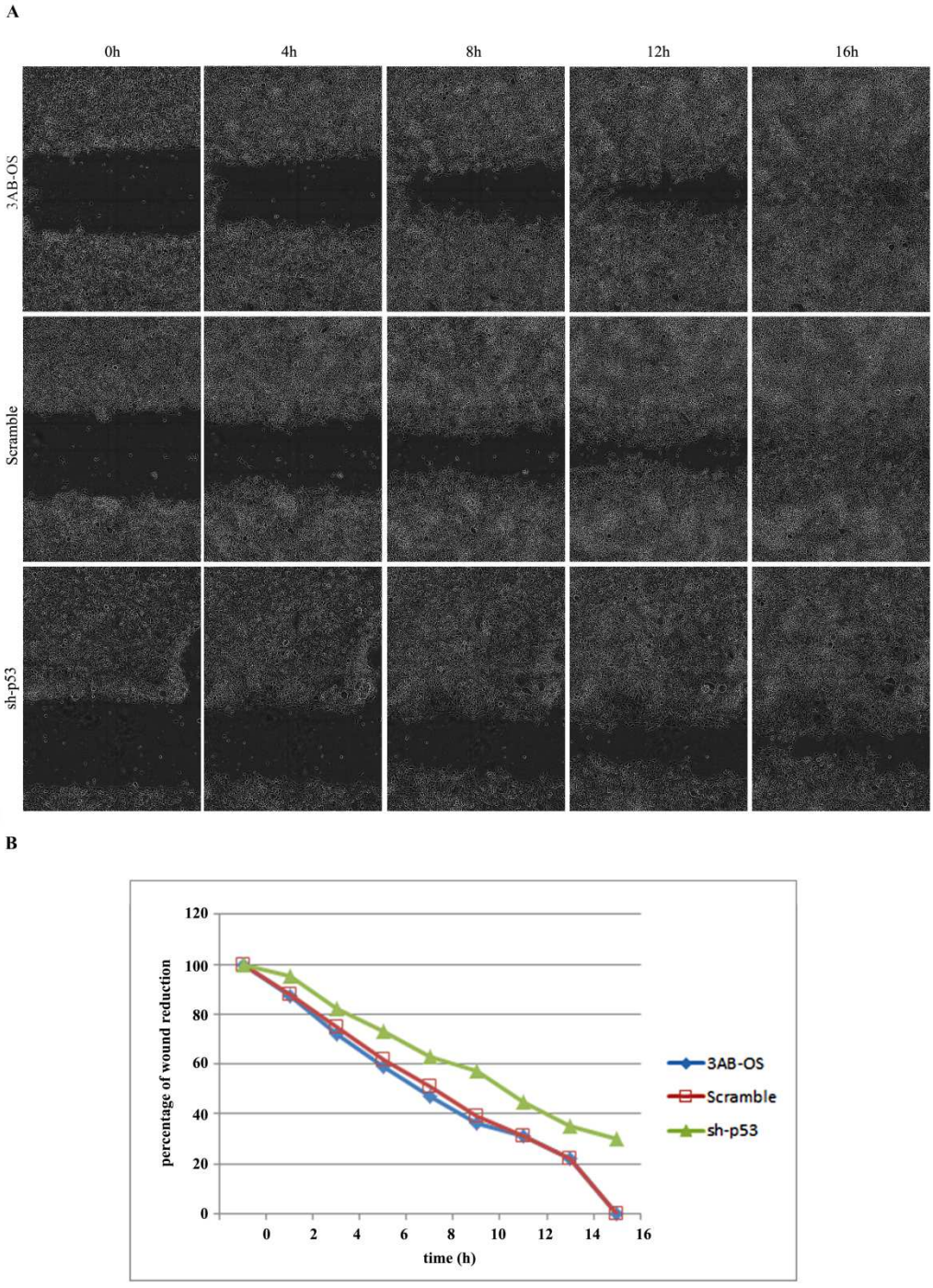

Fig.24. Study of migration ability of 3AB-OS cells after p53R248W/P672R stable knockdown. A)Incucyte images that show the wound repair ability of 3AB-OS, Scramble and sh-p53 cells among 0 and 16 hours after the scratch; B) data graphed.

As shown in figure 25A, mutant p53 stable knockdown determined a significant decrease of MMP2, VANGL1, CD44, SNAIL1, SNAIL2 and β-CATENIN mRNAs respect to the Scramble cells but not considerable differences in MMP9, ZEB1, ZEB2, VIM and N-CADHERIN mRNAs. From western blotting analysis (FIG.25B) a great decrease of MMP2,

MMP9, CD44 and N-CADHERIN protein expression levels were observed. A weird increase of VIM protein levels was evidenced and it could be explained by the presence of mechanisms like acetylation and detyrosination that usually stabilize this cytoskeletric protein (135). These data strongly confirmed that p53R248W/P72R plays an important role in the control of 3AB-OS cells migration and invasiveness. Recently, a few studies have shown that features of EMT (epithelial-mesenchymal transition) are closely associated with the signatures of CSCs, which could lead to tumor recurrence and drug resistance phenotype. It is proposed that while EMT may enhance the stemness of CSCS, MET (mesenchymal-epithelial transition) may attenuate the stemness of CSCs. Moreover, there are some evidences according to which EMT represents a mutant p53 gain of function (95)**.** The data described above are consistent with the hypothesis that p53R248W/P72R controls EMT in order to maintain 3AB-OS cells stemness. Moreover, one of the most important aspect of EMT process is the involvement of WNT/beta-catenin pathway that shows an increase of beta-catenin levels that translocates into the nuclei where it can exerts its co-transcriptional role. Immunofluorescence analyses (fig.25C), performed after mutant p53 stable knockdown, showed a clear β-catenin translocation from the nucleus to the cytoplasm reinforcing the hypothesis that this mutant leads the EMT in 3AB-OS stem cells.

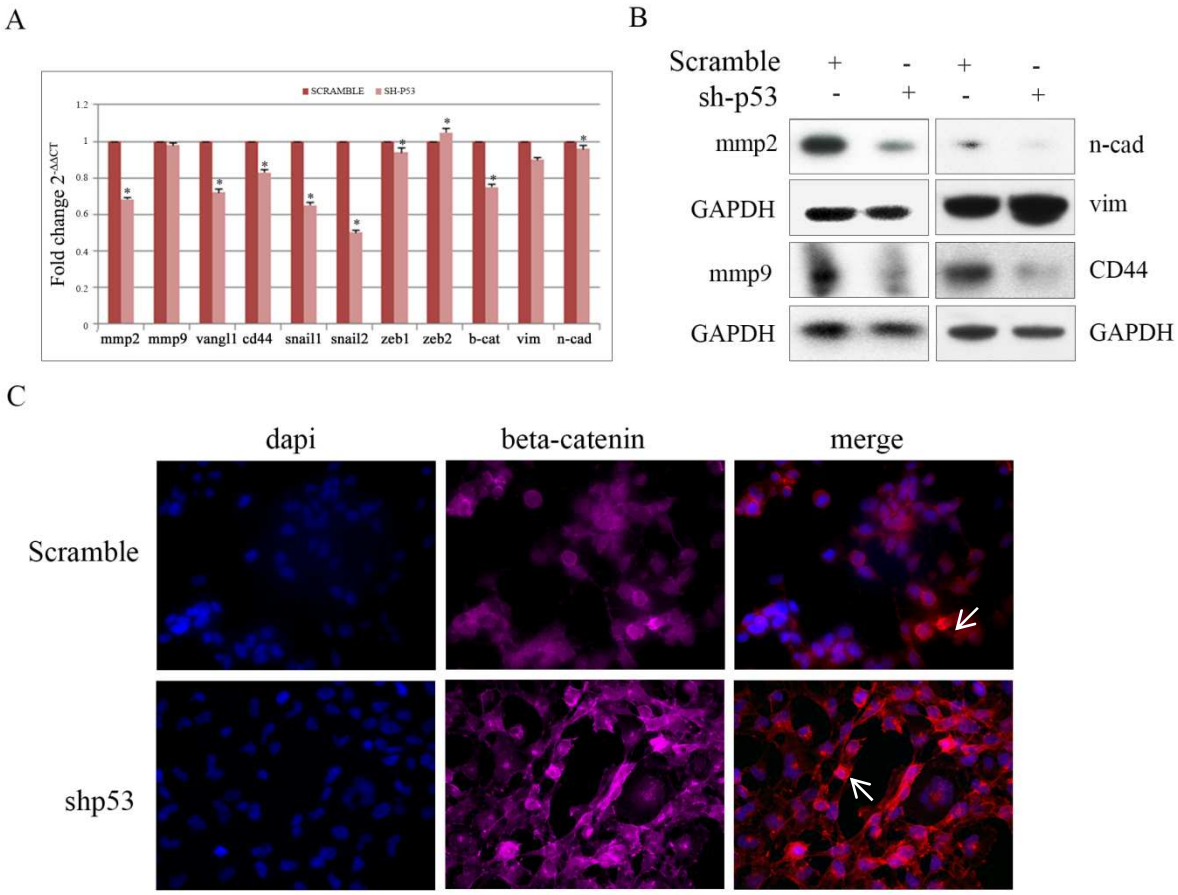

Fig.25. 3AB-OS migration and invasive abilities after p53-R248W/P72R stable knockdown. A) Real-time PCR analysis of migration and invasivness genes after stable mutant 53 knockdown. Data represent the mean with standard deviation (n = 4); *P < 0.05 compared to Scramble 3AB-OS cells. B) Western blotting analysis of important invasiveness protein. C) The arrows indicate the localization of □-catenin detected by using Alexa-fluo secondary antibody.

Thereafter, the expression levels of the main stemness markers such as KLF4, OCT4, NANOG, SOX2 and CD44 were evaluated by western blot (Fig.26A) and qPCR (Fig.26B) analyses. The results showed that they markedly decreased after p53R248W/P72R knockdown.

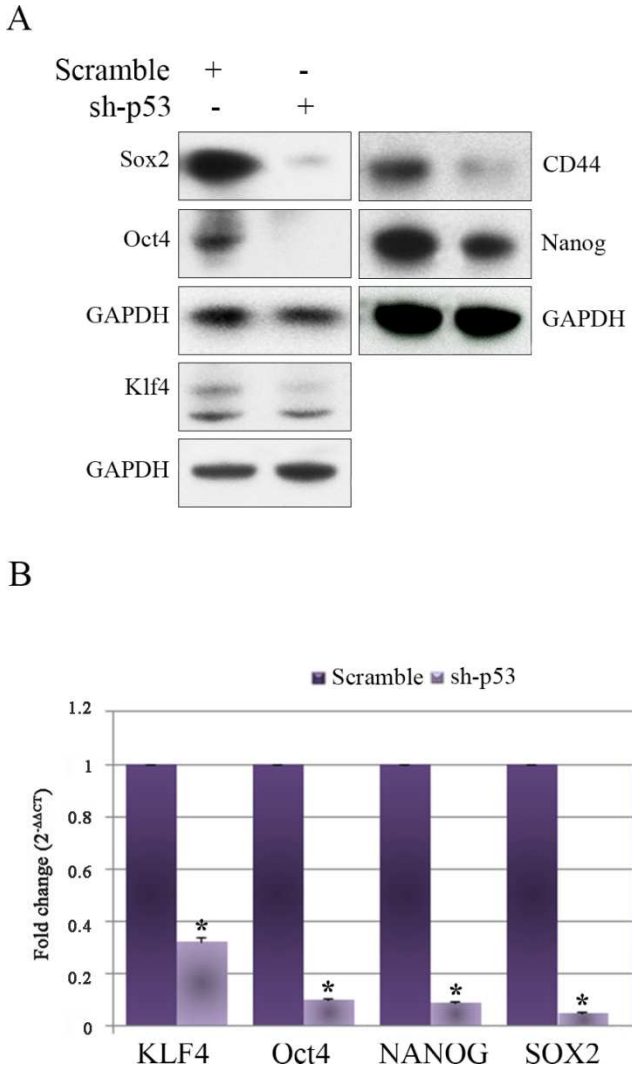

Fig.26. Stemness markers evaluation after p53-R248W/P72R stable knockdown. A) western blottin analysis of the main important stemness markers in 3AB-OS/shp53 cells compared with 3AB-OS Scramble cells. B) Real-time PCR analysis of important stemness genes after stable mutant 53 knockdown. Data represent the mean with standard deviation (n = 4); *P < 0.05 compared to Scramble 3AB-OS cells.

Also the ability of 3AB-OS/sh-p53 to form colonies markedly decreased (fig. 27) respect to 3AB-OS/Scramble. In particular, after ten days post seeding approximately 20 colonies with a mean diameter of 667,33 ± 43,09 μm were counted in silenced cells, respect to those counted on Scramble cells where more than 40 colonies with a mean diameter of 1280,33 ± 145,02μm were counted.

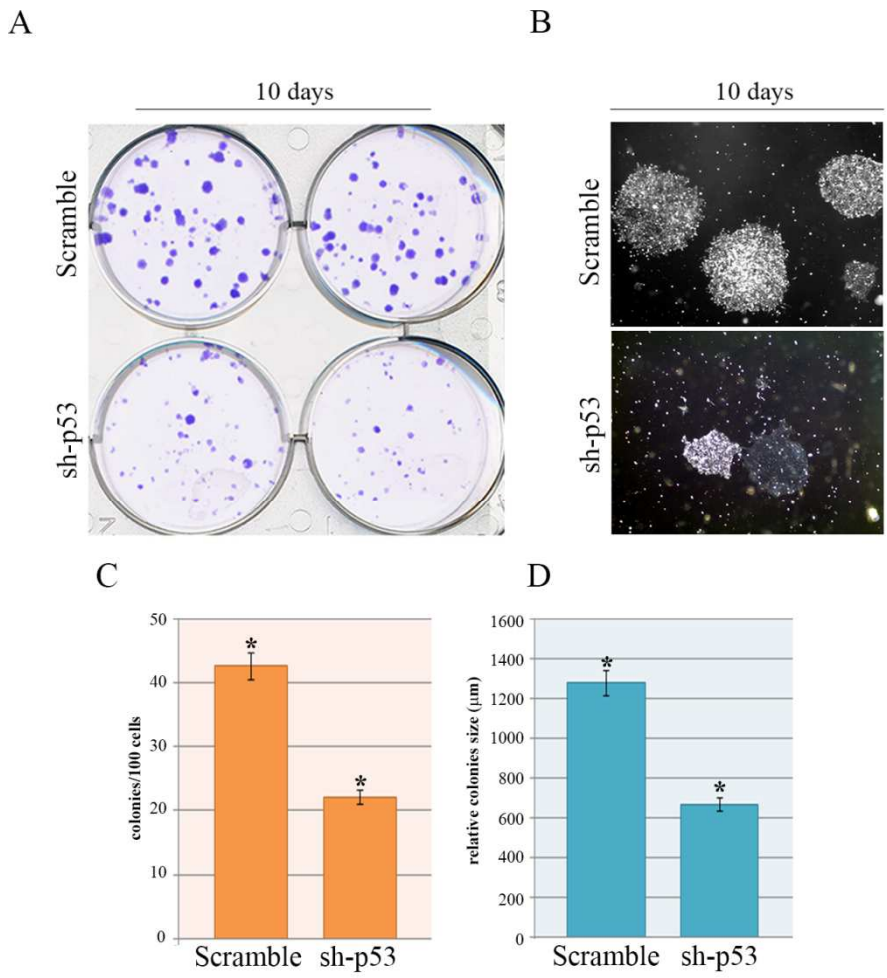

Fig.27.Colonies forming ability of p53-R248W/P72R knockdown cells. A) A picture of 6-well plate after staining with with crystal violet of 3AB-OS/Scramble (on the top) and 3AB-OS/sh-p53 (on the bottom) cells; B) phase contrast image (magnitude 2,5X) of 3AB-OS/Scramble (on the top) and 3AB-OS/sh-p53 (on the bottom); Graphs summarizing C) plate efficiency (colonies/100 cells) and D) relative colonies size. The data represent the mean with standard deviation (n = 4);*P < 0.05 and **P < 0.01 as compared with the Scramble cells. The data are representative of three independent experiments.

To test whether after p53-R248W/P72R knockdown 3AB-OS cells lost their ability to form spheres in low attachment 300 cells for both conditions, Scramble and sh-p53 were seeded. After 10 days (Fig.28) silenced cells formed less and smaller spheres than the Scramble cells. In particular (fig.28B and C), 3AB-Os/sh-p53 cells formed approximately 30 spheres with a mean diameter of 1336 ± 42 µm respect to Scramble cells which formed more than 50 spheres with a mean diameter of 2300 ± 92,8 µm. These data where confirmed by the total cell number obtained from the spheres of both cell conditions after 10 days post the seeding (Fig.28D). indeed, from 300 cells approximately $1{,}08x10^6$ 3AB-OS/Scramble cells and

$2{,}3x10^5$ 3AB-OS/sh-p53 cells were counted. Moreover, the analysis of secondary and tertiary spheres showed the same trend of the primary (data not shown).

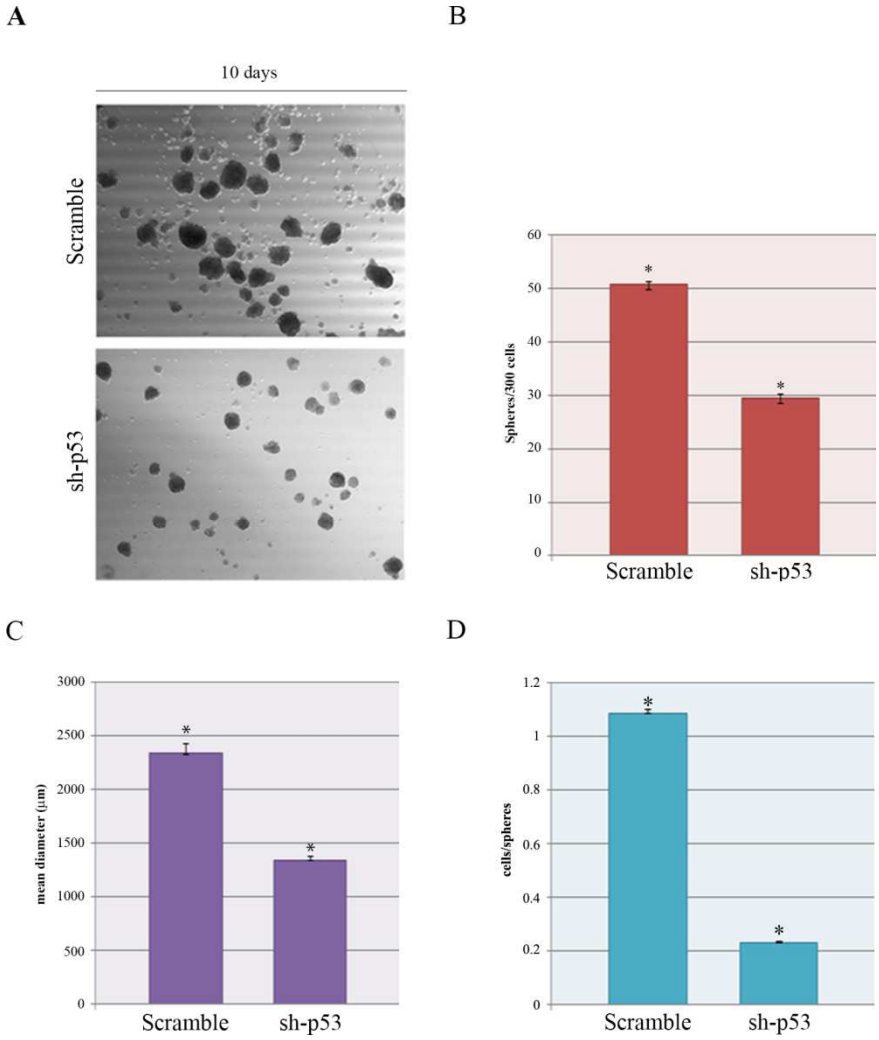

Fig.28.Spheres forming ability of p53-R248W/P72R knockdown cells. A) Phase contrast images of primary sarcospheres formed from 3AB-OS/Scramble and 3AB-OS/sh-p53 cells after 10 days post seeding (magnitudo2,5X). Graphs summarizing number (B) and size (C) of spheres from 300 cells (days 10) and number of cells/sphere on day 10 (D). The data represent the mean with standard deviation (n = 4); *P < 0.05 as compared to Scramble cells.

DISCUSSION

In about half of all human cancers, the tumor suppressor p53 protein is either lost or mutated and this often results in the expression of a transcriptionally inactive mutant p53 protein. Loss of p53 function influences cell cycle checkpoint controls, apoptosis, cell migration and invasion. Moreover, recent data suggests that expression of mutant p53 can acquire new oncogenic functions by which it drives tumor progression (136). P53 exerts its gain of function (GOF) increasing growth rate and motility, tumorigenicity metastatic progression and invasiveness and decreasing sensitivity to chemotherapeutic drugs. The GOF phenotypes can also be partially explained by a dominant-negative effect of mutant p53 on p73 and p63 (137). P53 mutational status may determine the efficacy of many of the chemotherapeutic drugs. Overall, in OS patients, alterations of TP53 occurs in 50%–60% of cases and consist of point mutations (20%–30%, mostly missense mutations), gene rearrangements (10%–20%) and allelic loss (75%–80%) (138). p53 mutation status is useful as a valuable indicator for predicting chemoresistance in OS patients (139). Moreover, patients with Li-Fraumeni syndrome, a disorder characterized by a germline mutation at the p53 locus, have a significantly higher risk of developing OS (140). Previous analyses (130) of the TP53 gene status/role showed that, in comparison with parental MG63 cells (where TP53 gene is wild type, hyper methylated, rearranged and in single copy), 3AB-OS cells have TP53 gene mutated at the codons 248 and 72, unmethylated, rearranged and in multiple copies. Moreover, this mutant p53 (p53-R248W/P72R) is post-translationally stabilized and localized in to the nucleus.

In this thesis it has been shown that this mutant p53 is involved in promoting proliferation, invasiveness, resistance to apoptosis and stemness of 3AB-OS. Moreover, it has been demonstrated that p53-R248W/P72R transient and stable knockdown strongly reduces the growth and replication rate of 3AB-OS cells and concomitantly increases the expression of

negative regulators of cell cycle such as pRb, p130, p107, E2F4, GADD45, p21, p27 and CDKN2C, while decreases the expression of positive regulators such as CDK4, CDK6, CycD1, CycD2, CycB1, CycE1 and CycE2. These data were accompanied by a significant accumulation of cells in G0/G1 cell cycle phase with a simultaneous decrease in S and G2 phases. The findings are in strong accordance with alteration of cell cycle genes, seen in up to 80% of pediatric/adult OS patients, suggesting that the genetic lesions that deregulate G1/S cell cycle checkpoint could be a constant feature in the pathogenesis of OS (141, 142, 143). Another distinctive feature of mutant p53 is its ability to confer on cells an elevated resistance to a variety of apoptotic signals (97). Analyses of death receptors in OS samples and in OS cell lines, including MG63 cells, have demonstrated alterations within the DR4 gene, suggesting that these genetic alterations may be implicated in OS formation (144). Previously, it has been shown that 3AB-OS cells highly express a great number of genes required for inhibiting apoptosis (105) .and much lower levels of FAS and DR4 receptors than parental MG63 cells (118). Here it has been shown that in 3AB-OS cells p53-R248W/P72R transient knockdown significantly increased the expression of DR4 and DR5 receptors and the sensitivity to TRAIL-induced apoptosis. Moreover, this transient silencing induced a decrease in anti-apoptotic factors such as Bcl-2 and Bcl-XL and an increase in pro-apoptotic factors such as Bax and Puma. Overall, these finding suggest that in 3AB-OS cells p53-R248W/P72R could hinder cell response to TRAIL-treatment. The stable knockdown of p53-R248W/P72R evidenced significant variations of expression levels of Bcl-2 family members with no measurable variations in Caspase-3 and its substrates. Moreover, the stable silencing of p53R248W/P72R in 3AB-OS CSCs seems to increase the amount of senescent cells respect to the Scramble cells. All these data demonstrated that the less number of cells after the knockdown was derived from the lower proliferation speed and the higher number of apoptotic and senescent cells respect to the Scramble condition.

Stemness acquisition is a key event in cancer development as it may induce progression, invasion, dissemination and metastasis. OS is a highly metastatic tumor and in patients with high-grade OS, increased MMPs expression was identified as prognostic marker for poor outcome (145,146).

Here, it has been shown that p53-R248W/P72R transient and stable knockdown causes a striking reduction of in vitro invasive ability of 3AB-OS cells with a decrease in the levels of invasion-related gene and protein such as MMP2, MMP9, ITGα5, ITGαV, Vangl1, CD44, Snail1, Snail2, N-cadherin and in transient silencing a concomitant marked increase of E-cadherin levels. This suggests that the oncogenic properties of p53-R248W/P72R could also enable 3AB-OS cells to promote invasion. The presence of OS stem-like cells has been reported in patient tumors (147) as well as in established human OS cell lines (148). Previously, it has been shown that 3AB-OS cells highly express a large panel of stemness-related genes/proteins and that efficiently trans-differentiate in vitro into cells of all the three primary germ layers, whereas when 3AB-OS cells were engrafted in nude mice, they potently induced malignant tumors, although preserving multilineage commitment. Here, it has been shown that, after in vitro 3AB-OS differentiation, in each derived cell lineage (hepatocytic, adipocytic, neurogenic, osteocytic), p53-R248W/P72R was profoundly down-regulated and after p53-R248W/P72R transient and stable knockdown the expression of pluripotent markers such as Oct3/4, Nanog, Sox2, nucleostemin, CD133 and Klf4 were markedly lowered. These data suggested that p53-R248W/P72R might be responsible for 3AB-OS cells pluripotency and self-renewal. In fact, after stable silencing 3AB-OS cells decreased their ability to form colonies and spheres in vitro. Indeed, in sh-p53 cells these were less numerous, smaller, containing less cells respect to the control condition of Scramble cells. Moreover, these cells showed lowered invasion and migratory properties.in addition, the transient ectopic expression of p53-R248W/P72R in osteosarcoma MG63 cells (3AB-OS parental cells)

promoted cancer stem-like properties. In particular, when MG63 cells were transfected with pcDNA3.1-p53-R248W/P72R showed strong positivity for p53 that resulted to be nuclear. Moreover, MG63 cells expressing p53-R248W/P72R, compared with the cells expression the empty vector, showed a higher proliferative output, were able to form 2-fold sarcospheres and more numerous and larger colonies. In addition, these cells showed a higher migratory and invasive activity respect to the control vector cells and significant increase in the expression of stemness markers.

In conclusion, the findings that in 3AB-OS cells p53-R248W/P72Rknockdown profoundly changed the expression of genes/proteins correlated to stemness, proliferation, apoptosis and invasiveness, and that in MG63 parental cells, the ectopic expression of p53-R248W/ P72R promoted cancer stem-like properties, suggest that the GOF property of p53-R248W/P72R can be at the root of the dedifferentiation of MG63 cells into 3AB-OS CSCs. Thus 3AB-OS cells could provide a best-fit to understand p53-R248W/P72R properties and its potential involvement in osteosarcomagenesis

WORK IN PROGRESS

The data described in this thesis, suggest that p53-R248W/P72R could be at the root of the dedifferentiation of osteosarcoma MG63 cell line in CSCs 3AB-OS cell line. For this reason I am aimed at evaluating the effects of the expression on this mutant-p53 in different osteosarcoma cell lines that are p53-null or p53-wild type. For my experiments I have chosen the cell lines SAOS-2 (p53-null because of a deletion), MG63 (p53-null because of the lack of gene expression) and U2-OS (p53-wild type). The production of SAOS-2, MG63 and U2-OS stable clones expressing the mutant p53- R248W/P72R is ongoing. I will also perform these experiments in the normal fibroblast cell line BJ-hTERT. I want to evaluate whether the stable ectopic expression of the mutant-p53 in these cell lines will induce the acquisition of stem-like features. Once obtained these clones, I will test in them the presence of stemness features such as high proliferation rate, spheres formation, clonogenic growth, high migration and invasive ability, high expression of stemness markers. I expect that these experiments confirm the results that I have discussed in the thesis. Once demonstrated the hypothesis that p53-R248W/P72R exerts its gain of function in 3AB-OS by keeping their stemness properties, the next step will be to find the possible mechanisms at the root of this gain of function. RNA-sequencing analysis, where 3AB-OS/Scramble cells are compared with 3AB-OS/sh-p53 cells, is ongoing. I am waiting the bioinformatics elaboration of the data. It is well known that point mutations, called “hotspot” (such as R175, G245, R248, R249, R273 and R282) at the DNA-binding domain (DBD) of wild type p53 affect its ability to bind the DNA and to exerts its tumor suppressor functions (149). Recent studies showed that these mutants can interact with the DNA binding sequences different from canonical wild type p53 consensus sequences using the C-terminal domain or recognizing particular DNA structures known as non-B DNA (150).

In order to understand if p53-R248W/P72R expressed in 3AB-OS cells, is able to bind the DNA, despite its hot spot mutation at the DBD, I performed a Chromatin Binding assay by which I could demonstrate that this mutant interacts with the DNA (Fig29). I will perform ChIP experiments in order to validate RNA-sequencing data with the aim of finding some known or unknown target involved in stemness or differentiation maintenance.

A

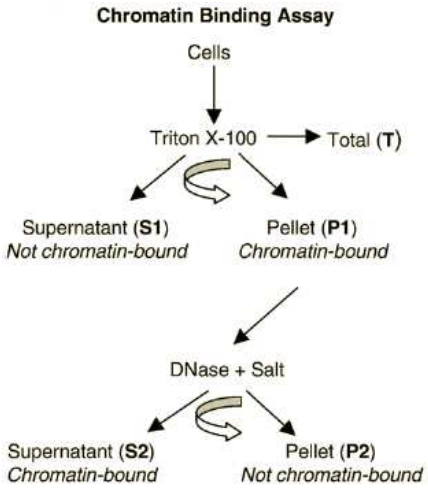

B

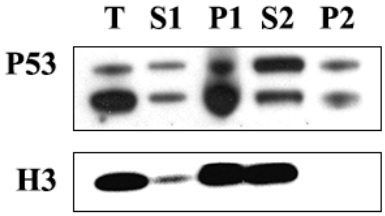

Fig.29.Evaluation of p53 DNA-binding in 3AB-OS cells by Chromatin binding assay. A) schematic description of the technique (151); B) western blotting analysis of the mutant p53 in the fractions. T, total fraction; S1, supernatant not chromatin-bound fraction; P1, pellet chromatin-bound fraction; S2, supernatant chromatin-bound; P2, pellet not chromatin-bound.

MATERIALS AND METHODS

Cell cultures

Human osteosarcoma MG63 cells were acquired from Interlab Cell Line Collection (ICLC, Genova, Italy). The human 3AB-OS cancer stem cells have been produced in our laboratory (105) and patented (Pluripotent cancer stem cells: their preparation and use. Renza Vento and Riccardo Di Fiore, Patent Appln. No. FI2008A000238, December 11, 2008). Cell lines were cultured as monolayers in T-75 flask in Dulbecco's modified Eagle medium (DMEM), supplemented with 10% (v/v) heat-inactivated fetal bovine serum (FBS), 2 mM L-glutamine, 100 U/ml penicillin and 50 μg/ml streptomycin (Euroclone, Pero, Italy) in a humidified atmosphere of 5% CO2 in air at 37 °C. When cells grew to approximately 80% confluence, they were sub-cultured or harvested using 0.025% trypsin–EDTA (Life Technologies Ltd, Monza, Italy).

Morphological observation

Cell morphology was evaluated using a Leica DM IRB inverted microscope (Leica Microsystems) and a Leica DMIL inverted microscope (Leica Microsystems) and images were captured computer-imaging systems(Leica DC300F and Leica EC3 cameras respectively)

Immunofluorescence Staining for p53

3AB-OS cells were fixed with 3.7% formaldehyde for 10 min at room temperature and permeabilized with 0.1% Triton® X-100 (all from Sigma) in phosphate-buffered saline (PBS) for 5 min. After washing with PBS, cells were incubated with anti-p53 primary antibody (diluted 1:100 in PBS + 1% BSA + 0.05% NaN3; Santa Cruz Biotechnology, Santa Cruz, CA, USA) at 4 °C, overnight. Cells were washed three times with PBS and incubated for 1 h at room temperature with Cy3-or Cy2-conjugated secondary antibody (diluted 1:100 in PBS + 1% BSA + 0.05% NaN3; Jackson ImmunoResearch Laboratories, West Grove, PA, USA).

Nuclei were counterstained with 2.5 μg/ml Hoechst 33342 (Sigma-Aldrich) for 10 min. After three washes, cells were examined on a Leica DMIRB inverted microscope equipped with fluorescence optics and suitable filters for DAPI, FITC and rhodamine detection; images were photographed and captured by a computer-imaging system (Leica DC300F camera and Adobe Photoshop for image analysis). 3AB-OS/sh-Scramble and 3AB-OS/sh-p53 were seeded in rounded coverslips placed in 24-well plate. When they were confluent to 80% they were washed with PBS and fixed and permeabilized as above. After washing some wells were incubated with anti-p53 primary antibody (diluted 1:100 in PBS + 1% BSA + 0.05% NaN3) and other with anti-b-catenin primary antibody (diluted 1:100 in PBS + 1% BSA + 0.05% NaN3) at 4 °C, overnight. Cells were washed three times with PBS and incubated for 1 h at room temperature with Alexa Fluor® 488 Donkey Anti-Mouse IgG (H+L) and Alexa Fluor® 647 Donkey Anti-Rabbit IgG (H+L) secondary antibodies respectively. At the end the cover slips were washed three times with PBS and one time in MilliQ sterile water and mounted by using ProLong® Gold Antifade Mountant with DAPI (Life Technologies)**.**

Transient down-regulation of p53 by short interfering RNA (siRNA)

Cells were plated in a six-well plate format and cultured in DMEM medium, supplemented with 10% FBS, for 24 h to reach approximately 60–80% confluence. Specific siRNAs directed against p53, obtained by St Cruz Biotechnology as a pool of double-stranded RNA oligonucleotides, were transfected for 5 h into the cells at a final concentration of 50 nM, in the presence of 5 μl Metafectene Pro (Biontex, Martinsried/Planegg, GmBH, Munich, Germany) in a final volume of 1 ml serum free DMEM. At the end, the reaction was stopped replacing the culture medium with DMEM + 10% FBS. Cells were examined for p53 down-regulation and other properties 24–72 h after transfection. siRNA, consisting in a scramble sequence, was used as a negative control.

Growth curve and cell viability assays

Total Scra-siRNA and p53-siRNA cells number and viability were evaluated by Trypan blue exclusion counting. Briefly, cells were harvested every 24 h and resuspended in PBS. Aliquots of cell suspensions were diluted with 0.4% trypan blue (Sigma-Aldrich Srl, Milano, Italy), pipetted onto a hemocytometer and counted under a microscope at 100× magnification. Live cells excluded the dye, whereas dead cells admitted the dye intensely staining with trypan blue. The number of viable cells for each experimental condition was counted and represented on a linear graph. Doubling time(DT)was estimated by the following equation: DT = (t2 − t1) ln2 / lnX2 / X1, where X2 and X1 are the number of cells at t2 and t1.

EdU in corporation assay

EdU (5-ethynyl-2′-deoxyuridine) incorporation Scra-siRNA and p53-siRNA cells ability was evaluated by using the Click-iT™ EdU Alexa Fluor High-Throughput Imaging Assay kit (Invitrogen, Life Technologies), according to the manufacturer's instructions. At the end nuclei were counterstained with 2.5 μg/ml Hoechst 33342 (Sigma-Aldrich), for 10 min and after three washes, cells were examined by fluorescence microscopy using filters for DAPI and FITC. The percentage of EdU-positive nuclei was determined by counting five random high-powered fields (400×). EdU (5-ethynyl-2′-deoxyuridine) incorporation 3AB-OS/sh-Scramble and 3AB-OS/sh-p53 cells ability was evaluated by using the Click-iT® EdU Alexa Fluor® 647 Flow Cytometry Assay Kit (Life Technologies), according to the manufacturer's instructions. Cells were examined by flowcytometry

MTS assay

3AB-OS/sh-Scramble and 3AB-OS/sh-p53 were seeded in 96-well plate at a density of $2x10^3$ cells/well with 100 µl of medium. Wells containing only medium were used as blank. 20 µl of

MTS reagent were added to each well and the plate was incubated at 37°C for 1 hour. At the end the absorbance of the plate was read at 490nm.

Cell cycle and proliferation analyses

Cell cycle phase distribution was studied by flow cytometry of DNA content. For DNA staining, trypsinized cell suspensions were centrifuged, washed 3 times with PBS and resuspended at 1 ×106 cells/ml in PBS. Cells were mixed with cold absolute ethanol and stored for 1 h at 4 °C. After centrifugation, cells were rinsed 3 times in PBS, and the pellet was suspended in 1 ml of propidium iodide (PI) staining solution (3.8 mM sodium citrate, 25 μg/ml PI, 10 μg/ml RNase A; Sigma-Aldrich Srl, Milano, Italy) and kept in the dark at 4 °C for 3 h prior to flow cytometry analysis. The proliferation index was calculated as the sum of cells in S and G2/M phases of cell cycle.

β-Galactosidase assay

To evaluate 3AB-OS senescence after p53-R248W/P72R Cell Signaling b-Galactosidase staining kit was used, according with the manufacturer's instructions.

Cell death assays

Apoptotic morphology was studied in cells stained with Hoechst 33342 (Sigma-Aldrich). In particular, cells were stained with Hoechst 33342 (2.5 μg/ml medium) for 30 min at 37 °C, visualized by fluorescence microscopy using an appropriate filter for DAPI; images were photographed and captured. Cells were evaluated on the basis of their nuclear morphology, noting the presence of homogeneous chromatin, condensed chromatin, and fragmented nuclei. Apoptosis was also studied by flowcytometry of either DNA content or annexin V labelling. The DNA staining protocol has been described in "Cell cycle and proliferation analyses". The proportion of cells giving fluorescence in the sub-G0/G1 peak of cell cycle was taken as a

measure of apoptosis. For annexin V labelling, trypsinized cell suspensionswere centrifuged, washed 3 times with PBS and resuspended in 1× annexin V binding buffer (BD Biosciences Pharmingen, San Diego, CA) at a concentration of 1 × 106 cells/ml. One hundred microliters of cell suspension was then incubated with 5μl of annexin V-FITC (BD Biosciences) and 5 μL of PI for 15 min at a room temperature in the dark. Double labelled with annexin V and PI allows a distinction of early apoptotic (annexin V+/PI−) and late apoptotic/necrotic (annexin V+/PI+) cells. Flow cytometry analyses were performed by a COULTER EPICS XL flow cytometer (Beckman Coulter Srl, Cassina De Pecchi (MI), Italy) equipped with a single Argon ion laser (emission wavelength of 488 nm) and Expo 32 software. The green fluorescence was measured in the FL1 channel using a 515-nm BP filter, and the red fluorescence was measured in the FL3 channel using a 620-nm BP filter. At least 1 × 104 cells per sample were analyzed and data were stored in list mode files.

Measurement of mitochondrial transmembrane potential (Δψm)

Mitochondrial membrane potential was measured by the cationic lipophilic fluorochrome 3,3-dihexyloxacarbocyanine (DiOC6 Molecular Probes, Eugene, OR), which exclusively emits within the spectrum of green light. Loss in DiOC6 staining indicates disruption of the mitochondrial inner transmembrane potential (ΔΨm). Cells were incubated with 40 nM DiOC6 for 20 min at 37°C, washed twice with PBS and analysed by flow cytometry. The green fluorescence was measured as above described.

In vitro Matrigel invasion assay

Invasion assays were performed using 6-well invasion chamber system (BD Biosciences, Discovery Labware, Becton Dickinson, Buccinasco, Italy). Cells were trypsinized and counted with a hemocytometer using trypan blue, and viable cells were seeded in the upper chamber at 1 ×105 cells/well in serum-free DMEM. DMEM supplemented with 10% FBS

(used as a chemoattractant)was placed in the bottom well. Incubation was carried out for 48 h at 37 °C in humidified air with 5% CO2. Non-migratory cells in the upper chamber were then removed with a cotton-tip applicator. Migrated cells on the lower surface were stained with Hoechst 33342 (2.5 μg/ml; Sigma-Aldrich) for 10 min and then visualized under an inverted microscope. The number of migrating cells was determined by counting five high-powered fields (200×) on each membrane. Four independent experiments were performed in

triplicate.

Construction of expression vector expressing p53 mutation p53-R248W/P72R and transfection in MG63 cells.

RNA from 3AB-OS cell line was isolated using TRI Reagent (Sigma- Aldrich), according to manufacturer's instructions. cDNA was amplified from 2 μg of RNA using M-MuLV reverse transcriptase (New England Biolabs, Euroclone, Pero, Italy). The following protocol was performed: RNA was incubated with dNTPs (Amersham Biosciences) and Random Examers (Promega Italia Srl, Milano, Italy) at 70 °C for 10 min and in ice for 1 min; then, after the addition of M-MuLV and the specific buffer, the incubation was performed at 42 °C for 1 h and at 90 °C for 10 min. The following primerswere used to amplified TP53 (≈1.2 kb): forward (BamHI restriction site-containing) 5′-CGTAGGATCCAGCCATGGAGGAGCCGCAG-3′ and reverse (XhoI restriction site-containig) 5′-CGGATCTCGAGCAATTCAGTCTGAGTCAGGCC-3′. For PCR amplification with Phusion Taq polymerase (New England Biolabs), the following protocol was performed: 98 °C for 2 min; 12 cycles at 98 °C for 10 s, 63 °C for 20 s and 72 °C for 30 s; 18 cycles at 98 °C for 10 s and 72 °C for 30 s; a final extension at 72 °C for 7 min. The amplified product was resolved by agarose gel electrophoresis (1% agarose and 0.5 μg/ml ethidium bromide; Sigma-Aldrich) and the band was extracted using Wizard SV Gel and PCR

Clean-up system (Promega Italia Srl). PCR product and pcDNA 3.1 vector (Invitrogen) were digested for 2 h at 37 °C with BamHI-HF and XhoI (New England Biolabs), resolved by agarose gel electrophoresis and extracted. Vector dephosphorylation and ligation reactions were performed using the Rapid Dephosphorylation and Ligation kit (Roche, Milano, Italy) according to manufacturer's instructions. The ligation mixture was transformed into calcium chloride-competent DH5α cells (Invitrogen). Plasmids after BamHI–XhoI digestion that showed the presence of a 1.2-kb insert were validated by sequencing (Ceinge Sequencing Service, Ceinge, Napoli, Italy). MG63 cells were plated in 6-well dishes until they reached 90% confluence and then transfected with p53-R248W/P72R-pcDNA 3.1 or empty vector, as a control, using Lipofectamine 2000 (Invitrogen) according to manufacturer's instructions. Two days after transfections, the cells were transferred in 100 mm dishes in selective medium containing 300 μg/ml G418 (Gibco, Life Technologies Ltd, Monza, Italy); the medium was replaced every 3–4 days. A plate of untrasfected cells was used as a control for the selection.

Construction of expression vector expressing a sh-p53 and transduction in 3AB-OS cells.

For transduction experiments shScramble-pLKO-1 puro and shp53-pLKO.1 puro vectors were used to construct 3AB-OS/sh-Scramble and 3AB-OS/sh-p53 cells respectively .

$2x10^6$ HEK-293FT cells were seeded in 10cm dish.

The day after the packaging was prepared as follow:

-7μg of shp53-PLKO.1 puro vector

-6μg of psPAX8-plasmid

- 5μg of CMV-VSVG plasmid

H_2O (to a final volume of 450μl)

To these 450µl, 50µl of $CaCl_2$ (2,5M) were added. After 10-20 minutes 500µl of HBS(2X) vortexing or making bubbles. The final volume of this mix is 1ml. After changing the medium to HEK-293FT putting 9ml of fresh DMEM, the mix above was added. The cells were incubated at 37°C. After 8-15 hours the medium was changed (using the medium used for the cells-DMEM). After approximately 36 hour the virus were harvest; polybrene (8µg/ml) was added to the medium that was filtered through a 0,45µm filter on a syringe and then added to 3AB-OS (incubated at 37°C). After 8-15 hours the medium was changed and after 48 hours the cells were put in selection with puromicyn

Sarcosphere formation assay

MG63 cells transfected with pcDNA3.1-p53-R248W/P72R or empty pcDNA3.1 vector were seeded in 6-well ultra-low attachment plates (Corning Costar, Euroclone) at a density of 500 cells/well with 3 ml stem cell medium consisting of DMEM/F12 (Gibco), B27 (1× Gibco), recombinant human epidermal growth factor (rhEGF, 20 ng/ml; Sigma-Aldrich) and basic fibroblast growth factor (bFGF, 20 ng/ml; Sigma-Aldrich). The stem cell medium was changed every 3 days, and cells were observed every day by microscopy. After the primary spheres reached approximately ≥50 µm in diameter (determined using the ImageJ software), they were collected by gentle centrifugation (800 rpm), enzymatically dissociated (10 min at 37 °C in 0.05% trypsin–EDTA; Life Technologies Ltd) to single cells and replanted into 6-well ultra-low attachment plates with 500 cells/well and cultured with stem cell medium to generate spheres of the next generation. For the 3AB-OS/sh-Scramble and 3AB-OS/sh-p53 cells the same protocols was followed but the cells were seeded at a density of 500 cells/well.

Colony formation assay

MG63 cells transfected with pcDNA3.1-p53-R248W/P72R or empty pcDNA3.1 vector were seeded in 6-well plates at a density of 100 cells/well with 3 ml culture medium and incubated

for 10 days. The medium was changed every 3 days, and cells were observed every day by microscopy. On the tenth day, media was removed from the wells and washed once with ice-cold PBS. The colonies were fixed with 50% EtOH and stained with 1% methylene blue (Sigma-Aldrich) for 10 min. After three washes with PBS, the colonies consisting of N50 cells were counted using microscopy. Colony size was determined by measuring the area with the ImageJ software. For the 3AB-OS/sh-Scramble and 3AB-OS/sh-p53 cells the same protocol was followed but at the end the cells were fixed with 4% of formaldeide and they were stained with 0,1% of crystal violet.

Scratch/wound-healing assay

To analyze cell migration by wound healing, confluent monolayers of MG63 cells transfected with pcDNA3.1-p53-R248W/P72R or empty pcDNA3.1 vector and cultured in 6-well plates were scratched with a 200-µl pipette tip to generate the wound. One hour before scratching, the medium was replaced with medium containing 0.1% FBS to minimize the cell proliferation. Phase-contrast photographs of the same region were taken with the same magnification (100×) at 0, 8 and 24 h post-wounding. The extent of wound closure was determined by measuring with the ImageJ software the area of cells that migrated into the wound and then dividing by the total area of wound. For the 3AB-OS/sh-Scramble and 3AB-OS/sh-p53 cells the Incucyte/wound-healing system was used and the cells were monitored among 0 and 16 hours post scratch insult. The Incucyte-system software measured the wound closure.

Flow cytometry analysis of CD133, ABCG2 and p53 expression

Cells were detached using 0.025% trypsin–EDTA in PBS, counted and washed in 0.1% BSA in PBS at 4 °C. At least 500,000 cells (in 100 µl PBS/ 0.5% BSA) were incubated with fluorescent-labelled monoclonal antibodies or respective isotype controls (1/10 diluted 4 °C for 30 min in the dark). After washing steps, the labelled cells were analyzed by flow

cytometry using COULTER EPICS XL (Beckman-Coulter Srl) and Expo 32 software. The antibodies used were mouse anti-human CD133/2 PE conjugated (Miltenyi Biotec S.r.l., Bologna, Italy), mouse anti-human ABCG2 nonconjugated (Santa Cruz Biotechnology) and mouse anti-human p53 nonconjugated (Santa Cruz Biotechnology). For indirect labelling, cellswere incubatedwith a compatible secondary antibody FITC conjugated (Santa Cruz Biotechnology, Inc.). For intracellular staining of CD133, ABCG2 and p53, cells were processed using the Caltag Fix & Perm Kit (Invitrogen) following the manufacturer's guidelines. The green fluorescence was measured as described in the Cell death assays section, and the phycoerythrin fluorescence was measured in the FL2 channel using a 575-nm BP filter. At least 1 × 104 cells per sample were analyzed, and data were stored in list mode files. The expression of cell markers was determined by comparison with isotype control.

RNA extraction and real-time RT-PCR

RNA was extracted by Trizol reagent (Life Technologies Ltd, Monza, Italy); a DNase I treatment step was included. One microgram of total RNA was reverse transcribed in a final volume of 20 μl reverse transcription (RT) by using a Super-Script First-Strand Synthesis kit for RT-PCR (Life Technologies Ltd) according to the manufacturer's instructions. The resulting cDNAs were used for quantitative analysis by real-time PCR (qPCR) using the primers reported in following table and the Power SYBR Green PCR Master Mix (Applied Biosystem, Warrington, UK). Reactions were performed in 96-well plates according to manufacturer's instructions, using Applied Biosystems StepOneTM instrument. levels were determined using the 2−ΔΔCt method and normalized to endogenous β-actin and GAPDH levels. The primer sequences used are listed in the following table.

Gene	**Forward Primer 5'-3'**	**Reverse Primer 5'-3'**
CD133	ttggctcagactggtaaatccc	ataggaaggactcgttgctggt
OCT4	ctgggggttctatttggga	ctggttcgctttctctttcg
Nanog	gcaagaactctccaacatcctga	gccacctcttagatttcattctctg
Sox2	cacccacagcaaatgacag	tacaaggtccattcccccg

Nucleostemin (NS)	gggaagataaccaagcgtgtg	cctccaagaagtttccaaagg
E-Cadherin	gcaaattcctgccattctgg	cgaagaaacagcaagagcagc
VIM	agagaggaagccgaaaacac	tgttcctgaatctgagcctg
N-Cadherin	tcaacttgccagaaaactccag	ccgcagtgaaaggtttttatctct
β-catenin	agtgctgaaggtgctatctg	tgaaagattcctgagagtcc
MMP-9	cctggagacctgagaaccaatc	gatttcgactctccacgcatc
MMP-2	acgaagacccacaggaggag	tagccagtcggatttgatgc
ITGA5	cccagacttctttggctctg	gcaagatctgagccttgtcc
ITGAV	ttgttgctactggctgttttg	tccctttcttgttcttcttgag
RB1	caccaatacctcacattcctc	ttctcagaagtcccgaatg
p107	gatgctacaaaaacacctgactg	gctgctgggaaatgcggc
RB2	tacacgctggagggaaat	ttccactgtccctttgcttac
E2F1	gacctgctgctcttcgccac	tttcacacctttttcctggatg
E2F4	ggacggcgtgcttgacctc	cccttccactggatgctgt
p21	ctgtcttgtacccttgtgcctc	aatctgtcatgctggtctgcc
p27	ctgcaaccgacgattcttct	gcttcttgggcgtctgctc
GADD45	agaccccggacctgcact	ccggcaaaaacaaataagttgact
CDK4	cggggctggcgtgagggtc	actgtggggatcacgggc
Bcl-2	ggataacggaggctgggat	ggcaggcatgttgacttcac
Bcl-xl	tccttgtctacgctttccac	ggtcgcattgtggccttt
Bax	cagaggcgggggggc	gtccacggcggcaatcatc
Puma	acgacctcaacgcacagtacg	tcccatgatgagattgtacaggac
α-actin	ggacttcgagcaagagatgg	agcactgtgttggcgtacag
P53	tagtgtggtggtgccctatg	cccatgcaggaactgttacac
Cyclin D1	ggcggaggagaacaaacaga	ctcctcaggttcaggccttg
Cyclin D2	gctggaggtctgtgaggaac	agttgcagatgggacttcgg
Cyclin E1	atacttgctgcttcggcctt	tcagttttgagctccccgtc
Cyclin E2	gcccagataatccaggcca	acaggtggccaacaattcct
CDKN2C	caggactctccccatctcca	tcaggctttctgctgtaggc
VANGL1	agtaaagaagcggaaagcaaggc	ctggagacgctgaatgtggatg
CD44	acagacagaatccctgctaccac	tgcctcttggttgctgtctcag
SNAIL1	gctgcaggactctaatccaga	atctccggaggtgggatg
SNAIL2	tggttgcttcaaggacacat	gttgcagtgagggcaagaa
ZEB1	gccaacagaccagacagtgtt	tttcttgcccttcctttctg
ZEB2	aagccagggacagatcagc	gccacactctgtgcattt
KLF-4	tgtgactatgcaggctgtg	aggtttctcgcctgtgtg

Western blotting analysis

Cells were washed in PBS and incubated on ice-cold lysis buffer (RIPA buffer 50 µl/106 cells) containing protease inhibitor cocktail for 30 min and sonicated three times for 10 s. Equivalent amounts of proteins (20-40 µg) were separated by SDS– polyacrylamide gel electrophoresis and transferred to a nitrocellulose membrane (Bio-Rad/Amersham) for detection with primary antibodies and the appropriate peroxidase–conjugated secondary

antibodies. Immunoreactive signals were detected using enhanced chemiluminescence (ECL) reagents (Bio-Rad/Pierce). The correct protein loading was confirmed by stripping the immunoblot and reprobing with primary antibody for actin (diluted 1:500; Sigma) and GAPDH (1:10000;Santa Cruz). To detect the protein expression levels during transient p53-knockdowm experiments Chemi Doc XRS (Bio-Rad) system was used while Amersham® Hyperfilm® ECL™ and MP Autoradiography Films,GE Healthcare were used to detect the expression levels of the proteins analyzed during stable p53-knockdown.Quantification was performed using Quantity One software, and the data (relative density normalized to actin) were expressed as mean ± SD of four experiments. The primary antibodies used during transient p53 silencing are listed below.

ANTIBODY	**HOST ORIGIN**	**DILUTION**	**COMPANY**	**PRODUCT NUMBER**
CD133	Rabbit	1:300	Abgent	AP2010b
Oct3/4	Mouse	1:300	Santa Cruz Biotechnology	sc-5279
Nanog	Goat	1:500	Santa Cruz Biotechnology	sc-30331
Sox2	Rabbit	1:300	Santa Cruz Biotechnology	sc-20088
Nucleostemin (NS)	Goat	1:500	Santa Cruz Biotechnology	sc-46218
mmp2	Rabbit	1:300	Santa Cruz Biotechnology	sc-10736
mmp9	Rabbit	1:1000	Cell Signaling	3852S
Itga5	Rabbit	1:300	Santa Cruz Biotechnology	sc-10729
Itgav	Rabbit	1:300	Santa Cruz Biotechnology	sc-10719
E-chaderin	Mouse	1:300	Santa Cruz Biotechnology	sc-1500
Vimentin	Mouse	1:500	Santa Cruz Biotechnology	sc-73259
N-chaderin	Mouse	1:500	Santa Cruz Biotechnology	sc-8424
□-catenin	Mouse	1:500	Santa Cruz Biotechnology	sc-7963
pRb	Mouse	1:500	Santa Cruz Biotechnology	sc-102
p107	Rabbit	1:200	Santa Cruz Biotechnology	sc-318
p130	Mouse	1:300	Santa Cruz Biotechnology	sc-9963

E2f1	Rabbit	1:500	Santa Cruz Biotechnology	sc-193
E2f4	Rabbit	1:300	Santa Cruz Biotechnology	sc-866
p53	Mouse	1:500	Santa Cruz Biotechnology	sc-126
p21	Rabbit	1:200	Santa Cruz Biotechnology	sc-397
p27	Rabbit	1:200	Santa Cruz Biotechnology	sc-1641
Gadd45	Mouse	1:300	Santa Cruz Biotechnology	sc-6850
Cdk4	Rabbit	1:200	Santa Cruz Biotechnology	sc-601
Bcl-2	Mouse	1:500	Santa Cruz Biotechnology	sc-509
Bcl-XL	Mouse	1:500	Santa Cruz Biotechnology	sc-8392
Bax	Mouse	1:500	Santa Cruz Biotechnology	sc-7480
Puma	Mouse	1:300	Santa Cruz Biotechnology	sc-377015
DR4	Rabbit	1:500	ProSci Incorporeted	1139
DR5	Rabbit	1:500	ProSci Incorporeted	2019
FAS	Mouse	1:300	Santa Cruz Biotechnology	sc-8009
actin	Rabbit	1:500	Sigma	A5060

The primary antibodies used during stable p53 silencing are listed below.

ANTIBODY	**HOST ORIGIN**	**DILUTION**	**COMPANY**	**PRODUCT NUMBER**
p53	Mouse	1:1000	Santa Cruz Biotechnology	sc-126
CyclinD1	Mouse	1:1000	Santa Cruz Biotechnology	sc-20044
CyclinB1	Mouse	1:1000	Cell Signaling	4135
p21	Mouse	1:1000	Santa Cruz Biotechnology	sc-6246
p27	Rabbit	1:1000	Cell Signaling	2552
CDK6	Rabbit	1:1000	Santa Cruz Biotechnology	sc-177
Bax	Mouse	1:1000	Santa Cruz Biotechnology	sc-7480
Bad	Rabbit	1:1000	Cell Signaling	9292
Bcl-2	Mouse	1:1000	Santa Cruz Biotechnology	sc-7382
Bcl-XL	Rabbit	1:1000	Cell Signaling	2762

LaminB1	Mouse	1:500	Santa Cruz Biotechnology	sc-377000
PARP	Rabbit	1:1000	Cell Signaling	9542
Caspase-3	Rabbit	1:1000	Cell Signaling	9662
MMP2	Rabbit	1:1000	Abcam	ab80737
MMP9	Rabbit	1:1000	Abcam	ab38898
N-cadherin	Rabbit	1:1000	Abcam	ab18203
Vimentin	Mouse	1:1000	Santa Cruz Biotechnology	sc-373717
CD44	Rabbit	1:100	Cell Signaling	3578
Oct4	Rabbit	1:1000	Abcam	ab19857
Nanog	Rabbit	1:200	Abcam	ab21603
Sox2	Mouse	1:500	R&D system	MAB2018
Klf4	Rabbit	1:100	Santa Cruz Biotechnology	sc-2069
GAPDH	Rabbit	1:10000	Santa Cruz Biotechnology	sc-25778

Chromatin binding assay

The ability of p53-R248W/P72R to bind the DNA was evaluated according to the protocol described by LIano M. (151).

Statistical Analysis

Data, represented as mean ± SD, were analyzed using the 2-tailed Student t-test using Microsoft Excel. Differences were considered significant when $P < 0.05$.

REFERENCES

1. ***Osteosarcoma originates from mesenchymal stem cells in consequence of aneuploidization and genomic loss of Cdkn2***. Mohseny AB, Szuhai K, Romeo S, Buddingh EP, Briaire-de Bruijn I, de Jong D, Van Pel M, Cleton-Jansen AM, Hogendoorn PC. J Pathol. 2009 Nov;219(3):294-305. doi: 10.1002/path.2603.
2. ***Malignant bone tumors***. Gibbs CP Jr, Weber K, Scarborough MT. Instr Course Lect. 2002;51:413-28. Review.Gibbs CP, Jr, Weber K, Scarborough MT. Malignant bone tumors. Instr Course Lect. 2002;51:413–428
3. ***Osteosarcoma: a randomized, prospective trial of the addition of ifosfamide and/or muramyl tripeptide to cisplatin, doxorubicin, and high-dose methotrexate.*** Meyers PA, Schwartz CL, Krailo M, Kleinerman ES, Betcher D, Bernstein ML, Conrad E, Ferguson W, Gebhardt M, Goorin AM, Harris MB, Healey J, Huvos A, Link M, Montebello J, Nadel H, Nieder M, Sato J, Siegal G, Weiner M, Wells R, Wold L, Womer R, Grier H. J Clin Oncol. 2005 Mar 20;23(9):2004-11.
4. ***Updates on the cytogenetics and molecular genetics of bone and soft tissue tumors: osteosarcoma and related tumors***. Sandberg AA, Bridge JA. Cancer Gene Cytogenet. 2003;145(1):1–30.
5. ***Alterations of the p53, Rb and MDM2 genes in osteosarcoma***. Miller CW, Aslo A, Won A, Tan M, Lampkin B, Koeffler HP. J Cancer Res Clin Oncol. 1996;122(9):559-65.
6. ***Loss of heterozygosity of the RB gene is a poor prognostic factor in patients with osteosarcoma***. Feugeas O, Guriec N, Babin-Boilletot A, Marcellin L, Simon P, Babin S, Thyss A, Hofman P, Terrier P, Kalifa C, Brunat-Mentigny M, Patricot LM,

Oberling F. J Clin Oncol. 1996 Feb;14(2):467-72. Erratum in: J Clin Oncol 1996 Aug;14(8):2411.

7. ***Osteosarcoma development and stem cell differentiation***. Tang N, Song WX, Luo J, Haydon RC, He TC. Clin Orthop Relat Res. 2008 Sep;466(9):2114-30. doi: 10.1007/s11999-008-0335-z. Epub 2008 Jun 18. Review.
8. ***P16INK4a overexpression and survival in osteosarcoma patients: a meta-analysis***. Bu J, Li H, Liu LH, Ouyang YR, Guo HB, Li XY, Xiao T. Int J Clin Exp Pathol. 2014 Aug 15;7(9):6091-6. eCollection 2014.
9. ***Wnt inhibitory factor 1 decreases tumorigenesis and metastasis in osteosarcoma***. Rubin EM, Guo Y, Tu K, Xie J, Zi X, Hoang BH. Mol Cancer Ther. 2010 Mar;9(3):731-41. doi: 10.1158/1535-7163.MCT-09-0147. Epub 2010 Mar 2.
10. ***A review of targeted therapies evaluated by the pediatric preclinical testing program for osteosarcoma***. Sampson VB, Gorlick R, Kamara D, Anders Kolb E. Front Oncol. 2013 May 31;3:132. doi: 10.3389/fonc.2013.00132. Collection 2013.
11. ***Etoposide and carbo-or cisplatin combination therapy in refractory or relapsed Ewing sarcoma: A large retrospective study***. Van Maldegem AM, Benson C, Rutkowski P, Blay JY, van den Berg H, Placzke J, Rasper M, Judson I, Juergens H, Dirksen U, Gelderblom H.

    Pediatr Blood Cancer. 2015 Jan;62(1):40-4. doi: 10.1002/pbc.25230. Epub 2014 Sep 22.
12. ***Multiple receptor tyrosine kinases promote the in vitro phenotype of metastatic human osteosarcoma cell lines***. Rettew AN, Young ED, Lev DC, Kleinerman ES, Abdul-Karim FW, Getty PJ, Greenfield EM. Oncogenesis. 2012 Nov 19;1:e34. doi: 10.1038/oncsis.2012.34.

13. ***A prognostic evaluation of vascular endothelial growth factor in children and young adults with osteosarcoma***. Ługowska I, Woźniak W, Klepacka T, Michalak E, Szamotulska K. Pediatr Blood Cancer. 2011 Jul 15;57(1):63-8. doi: 10.1002/pbc.23021. Epub 2011 Mar 17.

14. ***Phase I evaluation of cediranib, a selective VEGFR signalling inhibitor, in combination with gefitinib in patients with advanced tumours.*** Van Cruijsen H, Voest EE, Punt CJ, Hoekman K, Witteveen PO, Meijerink MR, Puchalski TA, Robertson J, Saunders O, Jürgensmeier JM, van Herpen CM, Giaccone G. Eur J Cancer. 2010 Mar;46(5):901-11. doi: 10.1016/j.ejca.2009.12.023. Epub 2010 Jan 12.

15. ***Targeted therapies in Ewing's sarcoma***. Scotlandi K. Adv Exp Med Biol. 2006;587:13-22. Review.

16. ***Inhibition of insulin-like growth factor-I receptor (IGF-IR) signaling and tumor cell growth by a fully human neutralizing anti-IGF-IR antibody***.Wang Y,Hailey J,Williams D, Wang Y, Lipari P, Malkowski M, Wang X, Xie L, Li G, Saha D, Ling WL, Cannon-Carlson S, Greenberg R, Ramos RA, Shields R,Presta L, Brams P, Bishop WR, Pachter JA. Mol Cancer Ther. 2005 Aug;4(8):1214-21.

17. ***Initial testing (stage1) of a monoclonal antibody (SCH 717454) against the IGF-1 receptor by the pediatric preclinical testing program*** Kolb E. A., Gorlick R., Houghton P. J., Morton C. L., Lock R., Carol H., et al. *Pediatr. Blood Cancer* 2008;50 1190–1197

18. ***Rapamycin inhibits ezrin-mediated metastatic behavior in a murine model of osteosarcoma***. Wan X, Mendoza A, Khanna C, Helman LJ. Cancer Res. 2005 Mar 15;65(6):2406-1

19. ***Review of the complexities of the PI3K/mTOR pathway presages similar handling of other critical topics.*** Alfred Yung WK. Neuro Oncol. 2010 Aug;12(8):763-4. doi: 10.1093/neuonc/noq083

20. ***Initial testing (stage 1) of the mTOR inhibitor rapamycin by the pediatric preclinical testing program.*** Houghton PJ, Morton CL, Kolb EA, Gorlick R, Lock R, Carol H, Reynolds CP, Maris JM, Keir ST, Billups CA, Smith MA. Pediatr Blood Cancer. 2008 Apr;50(4):799-805.

21. ***Stage 2 combination testing of rapamycin with cytotoxic agents by the Pediatric Preclinical Testing Program.***Houghton PJ, Morton CL, Gorlick R, Lock RB, Carol H, Reynolds CP, Kang MH, Maris JM, Keir ST, Kolb EA, Wu J, Wozniak AW, Billups CA, Rubinstein L, Smith MA. Mol Cancer Ther. 2010 Jan;9(1):101-12. doi: 10.1158/1535-7163.MCT-09-0952. Epub 2010 Jan 6.

22. ***Results of a phase II study of sirolimus and cyclophosphamide in patients with advanced sarcoma.*** Schuetze SM, Zhao L, Chugh R, Thomas DG, Lucas DR, Metko G, Zalupski MM, Baker LH. Eur J Cancer. 2012 Jun;48(9):1347-53. doi: 10.1016/j.ejca.2012.03.022. Epub 2012 Apr 21.

23. ***Phase II study of the mammalian target of rapamycin inhibitor ridaforolimus in patients with advanced bone and soft tissue sarcomas.*** Chawla SP, Staddon AP, Baker LH, Schuetze SM, Tolcher AW, D'Amato GZ, Blay JY, Mita MM, Sankhala KK, Berk L, Rivera VM, Clackson T, Loewy JW, Haluska FG, Demetri GD. J Clin Oncol. 2012 Jan 1;30(1):78-84. doi: 10.1200/JCO.2011.35.6329. Epub 2011 Nov 7.

24. ***Results of the phase III, placebo-controlled trial (SUCCEED) evaluating the mTOR inhibitor ridaforolimus (R) as maintenance therapy in advanced sarcoma patients (pts) following clinical benefit from prior standard cytotoxic chemotherapy (CT).*** S. P. Chawla, J. Blay, I. L. Ray-Coquard, A. Le Cesne, A. P. et al. J Clin Oncol 29: 2011 (suppl; abstr 10005)

25. ***Preliminary efficacy of the anti-insulin-like growth factor type 1 receptor antibody figitumumab in patients with refractory Ewing sarcoma***. Juergens H, Daw NC, Geoerger B, Ferrari S, Villarroel M, Aerts I, Whelan J, Dirksen U, Hixon ML, Yin D, Wang T, Green S, Paccagnella L, Gualberto A.J Clin Oncol. **2011** Dec 1;29(34):4534-40. doi: 10.1200/JCO.2010.33.0670. Epub **2011** Oct 24.
26. ***Combination mTOR and IGF-1R inhibition: phase I trial of everolimus and figitumumab in patients with advanced sarcomas and other solid tumors.***Quek R, Wang Q, Morgan JA, Shapiro GI, Butrynski JE, Ramaiya N, Huftalen T, Jederlinic N, Manola J, Wagner AJ, Demetri GD, George S. Clin Cancer Res. 2011 Feb 15;17(4):871-9. doi: 10.1158/1078-0432.CCR-10-2621. Epub 2010 Dec 22.
27. ***Combination testing (Stage2) of the Anti-IGF-1receptorantibodyIMC-A12 with rapamycin by the pediatric preclinical testing program.*** Kolb E. A., Gorlick R., Maris J. M., Keir S. T., Morton C. L., Wu J, et al. (2012). *Pediatr. Blood Cancer* 58 729–735
28. ***PI3-K/Akt-mediated anoikis resistance of human osteosarcoma cells requires Src activation.*** Díaz-Montero CM, Wygant JN, McIntyre BW. Eur Cancer. 2006 Jul;42(10):1491-500. Epub 2006 Jun 8.
29. ***Initial testing (stage 1) of the Akt inhibitor GSK690693 by the pediatric preclinical testing program.*** Carol H, Morton CL, Gorlick R, Kolb EA, Keir ST, Reynolds CP, Kang MH, Maris JM, Billups C, Smith MA, Houghton PJ, Lock RB. Pediatr Blood Cancer. 2010 Dec 15;55(7):1329-37. doi: 10.1002/pbc.22710. Epub 2010 Aug 25.
30. ***R1507, a fully human monoclonal antibody targeting IGF-1R, is effective alone and in combination with rapamycin in inhibiting growth of osteosarcoma xenografts***. Kolb E. A., Kamara D., Zhang W., Lin J., Hingorani P., Baker L., et al. (2010). *Pediatr. Blood Cancer* 55 67–75

31. ***Dinaciclib (SCH 727965), a novel and potent cyclin-dependent kinase inhibitor.*** Parry D, Guzi T, Shanahan F, Davis N, Prabhavalkar D, Wiswell D, Seghezzi W, Paruch K, Dwyer MP, Doll R, Nomeir A, Windsor W, Fischmann T, Wang Y, Oft M, Chen T, Kirschmeier P, Lees EM. Mol Cancer Ther. **2010** Aug;9(8):2344-53. doi: 10.1158/1535-7163.MCT-10-0324. Epub **2010** Jul 27.

32. ***Frequency and structure of p53 rearrangements in human osteosarcoma.*** Miller CW, Aslo A, Tsay C, Slamon D, Ishizaki K, Toguchida J, Yamamuro T, Lampkin B, Koeffler HP. Cancer Res. 1990 Dec 15;50(24):7950-4.

33. ***Characterization of the 12q15 MDM2 and 12q13-14 CDK4 amplicons and clinical correlations in osteosarcoma***. Mejia-Guerrero S, Quejada M, Gokgoz N, Gill M, Parkes RK, Wunder JS, Andrulis IL. Genes Chromosomes Cancer. 2010 Jun;49(6):518-25. doi: 10.1002/gcc.20761.

34. A ***phase I first-in-human pharmacokinetic and pharmacodynamic study of serdemetan in patients with advanced solid tumors***. Tabernero J, Dirix L, Schöffski P, Cervantes A, Lopez-Martin JA, Capdevila J, van Beijsterveldt L, Platero S, Hall B, Yuan Z, Knoblauch R, Zhuang SH. Clin Cancer Res. 2011 Oct 1;17(19):6313-21. doi: 10.1158/1078-0432.CCR-11-1101. Epub 2011 Aug 10.

35. ***MDM2 inhibitor Nutlin-3a suppresses proliferation and promotes apoptosis in osteosarcoma cells.*** Wang B, Fang L, Zhao H, Xiang T, Wang D. Acta Biochim Biophys Sin (Shanghai). 2012 Aug;44(8):685-91. doi: 10.1093/abbs/gms053.

36. ***Chemotherapeutic agents sensitize sarcoma cell lines to tumor necrosis factor-related apoptosis-inducing ligand-induced caspase-8 activation, apoptosis and loss of mitochondrial membrane potential.***Hotta T, Suzuki H, Nagai S, Yamamoto K, Imakiire A, Takada E, Itoh M, Mizuguchi J. J Orthop Res. 2003 Sep;21(5):949-57.

37. ***Initial testing (stage 1) of LCL161, a SMAC mimetic, by the Pediatric Preclinical Testing Program***. Houghton PJ, Kang MH, Reynolds CP, Morton CL, Kolb EA, Gorlick R, Keir ST, Carol H, Lock R, Maris JM, Billups CA, Smith MA. Pediatr Blood Cancer. 2012 Apr;58(4):636-9. doi: 10.1002/pbc.23167. Epub 2011 Jun 16.
38. ***The pediatric preclinical testing program: description of models and early testing results.*** Houghton PJ, Morton CL, Tucker C, Payne D, Favours E, Cole C, Gorlick R, Kolb EA, Zhang W, Lock R, Carol H, Tajbakhsh M, Reynolds CP, Maris JM, Courtright J, Keir ST, Friedman HS, Stopford C, Zeidner J, Wu J, Liu T, Billups CA, Khan J, Ansher S, Zhang J, Smith MA. Pediatr Blood Cancer. 2007 Dec;49(7):928-40.
39. ***Cancer stem cell detection and isolation***. Moghbeli M, Moghbeli F, Forghanifard MM, Abbaszadegan MR. Med Oncol. 2014 Sep;31(9):69. doi: 10.1007/s12032-014-0069-6. Epub 2014 Jul 27.
40. ***Cancer stem cell markers in esophageal cancer.*** Moghbeli M, Moghbeli F, Forghanifard MM, Garayali A, Abbaszadegan MR. Am J Cancer Sci. 2013;2(1):37–50.
41. ***Cancer stem cells: an old idea—a paradigm shift.*** Wicha MS, Liu S, Dontu G. Cancer Res. 2006;66(4):1883–90 discussion 95-6.
42. ***Cancer stem cells--important players in tumor therapy resistance.*** Colak S, Medema JP. FEBS J. 2014 Nov;281(21):4779-91. doi: 10.1111/febs.13023. Epub 2014 Sep 19.
43. ***CD44+ cancer cells express higher levels of the anti-apoptotic protein Bcl-2 in breast tumours***. Madjd Z, Mehrjerdi AZ, Sharifi AM, Molanaei S, Shahzadi SZ, Asadi-Lari M. Cancer Immun. 2009 Apr 23;9:4.
44. ***The anti-apoptotic genes Bcl-X(L) and Bcl-2are over-expressed and contribute to chemoresistance of non-proliferating leukaemic CD34+ cells.*** Konopleva, M., Zhao,

S., Hu, W., Jiang, S., Snell, V., Weidner, D., Jackson, C. E., Zhang, X., Champlin, R., Estey, E., Reed, J. C. & Andreeff, M. Br J Haematol. 2002 Aug;118(2):521-34.

45. ***Analysis of gene expression and chemoresistance of CD133+ cancer stem cells in glioblastom.*** Liu, G., Yuan, X., Zeng, Z., Tunici, P., Ng, H., Abdulkadir, I. R., Lu, L., Irvin, D., Black, K. L. & Yu, J. S. Mol Cancer. 2006 Dec 2;5:67.
46. ***Preferential expression of a high number of ATP binding cassette transporters in both normal and leukemic. CD34+CD38- cells***. De Grouw, E. P., Raaijmakers, M. H., Boezeman, J. B., van der Reijden, B. A., van de Locht, L. T., de Witte, T. J., Jansen, J. H. & Raymakers, R. A. Leukemia. 2006 Apr;20(4):750-4.
47. ***Expression of multidrug resistance genes in normal and cancer stem cells.*** Shervington, A. & Lu, C. Cancer Invest. 2008 Jun;26(5):535-42. doi: 10.1080/07357900801904140
48. ***Glioma stem cells promote radio-resistance by preferential activation of the DNA damage response.*** Bao, S., Wu, Q., Mc Lendon, R. E., Hao, Y., Shi, Q., Hjelmeland, A. B., Dewhirst, M. W., Bigner, D. D. & Rich, J. N. Nature. 2006 Dec 7;444(7120):756-60. Epub 2006 Oct 18.
49. ***CD133-targeted paclitaxel delivery inhibits local tumor recurrence in a mouse model of breast cancer.*** Swaminathan, S. K., Roger, E., Toti, U., Niu, L., Ohlfest, J. R. & Panyam, J. J Control Release. 2013 Nov 10;171(3):280-7. doi: 10.1016/j.jconrel.2013.07.014. Epub 2013 Jul 18.
50. ***Targeted inhibition of CD133+ cells in oral cancer cell lines.*** Damek-Poprawa, M., Volgina, A., Korostoff, J., Sollecito, T. P., Brose, M. S., O'Malley, B. W., Jr., Akintoye, S. O. & DiRienzo, J. M. J Dent Res. 2011 May;90(5):638-45. doi:10.1177/0022034510393511. Epub 2011 Jan 10.

51. ***Photochemical internalization (PCI) of immunotoxins targeting CD133 is specific and highly potent at femtomolar levels in cells with cancer stem cell properties.*** Bostad, M., Berg, K., Hogset, A., Skarpen, E., Stenmark, H. & Selbo, P. K. J Control Release. 2013 Jun 28;168(3):317-26. doi: 10.1016/j.jconrel.2013.03.023. Epub 2013 Apr 6.

52. ***CD47 is an adverse prognostic factor and therapeutic antibody target on human acute myeloid leukemia stem cells.*** Majeti, R., Chao, M. P., Alizadeh, A. A., Pang, W. W., Jaiswal, S., Gibbs, K. D., Jr., van Rooijen, N. & Weissman, I. L. Cell. 2009 Jul 23;138(2):286-99. doi: 10.1016/j.cell.2009.05.045.

53. ***The CD47-signal regulatory protein alpha (SIRPa) interaction is a therapeutic target for human solid tumors.*** Willingham, S. B., Volkmer, J. P., Gentles, A. J., Sahoo, D., Dalerba, P., Mitra, S. S. et al. Proc Natl Acad Sci U S A. 2012 Apr 24;109(17):6662-7. doi: 10.1073/pnas.1121623109. Epub 2012 Mar 26.

54. ***Identification of selective inhibitors of cancer stem cells by high-throughput screening,*** Gupta, P. B., Onder, T. T., Jiang, G., Tao, K., Kuperwasser, C., Weinberg, R. A. & Lander, E. S. Cell. 2009 Aug 21;138(4):645-59. doi: 10.1016/j.cell.2009.06.034. Epub 2009 Aug 13.

55. ***Salinomycin inhibits Wnt signaling and selectively induces apoptosis in chronic lymphocytic leukemia cells***. Lu, D., Choi, M. Y., Yu, J., Castro, J. E., Kipps, T. J. & Carson, D. A. Proc Natl Acad Sci U S A. 2011 Aug 9;108(32):13253-7. doi: 10.1073/pnas.1110431108. Epub 2011 Jul 25.

56. ***DLL4 blockade inhibits tumor growth and reduces tumor-initiating cell frequency.*** Hoey, T., Yen, W. C., Axelrod, F., Basi, J., Donigian, L., Dylla, S., Fitch-Bruhns, M., Lazetic, S., Park, I. K., Sato, A., Satyal, S., Wang, X., Clarke, M. F., Lewicki, J. & Gurney. Cell Stem Cell. 2009 Aug 7;5(2):168-77. doi: 10.1016/j.stem.2009.05.019.

57. ***A peri-vascular niche for brain tumor stem cells.*** Calabrese, C., Poppleton, H., Kocak, M., Hogg, T. L., Fuller, C., Hamner, B., Oh, E. Y., Gaber, M. W., Finklestein, D., Allen, M., Frank, A., Bayazitov, I. T., Zakharenko, S. S., Gajjar, A., Davidoff, A. & Gilbertson, R. J. Cancer Cell. 2007 Jan;11(1):69-82.

58. ***Targeting of CD44 eradicates human acute myeloid leukemic stem cells.*** Jin, L., Hope, K. J., Zhai, Q., Smadja-Joffe, F. & Dick, J. E. Nat Med. 2006 Oct;12(10):1167-74. Epub 2006 Sep 24.

59. ***Bone morphogenetic proteins inhibit the tumorigenic potential of human brain tumour-initiating cells.*** Piccirillo, S. G., Reynolds, B. A., Zanetti, N., Lamorte, G., Binda, E., Broggi, G., Brem, H., Olivi, A., Dimeco, F. & Vescovi, A. L. Nature. 2006 Dec 7;444(7120):761-5.

60. **p53 ubiquitination: Mdm2 and beyond.** Brooks, C. L. & Gu, W. Mol Cell. 2006 Feb 3;21(3):307-15. Review.

61. **Mdm2 is critically and continuously required to suppress lethal p53 activity *in vivo.*** Ringshausen, I., O'Shea, C. C., Finch, A. J., Swigart, L. B. & Evan, G. I. Cancer Cell. 2006 Dec;10(6):501-14.

62. **Regulating the p53 pathway: in vitro hypotheses, invivoveritas.** Toledo, F. & Wahl, G. M. Nat Rev Cancer. 2006 Dec;6(12):909-23.

63. **Mdm4 and Mdm2 cooperate to inhibit p53 activity in proliferating and quiescent cells in vivo.** Rancoz, S. et al. Proc Natl Acad Sci U S A. 2006 Feb 28;103(9):3232-7. Epub 2006 Feb 21.

64. **A dynamic role of HAUSP in the p53-Mdm2 pathway.** Li, M., Brooks, C. L., Kon, N. & Gu, W. Mol Cell. 2004 Mar 26;13(6):879-86.

65. **Critical role for Daxx in regulating Mdm2.** Tang, J. et al. Nat Cell Biol. 2006 Aug;8(8):855-62. Epub 2006 Jul 16.

66. **p53 in health and disease.** Vousden K. H. & Lane D. P. Nat Rev Mol Cell Biol. 2007 Apr;8(4):275-83. Review.

67. **Transcriptional control of human p53-regulated genes.** Riley, T., Sontag, E., Chen, P. & Levine, A. Nat Rev Mol Cell Biol. 2008 May;9(5):402-12. doi: 10.1038/nrm2395. Review

68. ***Ubiquitination, phosphorylation and acetylation: the molecular basis for p53 regulation.*** Brooks CL, Gu W. Curr Opin Cell Biol. 2003 Apr;15(2):164-71. Review

69. ***Tip60-dependent acetylation of p53 modulates the decision between cell-cycle arrest and apoptosis.*** Tang Y, Luo J, Zhang W, Gu W. Mol Cell. 2006 Dec 28;24(6):827-39.

70. ***Regulation of p53 responses by post-translational modifications.*** Xu Y. Cell Death Differ. 2003 Apr;10(4):400-3. Review.

71. ***The prolyl isomerase Pin1 is a regulator of p53 in genotoxic response.*** Zheng H, You H, Zhou XZ, Murray SA, Uchida T, Wulf G et al. Nature. 2002 Oct 24;419(6909):849-53. Epub 2002 Oct 2. Erratum in: Nature 2002 Nov 28;420(6914):445

72. ***Tumor suppression by p53 a role for the DNA DAMAGE RESPONSE?*** Meek DW.Nat Rev Cancer. 2009 Oct;9(10):714-23. doi: 10.1038/nrc2716. Epub 2009 Sep 4. Review.

73. ***P53:Its mutations and their impact on trascpription.*** Vaughan C, Pearsall I, Yeudall A, Deb SP, Deb S. Subcell Biochem. 2014;85:71-90. doi: 10.1007/978-94-017-9211-0_4. Review.

74. ***Molecular epidemiology of human cancer.*** Hussain SP, Harris CC. Toxicol Lett. 1998 Dec 28;102-103:219-25. Review.

75. ***Transcriptional regulation by mutant p53 and oncogenesis review*** Santoro R, Strano S, Blandino G. Subcell Biochem. 2014;85:91-103. doi: 10.1007/978-94-017-9211-0_5. Review.

76. ***Gain of function of mutant p53: the mutant p53/NF-Y protein complex reveals an aberrant transcriptional mechanism of cell cycle regulation.*** Di Agostino S, Strano S, Emiliozzi V, Zerbini V, Mottolese M, Sacchi A et al. Cancer Cell. 2006 Sep;10(3):191-202.

77. ***Mutant p53 cooperates with ETS and selectively up-regulates human MDR1 not MRP1.*** Sampath J, Sun D, Kidd VJ, Grenet J, Gandhi A, Shapiro LH et al. J Biol Chem. 2001 Oct 19;276(42):39359-67. Epub 2001 Aug 1.

78. ***Mutant p53 cooperates with ETS2 to promote etoposide resistance.*** Do PM, Varanasi L, Fan S, Li C, Kubacka I, Newman V et al. Genes Dev 2012 Apr 15;26(8):830–45; doi:10.1101/gad.181685.111.

79. ***A subset of tumor-derived mutant forms of p53 down-regulate p63 and p73 through a direct interaction with the p53 core domain.*** Gaiddon C, Lokshin M, Ahn J, Zhang T, Prives C. Mol Cell Biol. 2001 Mar;21(5):1874-87.;

80. ***Mutant p53: an oncogenic transcription factor.*** Strano S, Dell'Orso S, Di Agostino S, Fontemaggi G, Sacchi A, Blandino G (2007).. Oncogene Apr 2; 26(15);:2212–19; review.

81. ***Mutant p53 uses p63 as a molecular chaperone to alter gene expression and induce a pro-invasive secretome.*** Neilsen PM, Noll JE, Suetani RJ, Schulz RB, Al-Ejeh F, Evdokiou A et al (2011) Oncotarget 2011 Dec 2:1203–17.

82. ***Gain of function of p53 cancer mutants in disrupting critical DNA damage response.*** Song H, Xu Y. Cell Cycle. 2007 Jul 1;6(13):1570-3. Epub 2007 May 22.

83. ***Mutant p53 interactome identifies nardilysin as a p53R273H-specific binding partner that promotes invasion.*** Coffill CR, Muller PA, Oh HK, Neo SP, Hogue KA, Cheok CF et al.EMBO Rep 2012;13:638–644.

84. ***Mutant p53 is a transcriptional co-factor that binds to G-rich regulatory regions of active genes and generates transcriptional plasticity.*** Quante T, Otto B, Brazdova M, Kejnovska I, Deppert W, Tolstonog GV. Cell Cycle 2012; 11:3290–3303

85. ***Mutant p53 proteins bind DNA in a DNA structure-selective mode.*** Gohler T, Jager S, Warnecke G, Yasuda H, Kim E, Deppert W. Nucleic Acids Res 2005; 33:1087–1100;

86. ***Modulation of gene expression in U251 glioblastoma cells by binding of mutant p53 R273H to intronic and intergenic sequences.*** Brázdová M, Quante T, Tögel L, Walter K, Loscher C, Tichý V, Cincárová L, Deppert W, Tolstonog GV. Nucleic Acids Res. 2009 Apr;37(5):1486-500. doi: 10.1093/nar/gkn1085. Epub 2009 Jan 12)

87. ***Transcriptional activities of mutant p53: when mutations are more than a loss.*** Kim E, Deppert W. J Cell Biochem 2004 Nov 15;93(5):878–86; review.

88. ***Drastic effect of germline TP53 missense mutations in Li-Fraumeni patients.*** Zerdoumi Y, Aury-Landas J, Bonaiti-Pellie C, Derambure C, Sesboue R, Renaux-Petel M, Frebourg T, Bougeard G, Flaman JM. , 2013 Mar;34(3):453-61. doi: 10.1002/humu.22254. Epub 2013 Feb 11.

89. ***Transcription regulation by mutant p53.***Weisz L, Oren M, Rotter V. Oncogene 2007 Apr 2;26(15):2202–2211; review.

90. ***ChIP-on-chip analysis of in vivo mutant p53 binding to selected gene promoters.*** Dell'Orso S, Fontemaggi G, Stambolsky P, Goeman F, Voellenkle C, Levrero M et al. OMICS, 2011 May;15(5):305-12. doi: 10.1089/omi.2010.0084. Epub 2011 Feb 19.

91. ***ChIP-on-chip to identify mutant p53 targets.*** Goeman F, Fontemaggi G, Blandino G. Methods Mol Biol 2012;962:211–226.

92. ***ChIP sequencing to identify p53 targets.*** Vaughan C, Windle B, Deb S. Methods Mol Biol 2013;962:227–2369.

93. ***Modulation of gene expression by tumor-derived p53 mutants.*** Scian MJ, Stagliano KE, Ellis MA, Hassan S, Bowman M, Miles MF et al. Cancer Res 2004 Oct 15;64:7447–54

94. ***MicroRNA-128-2 targets the transcriptional repressor E2F5 enhancing mutant p53 gain of function.*** Donzelli S, Fontemaggi G, Fazi F, Di Agostino S, Padula F, Biagioni F et al. Cell Death Differ. 2012 Jun;19(6):1038-48. doi: 10.1038/cdd.2011.190. Epub 2011 Dec 23.

95. ***Mutant p53 gain-of-function induces epithelial-mesenchymal transition through modulation of the miR-130b-ZEB1 axis.*** Dong P, Karaayvaz M, Jia N, Kaneuchi M, Hamada J, Watari H et al. Oncogene. 2013 Jul 4;32(27):3286-95. doi: 10.1038/onc.2012.334. Epub 2012 Jul 30.

96. ***Gain of function mutp53 down-regulates miR223 contributing to chemoresistance of cultured tumor cells.*** Masciarelli S, Fontemaggi G, Di Agostino S, Donzelli S, Carcarino E, Strano S et al. Oncogene. 2014 Mar 20;33(12):1601-8. doi: 10.1038/onc.2013.106. Epub 2013 Apr 15.

97. ***Mutant p53 gain-of-function in cancer.*** Oren M, Rotter V. Cold Spring Harb Perspect Biol. 2010 Feb;2(2):a001107. doi: 10.1101/cshperspect.a001107. Review.

98. ***High metastatic potential in mice inheriting a targeted p53 missense mutation.*** Liu G, McDonnell TJ, Montes de Oca Luna R, Kapoor M, Mims B, El-Naggar AK, Lozano G. Proc Natl Acad Sci U S A. 2000 Apr 11;97(8):4174-9.

99. ***Chromosome stability, in the absence of apoptosis, is critical for suppression of tumorigenesis in Trp53 mutant mice.*** Liu G, Parant JM, Lang G, Chau P, Chavez-Reyes A, El-Naggar AK, Multani A, Chang S, Lozano G. Nat Genet. 2004 Jan;36(1):63-8. Epub 2003 Dec 21.

100. ***Analysis of centrosome abnormalities and angiogenesis in epidermal-targeted p53172H mutant and p53-knockout mice after chemical carcinogenesis: evidence for a gain of function.*** Wang XJ, Greenhalgh DA, Jiang A, He D, Zhong L, Brinkley BR, Roop DR. Mol Carcinog. 1998 Nov;23(3):185-92.

101. ***A gain of function p53 mutant promotes both genomic instability and cell survival in a novel p53-null mammary epithelial cell model.*** Murphy KL, Dennis AP, Rosen JM. FASEB J, 2000 Nov; 14:2291–302.

102. ***The inherent instability of mutant p53 is alleviated by Mdm2 or p16INK4a loss.*** Terzian T, Suh YA, Iwakuma T, Post SM, Neumann M, Lang GA, Van Pelt CS, Lozano G. Genes Dev. 2008 May 15;22(10):1337-44. doi: 10.1101/gad.1662908.

103. ***The cancer stem cell: Premises, promises and challenges.*** Clevers H. Nat Med 2011; 17:313-3199

104. ***Carcinogenesis and environment: the cancer stem cell hypothesis and implications for the development of novel therapeutics and diagnostics.*** Giordano A, Fucito A, Romano G, Marino IR. Front Biosci 2007; 12:3475-3482.

105. ***Identification and expansion of human osteosarcoma-cancer-stem cells by long-term 3-aminobenzamide treatment.*** Di Fiore R, Santulli A, Ferrante RD, Giuliano M, De Blasio A, Messina C, et al. J Cell Physiol 2009; 219:301-313.

106. ***The effect of 3-aminobenzamide, inhibitor of poly (ADP-ribose) polymerase, on human osteosarcoma cells.*** De Blasio A, Musmeci MT, Giuliano M, Lauricella M, Emanuele S, D'Anneo A, et al.. Int J Oncol 2003; 23:1521-1528.

107. ***Differentiative pathway activated by 3-aminobenzamide, an inhibitor of PARP, in human osteosarcoma MG63 cells.*** De Blasio A, Messina C, Santulli A, Mangano V, Di Leonardo E, D'Anneo A, et al.. FEBS Lett 2005; 579:615-620.

108. ***Differentiation of human osteosarcoma 3AB-OS stem-like cells in derivatives of the three primary germ layers as an useful in vitro model to develop several purposes.*** Di Fiore R, Drago-Ferrante R, D'Anneo A, De Blasio A, Santulli A, Messina C, et al.. Stem Cell Discovery 2013;3:188-201.

109. ***Modelling human osteosarcoma in mice through 3AB-OS cancer stem cell xenografts.*** Di Fiore R, Guercio A, Puleio R, Di Marco P, Drago-Ferrante R, D'Anneo A, et al. J Cell Biochem 2012 Nov;113(11):3380-92. doi: 10.1002/jcb.24214.

110. ***Hallmarks of cancer: the next generation***. Hanahan D, Weinberg RA. vCell. 2011 Mar 4;144(5):646-74. doi: 10.1016/j.cell.2011.02.013. Review.

111. ***On the origin of cancer cells***. Warburg O. Science. 1956 Feb 24;123(3191):309-14.

112. ***Tumor suppressors and cell metabolism: a recipe for cancer growth***. Jones RG, Thompson CB.Genes Dev. 2009 Mar 1;23(5):537-48. doi: 10.1101/gad.1756509. Review.

113. ***HIF1α induced switch from bivalent to exclusively glycolytic metabolism during ESC-to-EpiSC/hESC transition***. Zhou W, Choi M, Margineantu D, Margaretha L, Hesson J, Cavanaugh C, Blau CA, Horwitz MS, Hockenbery D, Ware C, Ruohola-Baker H.

EMBO J. 2012 May 2;31(9):2103-16. doi: 10.1038/emboj.2012.71. Epub 2012 Mar 23.

114. ***Energy metabolism in human pluripotent stem cells and their differentiated counterparts.*** Varum S, Rodrigues AS, Moura MB, Momcilovic O, Easley CA 4th,

Ramalho-Santos J, Van Houten B, Schatten G. PLoS One. 2011;6(6):e20914. do10.1371/journal.pone.0020914. Epub 2011 Jun 17.

115. ***Oct1 loss of function induces a coordinate metabolic shift that opposes tumorigenicity.*** Shakya A, Cooksey R, Cox JE, Wang V, McClain DA, Tantin D. Nat Cell Biol. 2009 Mar;11(3):320-7. doi: 10.1038/ncb1840. Epub 2009 Feb 15.

116. ***Energy metabolism characterization of a novel cancer stem cell-like line 3AB-OS***. Palorini R, Votta G, Balestrieri C, Monestiroli A, Olivieri S, Vento R, Chiaradonna F. J Cell Biochem. 2014 Feb;115(2):368-79. doi: 10.1002/jcb.24671.

117. ***Cancer stem cells with genetic instability: the best vehicle with the best engine for cancer.*** Lagasse E. Gene Ther. 2008 Jan;15(2):136-42. Epub 2007 Nov 8. Review.

118. ***Genetic and molecular characterization of the human osteosarcoma 3AB-OS cancer stem cell line: a possible model for studying osteosarcoma origin and stemness.*** Di Fiore R, Fanale D, Drago-Ferrante R, Chiaradonna F, Giuliano M, De Blasio A, Amodeo V, Corsini LR, Bazan V, Tesoriere G, Vento R, Russo A. J Cell Physiol. 2013 Jun;228(6):1189-201. doi: 10.1002/jcp.24272.

119. ***Cytogenetic findings in 73 osteosarcoma specimens and a review of the literature***. Bridge JA, Nelson M, McComb E, McGuire MH, Rosenthal H, Vergara G, Maale GE, Spanier S, Neff JR. Cancer Genet Cytogenet. 1997 May;95(1):74-87. Review.

120. ***Evaluation of paediatric osteosarcomas by classic cytogenetic and CGH analyses.*** Batanian JR, Cavalli LR, Aldosari NM, Ma E, Sotelo-Avila C, Ramos MB, Rone JD, Thorpe CM, Haddad BR. Mol Pathol. 2002 Dec;55(6):389-93.

121. ***Array comparative genomic hybridization reveals frequent alterations of G1/S checkpoint genes in undifferentiated pleomorphic sarcoma of bone.*** Niini

T, Lahti L, Michelacci F, Ninomiya S, Hattinger CM, Guled M, Böhling T, Picci P, Serra M, Knuutila S. Genes Chromosomes Cancer. 2011 May;50(5):291-306. doi: 10.1002/gcc.20851. Epub 2011 Jan 19.

122. ***Profiling of high-grade central osteosarcoma and its putative progenitor cells identifies tumourigenic pathways.*** Cleton-Jansen AM, Anninga JK, Briaire-de Bruijn IH, Romeo S, Oosting J, Egeler RM, Gelderblom H, Taminiau AH, Hogendoorn PC. Br J Cancer. 2009 Dec 15;101(12):2064. doi: 10.1038/sj.bjc.6605482.

123. ***Analysis of miRNA-gene expression-genomic profiles reveals complex mechanisms of microRNA deregulation in osteosarcoma***. Maire G, Martin JW, Yoshimoto M, Chilton-MacNeill S, Zielenska M, Squire JA. Cancer Genet. 2011 Mar;204(3):138-46. doi: 10.1016/j.cancergen.2010.12.012.

124. ***miRNA signatures associate with pathogenesis and progression of osteosarcoma.***

Jones KB, Salah Z, Del Mare S, Galasso M, Gaudio E, Nuovo GJ, Lovat F, LeBlanc K, Palatini J, Randall RL, Volinia S, Stein GS, Croce CM, Lian JB, Aqeilan RI.

Cancer Res. 2012 Apr 1;72(7):1865-77. doi: 10.1158/0008-5472.CAN-11-2663. Epub 2012 Feb 20.

125. ***Surface proteomic analysis of differentiated versus stem-like osteosarcoma human cells.*** Gemei M, Corbo C, D'Alessio F, Di Noto R, Vento R, Del Vecchio L. Proteomics. 2013 Nov;13(22):3293-7. doi: 10.1002/pmic.201300170. Epub 2013 Oct 9.

126. ***Surfing the p53 network.*** Vogelstein B, Lane D, Levine AJ. Nature. 2000 Nov 16;408(6810):307-10.

127. ***Live or let die: the cell's response to p53.*** Vousden KH, Lu X. Nat Rev Cancer. 2002 Aug;2(8):594-604. Review.

128. ***Mutant p53: an oncogenic transcription factor***. Strano S, Dell'Orso S, Di Agostino S, Fontemaggi G, Sacchi A, Blandino G. Oncogene. 2007 Apr 2;26(15):2212-9. Review.

129. ***Mutant p53 gain-of-function in cancer.*** Oren M, Rotter V. Cold Spring Harb Perspect Biol. 2010 Feb;2(2):a001107. doi: 10.1101/cshperspect.a001107. Review.

130. ***Mutant p53 gain of function can be at the root of dedifferentiation of human osteosarcoma MG63 cells into 3AB-OS cancer stem cells***. Di Fiore R, Marcatti M, Drago-Ferrante R, D'Anneo A, Giuliano M, Carlisi D, De Blasio A, Querques F, Pastore L, Tesoriere G, Vento R. Bone. 2014 Mar;60:198-212. doi: 10.1016/j.bone.2013.12.021. Epub 2013 Dec 27.

131. ***Cancer stem cells and tumor metastasis*** (Review). Li S, Li Q. Int J Oncol. 2014 Jun;44(6):1806-12. doi: 10.3892/ijo.2014.2362. Epub 2014 Apr 2. Review.

132. ***Tumor stem cells derived from glioblastomas cultured in bFGF and EGF more closely mirror the phenotype and genotype of primary tumors than do serum-cultured cell lines.*** Lee J, Kotliarova S, Kotliarov Y, Li A, Su Q, Donin NM, Pastorino S, Purow BW, Christopher N, Zhang W, Park JK, Fine HA.Cancer Cell. 2006 May;9(5):391-403.

133. ***Side population is enriched in tumorigenic, stem-like cancer cells, whereas ABCG2+ and ABCG2- cancer cells are similarly tumorigenic***. Patrawala L, Calhoun T, Schneider-Broussard R, Zhou J, Claypool K, Tang DG. Cancer Res. 2005 Jul 15;65(14):6207-19.

134. ***Quantitative assay of senescence-associated β-galactosidase activity in mammalian cell extractas.*** R.K. Gary, S. M. Kindell. Analytical Biochemistry; 2005 August 15; 329-334.

135. ***A novel taxol-induced vimentin phosphorylation and stabilization revealed by studies on stable microtubules and vimentin intermediate filaments***. Vilalta PM, Zhang L, Hamm-Alvarez SF. J Cell Sci. 1998 Jul;111 (Pt 13):1841-52.

136. ***p53 and its mutants in tumor cell migration and invasion***. Muller PA, Vousden KH, Norman JC. J Cell Biol. 2011 Jan 24;192(2):209-18. doi: 10.1083/jcb.201009059. Review.

137. ***Gain-of-Function Activity of Mutant p53 in Lung Cancer through Up-Regulation of Receptor Protein Tyrosine Kinase Axl.*** Vaughan CA, Singh S, Windle B, Yeudall WA, Frum R, Grossman SR, Deb SP, Deb S. Genes Cancer. 2012 Jul;3(7-8):491-502. doi: 10.1177/1947601912462719.

138. ***Osteosarcoma development and stem cell differentiation***. Tang N, Song WX, Luo J, Haydon RC, He TC. Clin Orthop Relat Res. 2008 Sep;466(9):2114-30. doi:10.1007/s11999-008-0335-z. Epub 2008 Jun 18. Review.

139. ***Impact of mutant p53 functional properties on TP53 mutation patterns and tumor phenotype: lessons from recent developments in the IARC TP53 database.*** Petitjean A, Mathe E, Kato S, Ishioka C, Tavtigian SV, Hainaut P, Olivier M. Hum Mutat. 2007 Jun;28(6):622-9.

140. ***Germline mutations of the p53 tumor-suppressor gene in children and young adults with second malignant neoplasms***. Malkin D, Jolly KW, Barbier N, Look AT, Friend SH, Gebhardt MC, Andersen TI, Børresen AL, Li FP, Garber J, et al. N Engl J Med. 1992 May 14;326(20):1309-15. Erratum in: N Engl J Med. 1997 Mar 6;336(10):734.

141. ***CDK4 gene amplification in osteosarcoma: reciprocal relationship with INK4A gene alterations and mapping of 12q13 amplicons***. Wei G, Lonardo F, Ueda

T, Kim T, Huvos AG, Healey JH, Ladanyi M. Int J Cancer. 1999 Jan 18;80(2):199-204.

142. ***p53 and MDM2 alterations in osteosarcomas: correlation with clinicopathologic features and proliferative rate***. Lonardo F, Ueda T, Huvos AG, Healey J, Ladanyi M. Cancer. 1997 Apr 15;79(8):1541-7.

143. ***CDKN2A gene deletions and loss of p16 expression occur in osteosarcomas that lack RB alterations***. Nielsen GP, Burns KL, Rosenberg AE, Louis DN.Am J Pathol. 1998 Jul;153(1):159-63.

144. ***Mutation analysis of the apoptotic "death-receptors" and the adaptors TRADD and FADD/MORT-1 in osteosarcoma tumor samples and osteosarcoma cell lines.*** Dechant MJ, Fellenberg J, Scheuerpflug CG, Ewerbeck V, Debatin KM. Int J Cancer. 2004 May 1;109(5):661-7.

145. ***Matrix metalloproteinases participate in osteosarcoma invasion.*** Bjørnland K, Flatmark K, Pettersen S, Aaasen AO, Fodstad O, Maelandsmo GM. J Surg Res. 2005 Aug;127(2):151-6. Epub 2005 Apr 14.

146. ***Role of MMP-9 and its tissue inhibitor TIMP-1 in human osteosarcoma: findings in 42 patients followed for 1-16 years.*** Ferrari C, Benassi S, Ponticelli F, Gamberi G, Ragazzini P, Pazzaglia L, Balladelli A, Bertoni F, Picci P. Acta Orthop Scand. 2004 Aug;75(4):487-91.

147. ***Human primary bone sarcomas contain CD133+ cancer stem cells displaying high tumorigenicity in vivo.*** Tirino V, Desiderio V, Paino F, De Rosa A, Papaccio F, Fazioli F, Pirozzi G, Papaccio G. FASEB J. 2011 Jun;25(6):2022-30. doi: 10.1096/fj.10-179036. Epub 2011 Mar 8

148. ***Characterization of stem cell attributes in human osteosarcoma cell lines.*** Wang L, Park P, Lin CY. Cancer Biol Ther. 2009 Mar 15;8(6):543-52. doi: 10.4161/cbt.8.6.7695. Epub 2009 Mar 15.

149. ***Mutant p53 is a transcriptional co-factor that binds to G-rich regulatory regions of active genes and generates transcriptional plasticity.***Quante T, Otto B, Brázdová M, Kejnovská I, Deppert W, Tolstonog GV. Cell Cycle. 2012 Sep 1;11(17):3290-303. doi:10.4161/cc.21646. Epub 2012 Aug 21.

150. ***Preferential binding of hot spot mutant p53 proteins to supercoiled DNA in vitro and in cells.*** Brázdová M, Navrátilová L, Tichý V, Němcová K, Lexa M, Hrstka R, Pečinka P, Adámik M, Vojtesek B, Paleček E, Deppert W, Fojta M. PLoS One. 2013;8(3):e59567. doi: 10.1371/journal.pone.0059567. Epub 2013 Mar 26.

151. ***Identification*** *and* ***characterization*** *of the* ***chromatin-binding domains*** *of the* ***HIV-1 integrase interactor LEDGF/p75.*** Llano M, Vanegas M, Hutchins N, Thompson D, Delgado S, Poeschla EM. J Mol Biol. 2006 Jul 21;360(4):760-73. Epub 2006 May 17.

AKNOLEDMGEMENTS

During these last three years I worked with all my power to realize this thesis and at the end I got it! But I want to thanks all people that helped me in my iter. First of all I want to say thanks to my tutor, the Prof. Renza Vento that gave me the great opportunity to develop my PhD project in her research group. She has been a really good guide both scientifically and humanly and she teached me so many things. She also scolded me several times during these years but I know that she has always done it for my own good. In her research group I found not only colleagues but also friends with who I shared many good and bad moments. I will cherish in my heart all people that I met in the laboratories of the Department of Experimental Biomedicine and Clinical Neurosciences. All of them stayed close to me especially when I had more need and all of them gave me something good. I will never forget Anna De Blasio, her way to convey her great love for research and her friendship. I want to say thank you to Riccardo Di Fiore that teached me a lot using humor, smiles and also reproaches and his really nice wife Rosi Drago-Ferrante with whom I am linked by a particular shared experience. I wanted to say thanks to Selenia Sabella and Antonietta Notaro for all the times that we had fun or we cried together. Thanks to Daniela Carlisi that never made me feel alone. Thanks also to all the others colleagues (Antonella D'Anneo, Giuseppina Buttitta, Roberta Martinez; Dario La Sala) and all professors (Giovanni Tesoriere, Michela Giuliano, Marianna Lauricella) above all the Prof. Giuseppe Calvaruso and his niceness.

I spent my last year at the BRIC centre of the University of Copenhagen and I am grateful for this to the Prof.Anders Lund that accepted me in his laboratories. From the beginning he welcomed me as a real member of his research group, appreciating my work qualities and giving me many advice that allowed me to improve my skills. He is a really nice person whit

whom you can really feel at ease. Here I found very professional, available and patient people: Nkerorema Djodji Damas, Martin Jannsson, Giulia Maglieri, Roland Baumgartner, Marta Montes, Alison Louw, Imke Ulken, Helene Gylling, Lisa Frankel, Christophe Come, Disa Theler and Michal Lubas. I want to say thanks to all of them and above all to Nkerorema Djodji Damas with whom I collaborated. He has been a really good guide but especially he has been a very good friend. Thanks to him I met a really nice people (from the BRIC and from outside) and I have never felt alone in Copenhagen above all at the beginning when I did not know anybody. I also found in Giulia Maglieri a sincere friend that I would like to bring with me wherever I will live.

I am really grateful to Francesco Niola for all his advice and his typical Roman humor that kept me company when I needed it.

I want to say thanks also to all my best Italian friends (Francesca, Piero, Rosaria, Nino, Costa, Elena, Lilli and all the others) that gave me support during all my PhD period mostly when I was so far from them. I dedicate a big hug to all of them.

When I knew that I had won the competition for the admission for this PhD course I was with my father Aldo. I will never forget his happiness and pride in his eyes. Unfortunately, after few days he died and his memories and teachings had allowed to me to achieve this aim. I think that he would be proud of me now more than before. This is the reason why I dedicate this thesis to him.

Despite the difficult time all my family stayed close to me and encouraged all my decisions . This is the reason why I want to say thanks to my mother Enza, my sister Connie, my brother Marco and his wife Bea and his kids Viscardo e Sveva, my brother Antonino and his wife Yvhonne and his daughter Aiko. A good thought is also for my husband's family because all

of them (my mother in low Grazia, my father in low Enzo, my sister in low Giulia and my brother in low Davide) supported me and showed to be very proud of me every time.

Lastly, but not because he is less important than the others, I want to say thanks to my great husband Mauro. Thanks for his support, his advice, his encouragement. Thanks above all because, despite the huge distance between us, he has always managed to make me feel his great love through which I was able to overcome these last months.